

2003-04-24

Development of an Automated Anesthesia System for the Stabilization of Physiological Parameters in Rodents

Kevin Michael Hawkins
Worcester Polytechnic Institute

Follow this and additional works at: <https://digitalcommons.wpi.edu/etd-theses>

Repository Citation

Hawkins, Kevin Michael, "*Development of an Automated Anesthesia System for the Stabilization of Physiological Parameters in Rodents*" (2003). *Masters Theses (All Theses, All Years)*. 256.
<https://digitalcommons.wpi.edu/etd-theses/256>

This thesis is brought to you for free and open access by [Digital WPI](#). It has been accepted for inclusion in Masters Theses (All Theses, All Years) by an authorized administrator of Digital WPI. For more information, please contact wpi-etd@wpi.edu.

Development of an Automated Anesthesia System for the Stabilization of Physiological Parameters in Rodents

A Thesis

Submitted to the Faculty

of the

WORCESTER POLYTECHNIC INSTITUTE

in partial fulfillment of the requirements for the

Degree of Master of Science

by

Kevin M. Hawkins

Date: April 24, 2003

Approved:

Professor Ross D. Shonat, Ph.D., Major Advisor

Professor Yitzhak Mendelson, Ph.D., Committee Member

Professor Fred J. Looft, Ph.D., Committee Member

ACKNOWLEDGEMENTS

Funding for this project was provided by a biomedical engineering grant from the Whitaker Foundation, Rosslyn VA.

I would like to extend my gratitude to my wife Lisa and the rest of my family and friends for their support, and to:

Professor Mendelson and Professor Looft, for their technical input and constructive criticism.

Ross D, Shonat, for his guidance, support and confidence in me throughout this experience.

ABSTRACT

The testing of any physiological diagnostic system in-vivo depends critically on the stability of the anesthetized animal used. That is, if the systemic physiological parameters are not tightly controlled, it is exceedingly difficult to assess the precision and accuracy of the system or interpret the consequence of disease. In order to ensure that all measurements taken using the experimental system are not affected by fluctuations in physiological state, the animal must be maintained in a tightly controlled physiologic range. The main goal of this project was to develop a robust monitoring and control system capable of maintaining the physiological parameters of the anesthetized animal in a predetermined range, using the instrumentation already present in the laboratory, and based on the LabVIEW^R software interface. A single user interface was developed that allowed for monitoring and control of key physiological parameters including body temperature (BT), mean arterial blood pressure (MAP) and end tidal CO₂ (ETCO₂). Embedded within this interface was a fuzzy logic based control system designed to mimic the decision making of an anesthetist. The system was tested by manipulating the blood pressure of a group of anesthetized animal subjects using bolus injections of epinephrine and continuous infusions of phenylephrine (a vasoconstrictor) and sodium nitroprusside (a vasodilator). This testing showed that the system was able to significantly reduce the deviation from the set pressure (as measured by the root mean square value) while under control in the hypotension condition ($p < 0.10$). Though both the short-term and hypertension testing showed no significant improvement, the control system did successfully manipulate the anesthetic percentage in response to changes in MAP. Though currently limited by the control variables being used, this system is an important first step towards a fully automated monitoring and control system and can be used as the basis for further research.

TABLE OF CONTENTS

ACKNOWLEDGEMENTS	ii
ABSTRACT	iii
TABLE OF CONTENTS	iv
TABLE OF FIGURES	vi
TABLE OF TABLES	ix
1. INTRODUCTION	1
2. BACKGROUND	4
2.1. Anesthetic Agents	4
2.2. Physiological Monitoring	6
2.3. Physiologic Control	7
3. DESIGN	10
3.1. LabVIEW ^R Interface	10
3.2. Monitoring/Communication System	11
3.2.1. Body Temperature Monitoring	11
3.2.2. Analog Waveform Monitoring	11
3.3. Instrument Control System	14
3.3.1. Anesthetic Control	14
3.3.2. Ventilator Control	19
3.3.3. Body Temperature Control	21
3.4. Fuzzy Logic Control Systems	23
3.4.1. Blood Pressure	25
3.4.2. End Tidal CO ₂ Control	30
3.5. Data Transfer System	35
3.6. User Interface	38
3.6.1. Interface Hierarchy	41
4. METHODS	42
4.1. In-Vitro Testing	42
4.2. In-Vivo Experiments	42
4.2.1. Short-term Perturbation	45
4.2.2. Long-term Perturbation	46
5. RESULTS	48
5.1. Body Temperature Results	48
5.2. Short term Perturbation Results	49
5.3. Long-term Perturbation results	54
5.4. CO ₂ controller Results	62
5.5. Steady state observations	63
6. DISCUSSION	66
6.1. Significance of results	66
6.2. Future Work	67
6.3. Conclusions	69
7. REFERENCES	71

Appendix A: Epinephrine Injection Data Plots.....	75
Appendix B: Neo-Synephrine Infusion Data plots	78
Appendix C: Sodium Nitroprusside Infusion Data Plots	82
Appendix D: ETCO ₂ Data Plots.....	88

TABLE OF FIGURES

Figure 2.1-1: Anesthesia vaporizer and flow control hardware (Boutillette et al 2000).....	5
Figure 2.3-1: Block diagram of a traditional control scheme (Rao et al 2000).....	8
Figure 3.2-1: Body temperature VI block diagram (a) and front panel display(b). Dashed boxes show different sections of the block diagram: voltage measurement (1), temperature conversion voltage to °K (2), and temperature conversion °K to °C.....	11
Figure 3.2-2: Waveform processing section (a) consisting of a waveform acquisition VI (box (1)), airway pressure rate (box (2)), airway Min/Max (box (3)), airway pressure and %CO ₂ waveform display (box (4)), %CO ₂ Min/Max (box (5)), %CO ₂ rate (box (6)), blood pressure rate (box (7)), blood pressure two point calibration and scaling for Min/Max and waveform display (box (8)). Blood pressure VI front panel (b), and block diagram (c).....	13
Figure 3.3-1: Anesthetic Concentration / Flow Control VI block diagram (a), showing the Anesthetic Calculator (box1) and the Basic Gas Mixer (box 2) VI, and front panel (b).	15
Figure 3.3-2: Anesthetic Flow rate Calculator VI block diagram (a) and front panel (b). (Based on work done by Dr. Ross Shonat).....	17
Figure 3.3-3: Basic Gas Flowmeter VI block diagram (a) and front panel (b). (Based on work done by Dr. Ross Shonat).....	18
Figure 3.3-4: The Ventilator Control VI block diagram (a) and front panel display (b). (Based on work done by Amanda Kight).....	19
Figure 3.3-5: Inspira Control VI Block diagram (a) and front panel (b).....	20
Figure 3.3-6: The water bath control VI block diagram (a) and front panel display (b).....	22
Figure 3.3-7: Duty cycle VI block diagram (a) and front panel (b).....	23
Figure 3.4-1: Preliminary membership functions for blood pressure control system.....	26
Figure 3.4-2: Blood Pressure Control VI block diagram (a) showing the fuzzification, inference, defuzzification operations and the safety limits (boxes 1, 2, 3 and 4 respectively) and front panel display (b).	29
Figure 3.4-3: Mean Arterial Pressure VI block diagram (a) and front panel (b)..	29
Figure 3.4-4: Plots of (A) increased ventilation with increased pCO ₂ levels, due to (B) increased RR and (C) increased TV (Letsky 1992)	31
Figure 3.4-5: Fuzzification membership functions for the E input rule base.....	32
Figure 3.4-6: Graph showing the change in ventilation due to changes in oxygen concentration (Letsky 1992)	34
Figure 3.4-7: ETCO ₂ Control VI block diagram (a) showing the fuzzification, inference and defuzzification operations (boxes 1, 2 and 3 respectively) and (b) front panel display.....	35
Figure 3.5-1: the Write to File VI block diagram (a) and front panel display (b).	37

Figure 3.5-2: An example of the data collected using the write to file VI and analyzed using Excel, note the vertical lines indicating a marked event (in this case images being taken).....	38
Figure 3.6-1: User interface VI block is made up of the previously discussed VIs	39
Figure 3.6-2: Interfacev2 VI block diagram (a) and front panel interface (b)	40
Figure 3.6-3: Block diagram showing the hierarchy of the sub-VIs used to make the interface VI.	41
Figure 4.2-1: Digital images of a rat (a) in an induction chamber (b) with the anesthesia mask over its snout and (c) with the tracheal cannula inserted and connected to the ventilator inhalation and exhalation tubing.	45
Figure 5.1-1: Test data for control of water temperature in a rat substitute (With a set point of 37 degrees Celsius).....	48
Figure 5.1-2:A sample of the data collected during a preliminary animal procedure (set point Temperature of 38 degrees Celsius).	49
Figure 5.2-1: Animal R-1 epinephrine test data showing MAP under control (closed circles) and no- control (open circles) conditions and % anesthetic (closed triangles) vs. time.....	51
Figure 5.2-2 Animal R-1 epinephrine test data showing % MAP deviation under control (closed circles) and no- control (open circles) conditions and % anesthetic (closed triangles) vs. time.	52
Figure 5.3-1: Animal LTP-6 Neo-Syneprhine infusion test data showing MAP under control (closed circles) and no- control (open circles) conditions and % anesthetic (closed triangles) vs. time.	57
Figure 5.3-2: Animal LTP-6 Neo-Syneprhine infusion test data showing % MAP deviation under control (closed circles) and no- control (open circles) conditions and % anesthetic (closed triangles) vs. time.	57
Figure 5.3-3: Animal LTP-6 sodium nitroprusside infusion test data showing MAP under control (closed circles) and no- control (open circles) conditions and % anesthetic (closed triangles) vs. time.	58
Figure 5.3-4: Animal LTP-6 sodium nitroprusside infusion test data showing % MAP deviation under control (closed circles) and no- control (open circles) conditions and % anesthetic (closed triangles) vs. time.	59
Figure 5.3-5: Neo-syneprhine testing mean and standard deviation vs. tome for control (closed circles, negative error bars) and no-control (open circles, positive error bars).	61
Figure 5.3-6: Sodium nitroprusside testing mean and standard deviation vs. tome for control (closed circles, negative error bars) and no-control (open circles, positive error bars).	61
Figure 5.4-1: Representative plot of % CO ₂ (closed circle) tidal volume (closed triangle) and respiratory rate (Closed square) vs. time for animal LTP-3.	62
Figure 5.4-2: Representative plot of % CO ₂ deviation (closed circle) change in TV set point (closed triangle) and change in RR set point (Closed square) vs. time for animal LTP-3.	63
Figure 5.5-1: Animal LTP-5 steady state test data showing MAP under control (closed circles) and % anesthetic (closed triangles) vs. time.	64

- Figure 5.5-2: Animal LTP-5 steady state test data showing % MAP deviation under control (closed circles) and % anesthetic (closed triangles) vs. time. 64*
- Figure 5.5-3: Animal LTP-5 steady state data showing % CO₂ (closed circle) tidal volume (closed triangle) and respiratory rate (Closed square) vs. time. ... 65*
- Figure 5.5-4: Animal LTP-5 steady state data showing % CO₂ deviation (closed circle)% change in tidal volume (closed triangle) and % change in respiratory rate (Closed square) vs. time. 65*

TABLE OF TABLES

<i>Table 3.3-1: Summary of temperature difference ranges and the corresponding duty cycles</i>	21
<i>Table 3.4-1: Pros and Cons of the traditional and fuzzy logic approach to anesthesia control.</i>	25
<i>Table 3.4-2: Pressure controller rule base definition summary.</i>	27
<i>Table 3.4-3: ETCO₂ controller rule base definition summary.</i>	33
<i>Table 3.4-4: Correction value scaling factors for various pO₂ ranges.</i>	34
<i>Table 5.2-1 Representative data set for animal R-1 showing formatted data for an epinephrine injection test under no- control conditions.</i>	53
<i>Table 5.2-2: Summary of calculated RMS values and Paired t-test results</i>	54
<i>Table 5.3-1: Representative data set for animal LTP-3 showing formatted data for an Sodium Nitroprusside infusion test under control conditions.</i>	56
<i>Table 5.3-2: Summary of calculated RMS values and Paired t-test results for the Neo-Synephrine infusion experiments.</i>	59
<i>Table 5.3-3: Summary of calculated RMS values and Paired t-test</i>	60

1. INTRODUCTION

The presence of low O_2 levels in the vasculature and tissues of the retina, termed retinal hypoxia, has been linked to the development of many eye diseases including diabetic retinopathy and glaucoma. It is recognized that imaging technologies to identify and monitor oxygen levels in the retina would substantially advance our understanding and treatment of these devastating diseases and the laboratory is currently developing a non-invasive diagnostic imaging technique, based on phosphorescence lifetime imaging (PLI), to produce two-dimensional maps of pO_2 in the rodent retina. This technique is undergoing *in-vivo* testing, using rats and mice, and has shown promising results.

The testing of this technology *in-vivo* depends critically on the stability of the anesthetized animal. That is, if the systemic physiological parameters are not tightly controlled, it is exceedingly difficult to assess the precision and accuracy of the PLI system or interpret the consequence of disease. Any variation in physiological parameters such as Blood Pressure (BP), Body Temperature (BT) and Pulmonary Function (pO_2 and pCO_2 levels) can be a potential source of variation in the data being gathered using PLI. In order to ensure that all measurements taken using PLI are not affected by fluctuations in the systemic physiological state, each animal must be maintained within a tightly controlled physiologic range. The main goal of this project was to develop a robust monitoring and control system capable of maintaining the physiological parameters of an anesthetized animal in a predetermined range, using the instrumentation already present in the laboratory, and based on the LabVIEWTM software interface. The specific aims were to:

- Develop a computer-controlled monitoring system (based on LabVIEW™) capable of “real time” data acquisition and display of BT, end tidal CO₂ (ETCO₂), ventilator pressure and BP.
- Develop a communications capability allowing for the control of laboratory instrumentation, such as the ventilator, heating bath and gas flow meters.
- Develop a computer-based control system (using LabVIEW™) for maintaining BT, ETCO₂, and BP. Fuzzy logic control theory was employed to mimic the complex decision processes that a trained anesthesiologist might make.
- Design a user interface that incorporates the above subsystems and an event marker and file transfer system.

By developing a system that can maintain the physiologic state of the animal within narrow limits, better characterization of the PLI system in the laboratory is possible. At the same time, the system can free the experimentalist to concentrate on the acquisition of retinal oxygen data using the PLI system.

In order to achieve the above goals a design had to be developed that allowed for the most elegant solution possible. A fuzzy logic control strategy was developed to mimic the decision making of an anesthetist allowing for the automated maintenance of ETCO₂ and BP. The monitoring, control and file transfer systems were developed in LabVIEW™ and combined to create a single user interface. This interface was tested on a total of ten rats in both short and long-term perturbation experiments using bolus and maintained drug infusions to mimic various systemic physiological conditions. This testing revealed that the system had limited abilities to control short-term perturbations

but was able to significantly reduce the deviation of the mean arterial blood pressure (MAP) from the control set point in simulated hypotension experiments.

2. BACKGROUND

Before developing a monitoring/control system, it is important to first understand anesthesia and its control. The following sections provide some background in anesthesia, physiological monitoring and physiological control systems that have been used to date.

2.1. *Anesthetic Agents*

General anesthetics can be separated into two major categories, injectable anesthetics and inhalant anesthetics. Injectable anesthetics can be further divided into sub-categories based on the route of administration, including Intra-peritoneal (IP), Intra-Muscular (IM), Sub-Cutaneous (SC), Intra-Cardiac (IC) and Intra-Venous (IV). In past experiments in the laboratory, an injectable anesthetic, Avertin, was administered IP to achieve the desired anesthetic depth. Though safe for the test subject and easy for the researcher to administer, bolus injection made it impossible to control the physiology of the animal through anesthetic manipulation during the procedure. Since the control of the animal's physiology is one of the main goals of this project, a new anesthetic agent had to be chosen for future experimentation. IV anesthetics, such as Propofol, afford the researcher the ability to control the depth of anesthesia throughout the procedure by manipulating the rate of infusion, but this approach requires the use of syringe pumps, which are not always available in the laboratory. Other injectable agents can also be used once the animal is under anesthesia to manipulate its physiological parameters. Some examples of these chemical agents are vasodilators, such as sodium nitroprusside, which cause a drastic drop in systemic BP and vasoconstrictors, such as phenylephrine, which cause a drastic rise in systemic BP.

Inhalant anesthetics, on the other hand, allow for a controlled depth of anesthesia due to the fairly rapid physiological response time to changes in concentration. Some common inhalant anesthetics include Halothane, Isoflurane, and Enflurane. For this project, Halothane was chosen as the anesthetic based on its rapid uptake, pleasant induction and availability (Short 1987). In order to deliver a precise concentration of anesthetic, a copper kettle vaporizer constructed by a previous undergraduate project group was used (*figure 2.1-1*). The copper kettle vaporizer produces O₂ saturated with the anesthetic agent, which is then mixed with humidified N₂ and O₂ and delivered to the test animal (Boutillette *et al* 2000). The overall inhalant anesthesia and gas flow system is shown in *figure 2.1-1*.

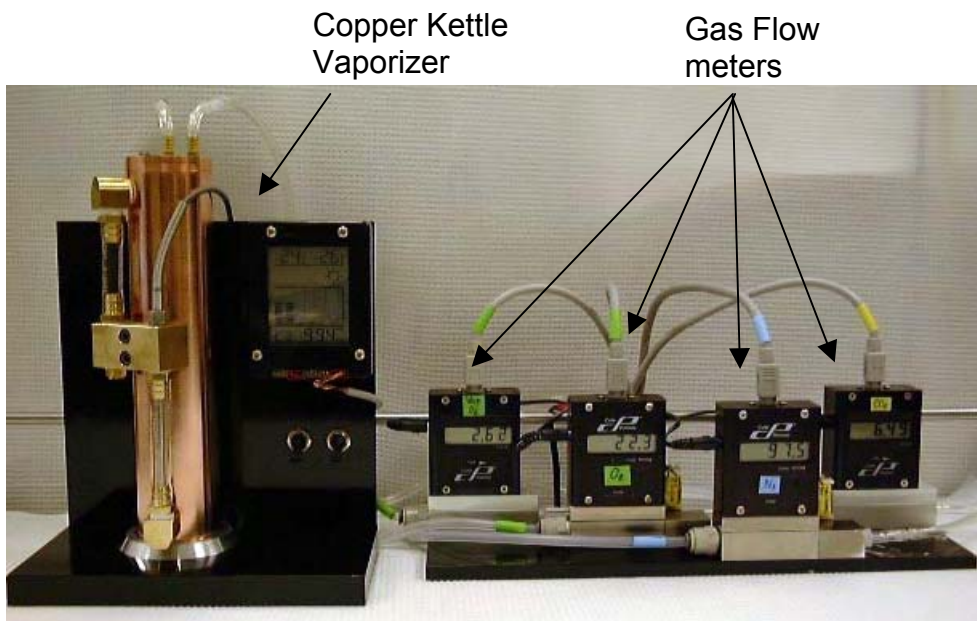


Figure 2.1-1: Anesthesia vaporizer and flow control hardware (Boutillette et al 2000).

2.2. Physiological Monitoring

While under anesthesia, it is important to closely monitor the animal subject to ensure anesthetic depth is maintained at a point that ensures that it will not experience any discomfort throughout the procedure. The parameters that are traditionally monitored and analyzed to assess current physiological state and anesthetic depth include BT, BP, Electro-cardiogram (ECG), pulmonary function (CO₂ and O₂) and blood gas values. Due to the small size of the animals being used for this research (rats and mice) special considerations of the animal's parameters to be accurately collected and analyzed is required (Short 1987).

One of the parameters that requires special considerations due to the small size of the animals is the ETCO₂. The instrument used to sample CO₂ concentration is called a capnometer. Traditional capnometers require a sample size that is quite large in comparison to the dead space of the animal's lungs. This produces a situation in which serious damage or death can occur due to suffocation during sampling. To ensure that there is no danger to the animal, a micro-capnometer must be used. The micro-capnometer chosen for this research was the Columbus Instruments Micro-Capnometer, which is able to take wet samples of either 20 cc or 5 cc. These smaller sample volumes allow for the sampling of CO₂ without risk of injury to the animal.

Blood pressure is another parameter that is important to monitor throughout the procedure. The BP of the animal is an important indicator of anesthetic depth and can be an indicator of distress. To measure BP for this study, an arterial catheter is placed in a femoral artery and pressure readings are taken using the Biopac RX104A pressure transducer connected to the National Instruments SCXI module. The National

Instruments SCXI module allows for the measurement of voltage and, using a two-point calibration factor, allows for the direct measurement of BP. Heart rate is another important parameter to measure, which can be extracted from the BP waveform data.

Though ECGs are often an important parameter to monitor, the small size of the animal can make it difficult to obtain a useful waveform. In addition, the intervals of the ECG can be difficult to measure consistently in small animals due to the high heart rate and variation from animal to animal.

Blood gas measurements are very indicative of the physiological state of the animal, providing such information as pO_2 , pH and pCO_2 . The issue with the measurement of blood gases is that the sampling of blood can quickly reduce the test subject's blood volume and there is currently no way to automate the sampling process and data transfer with the equipment currently available in the laboratory. Instead, manual samples can be taken and entered into the user interface, allowing these valuable parameters to be taken into consideration, during anesthetic control.

2.3. Physiologic Control

The automated control of anesthesia has received quite a bit of attention in the last few years. The two major areas of control theory that have received this attention are traditional, mathematical model based, controls (Hang *et al* 1999, Dalkara *et al* 1995, Prie *et al* 1997, Rao *et al* 2000) and fuzzy logic control theory (Apshari *et al* 1994, Becker *et al* 1997, Dojat 1997, Graaf *et al* 1997, Held *et al* 2000, Linkens 1999, Lowe *et al* 1999, Meier *et al* 1992, Shing *et al* 1999). The model based control theory uses mathematical models of the test subject's physiology and the theoretical reaction of

stimulus, such as anesthetic concentration, to produce estimates of the physiologic reactions. Based on these estimates, control algorithms are developed and used in a feedback (most often negative) system. The traditional control system is able to take inputs from the entire system and produce multiple outputs for control. A block diagram representing such a control system that takes advantage of feedback to increase stability is seen in *figure 2.3-1* (Rao *et al* 2000).

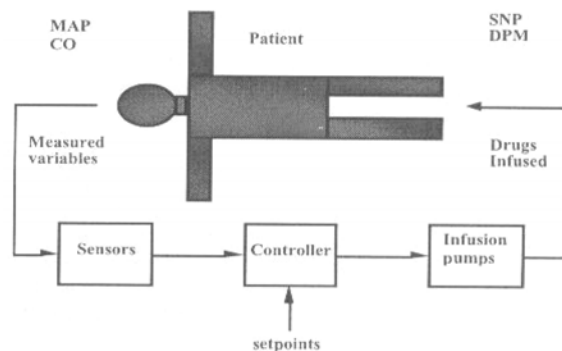


Figure 2.3-1: Block diagram of a traditional control scheme (Rao *et al* 2000).

The past work done in the area of anesthetic control using traditional control theory is somewhat limited due to the complexity of the models. A majority of the past research relies on the use of electroencephalogram (EEG) or electrocardiogram (ECG) waveforms as the primary parameter for the detection of anesthetic depth (Seiber *et al* 2000) (Mortier and Stuyts 2001). Though this is a valid and highly accurate method for human patients, the measurement of EEG and ECG data can be problematic in small animals such as mice and rats, and the equipment needed to acquire these waveforms is currently unavailable in the laboratory.

In contrast, fuzzy logic control attempts to use fuzzy set theory to model the decisions of an anesthetist, given inputs of physiologic states. Fuzzy set theory allows for

the computation of partial membership, or partial truth, for a set of membership functions and provides a crisp output based on a corresponding rule set. The rule sets used in fuzzy logic controls are based on the previous knowledge of a specialist, or a number of specialists, and can take single or multiple inputs into account to make the decision. The process of producing a crisp output using fuzzy logic consists of three major steps: fuzzification, inference and defuzzification. Fuzzification consists of the calculation of membership, based on the membership functions, for the input values. Inference takes the results of the fuzzification process and produces a fuzzy output based on the rule set. Defuzzification produces a crisp output based on the inference process results (Qingyang Hu and Petr 2000).

In recent years an increasing number of studies have focused on the use of fuzzy logic controls to control BP and anesthetic depth (Apsari *et al* 1994, Becker *et al* 1997, Dojat 1997, Graaf *et al* 1997, Held *et al* 2000, Linkens 1999, Lowe *et al* 1999, Meier *et al* 1992, Shing *et al* 1999). The control outputs for these systems have been both inhalant and injectable anesthetics and have focused primarily on BP for the input parameter (Meier *et al* 1997, de Graaf *et al* 1997, Shieh *et al* 1999).

3. DESIGN

The use of the LabVIEW™ interface is integral to the successful development of the communication and control systems that are required to successfully implement the objectives set forth for this project. This section outlines the design process that was followed in order to develop the various components of the monitoring, instrument control, fuzzy logic control and data transfer systems as well as the final user interface.

3.1. *LabVIEW^R Interface*

The LabVIEW™ platform was used for all components of this project, including monitoring, instrument control and fuzzy logic control. LabVIEW^R is a program that allows for the development of “Virtual Instruments” (VI) capable of sending information to and receiving information from devices using embedded virtual channels that can be setup for each input and output function, incorporating conversion factors and handling the transfer of data. This platform also has substantial mathematical capabilities. The LabVIEW™ platform was ideal for this project because it allowed existing VIs to be used as sub-sets, sub-VIs, in larger more complex VIs. This allowed for the creation of small specialized VIs capable of monitoring a single parameter or controlling a single instrument and which could be used as building blocks for a highly complex single VI capable of monitoring, display, data acquisition, instrument control and fuzzy logic control. The VIs developed for this project are described in the following sections.

3.2. Monitoring/Communication System

3.2.1. Body Temperature Monitoring

The Body Temp VI is able to obtain and display the animal's rectal body temperature (*figure 3.2-1*). The hardware measures the voltage drop across a thermistor based temperature probe excited with 0.15 mA of current. The measured voltage is converted to a temperature in degrees Kelvin using constants provided by the manufacturer, and is ultimately converted to degrees Celsius using a standard conversion factor (*figure 3.3-1(a)*). The resulting front panel display for the VI displays the measured voltage, numeric measurement of temperature and a graphical representation of temperature (*figure 3.2-1 (b)*)

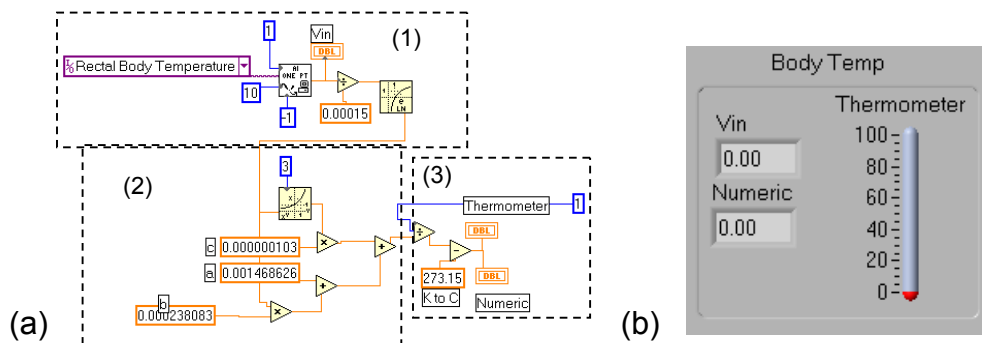


Figure 3.2-1: Body temperature VI block diagram (a) and front panel display(b). Dashed boxes show different sections of the block diagram: voltage measurement (1), temperature conversion voltage to °K (2), and temperature conversion °K to °C.

3.2.2. Analog Waveform Monitoring

The acquisition of %CO₂, airway pressure and BP waveform data is done using a modified waveform acquisition VI supplied by LabVIEW^R (*figure 3.2-2 (a) box (1)*).

This VI uses “Virtual Channels” (VCs) to obtain scaled waveform data for the above

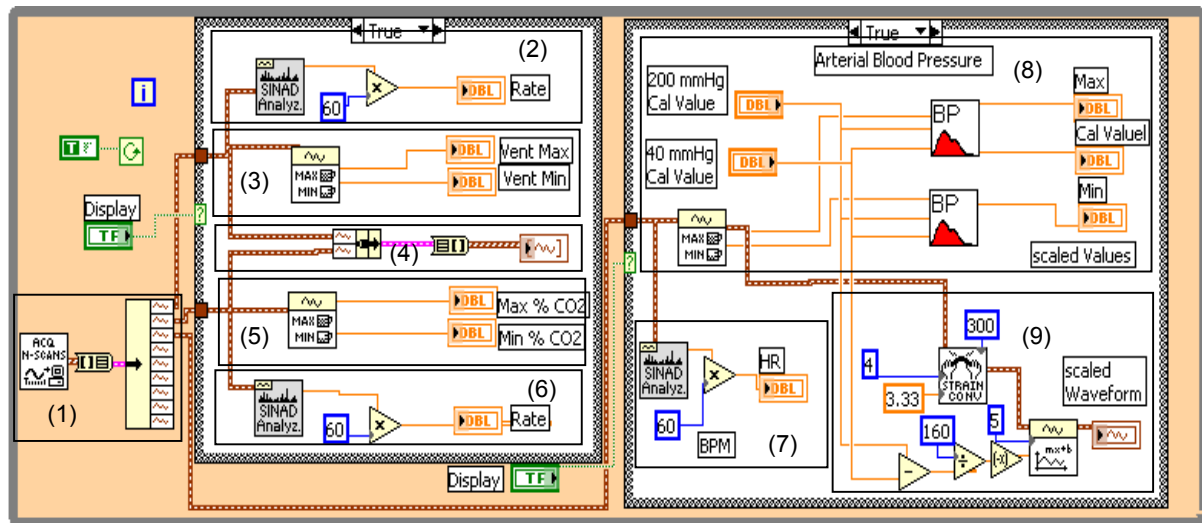
parameters at a rate of 250 Hz. Additional conditioning of the waveform signals is completed to obtain the min/max values and the rate of the waveforms. To provide the user with more flexibility the airway pressure and %CO₂ waveforms are conditioned in one section while the BP waveform is conditioned in another. Each of the waveform conditioning sections can be turned on and off independently.

The airway pressure conditioning section can handle waveform data from two different ventilators, one from Columbus Instruments (CIV-101) and the other from Harvard Apparatus (Inspira). Two VCs, “Columbus” and “Inspira”, are set up to measure an analog output of 0-5 V from a ventilator and use a conversion factor to produce the manufacturer specified pressure range (-10 - 40 mmHg for Columbus Instruments, and -50 - 50 mmHg for the Harvard Apparatus Inspira). After the airway pressure waveform is acquired, the data is processed for rate and minimum and maximum values (*figure 3.2-2 (a) boxes (2) and (3,) respectively*)

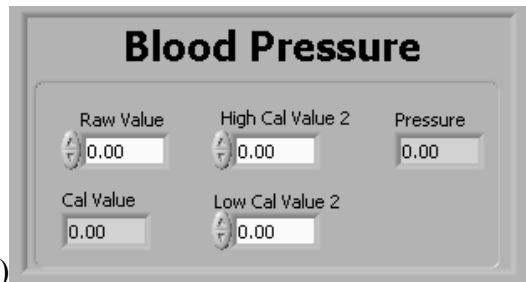
The design of the %CO₂ waveform conditioning section closely resembles that of the airway pressure section. A VC, “Capnometer Read”, measures an analog output of 0-5 V directly from the micro-capnometer and converts the signal to a range of 0-10 %CO₂. The acquired waveform data is processed for min/max values and rate (*figure 3.2-2 (a) boxes (5) and (6) respectively*). The waveform data for both the airway pressure and %CO₂ are then clustered together and displayed on a single waveform graph (*figure 3.3-2 (a) box (5)*).

The arterial BP waveform is processed in a different section because it requires a two-point calibration factor (calibration points at 40 mmHg and 200 mmHg). A separate VI, Blood Pressure (*figure 3.2-2 (a) and (b)*), is used to scale the waveform and min/max

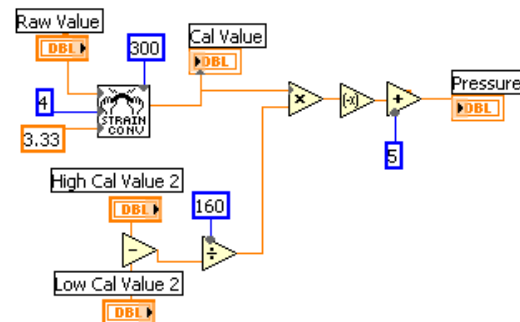
values to the correct level once the user entered the 40 mmHg and 200 mmHg calibration points (*figure 3.2-2 (a) box (8)*). The waveform is also processed to obtain the rate of the signal in beats per minute (BPM) (*figure 3.2-2 (a) box (9)*)



(a)



(b)



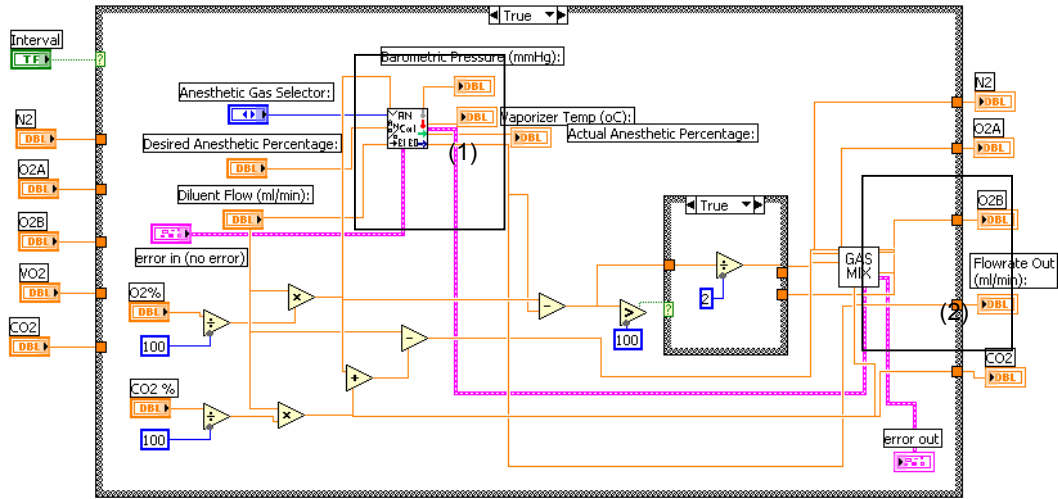
(c)

Figure 3.2-2: Waveform processing section (a) consisting of a waveform acquisition VI (box (1)), airway pressure rate (box (2)), airway Min/Max (box (3)), airway pressure and %CO₂ waveform display (box (4)), %CO₂ Min/Max (box (5)), %CO₂ rate (box (6)), blood pressure rate (box (7)), blood pressure two point calibration and scaling for Min/Max and waveform display (box (8)). Blood pressure VI front panel (b), and block diagram (c).

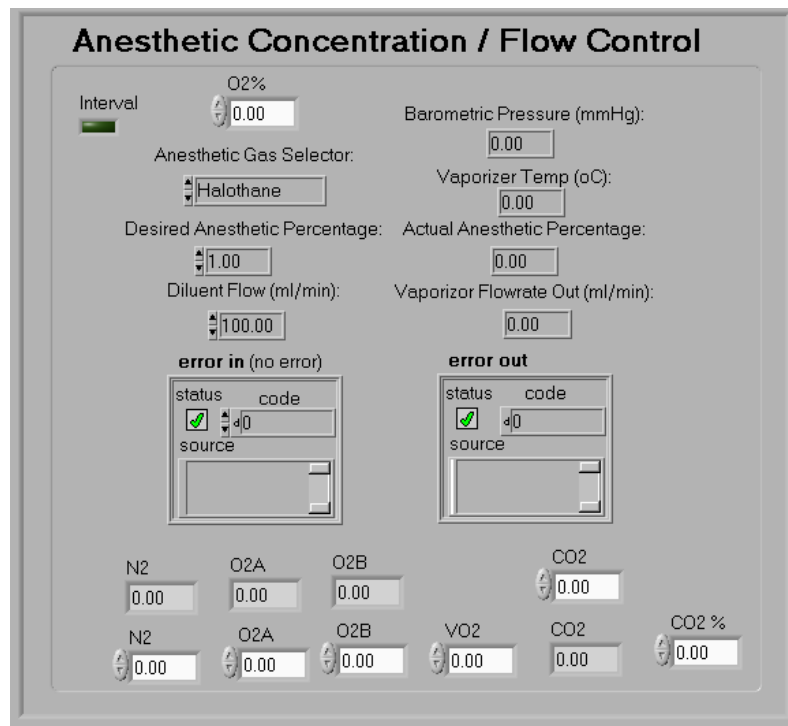
3.3. Instrument Control System

3.3.1. Anesthetic Control

The Anesthetic Concentration/Flow Control VI is able to monitor the gas flow valves and calculate the correct flow rates to obtain the requested anesthetic percentages (*figure 3.3-1*). This VI takes advantage of two major sub-VIs, Anesthetic Calculator and Basic Gas Mixer (*figure 3.3-3 (a) box (1) and (2) respectively*), to perform the majority of the calculations and act primarily as the input point for the user.



(a)

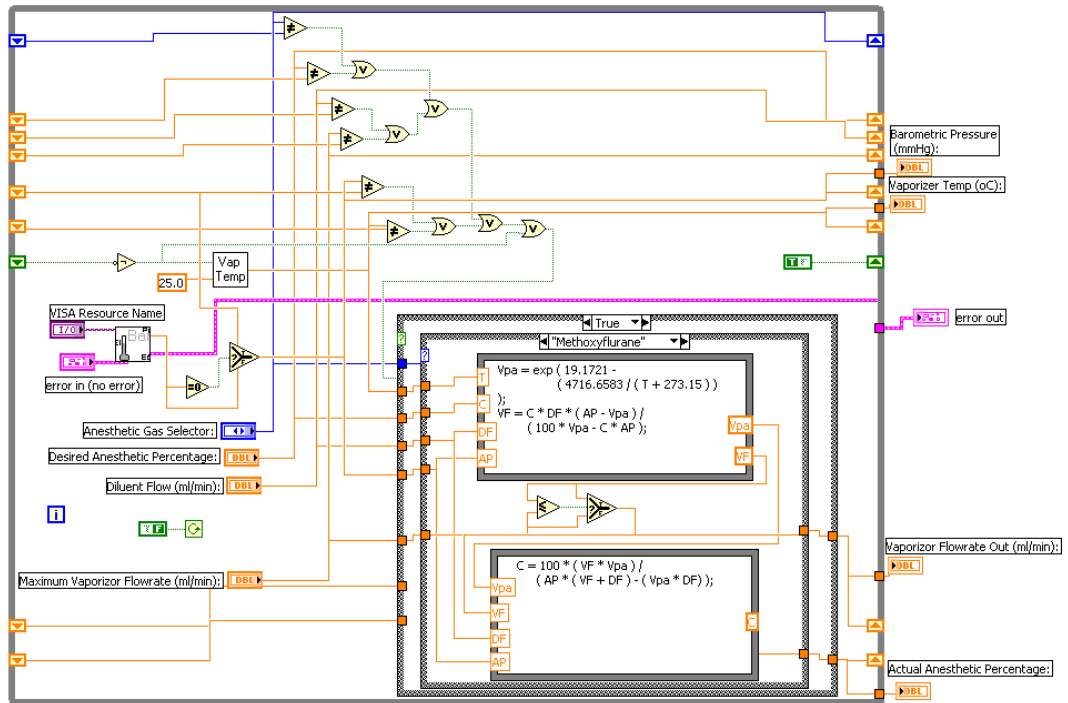


(b)

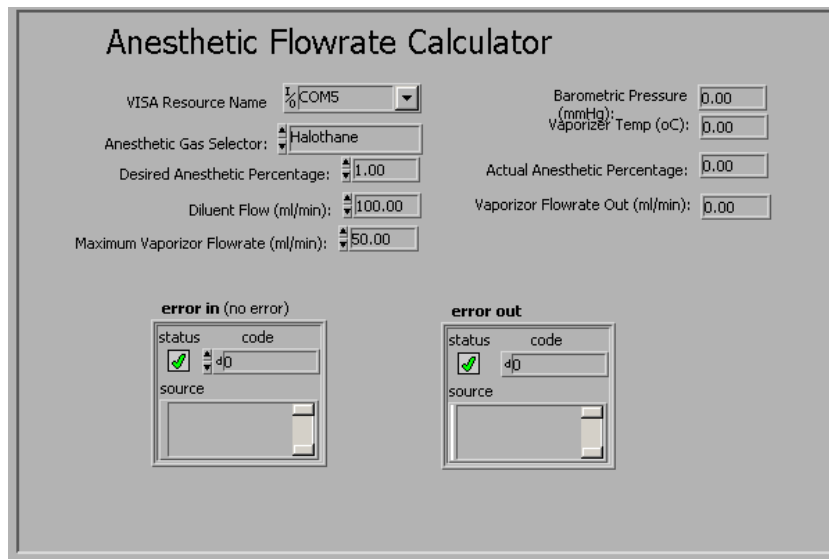
Figure 3.3-1: Anesthetic Concentration / Flow Control VI block diagram (a), showing the Anesthetic Calculator (box1) and the Basic Gas Mixer (box 2) VI, and front panel (b).

The Anesthetic Flow Rate Calculator VI (*figure 3.3-2*) is designed to take the user input values sent to it by the Anesthetic Concentration/Flow Control VI and environmental conditions, including barometric pressure and the internal temperature of the copper kettle vaporizer, to calculate the correct flow rates for the nitrogen (N₂, flow rate 0 –500 ml/min), oxygen A (O₂A, flow rate 0 –100 ml/min), oxygen B (O₂B, flow rate 0 –100 ml/min), vaporizer (VO₂, flow rate 0 –50 ml/min) and carbon dioxide (CO₂, flow rate 0 –50 ml/min) flow meters and send them to the “Basic Gas Mixer” VI. The VI is also designed to evaluate the input and environmental parameters so that new flow values are only sent on to the next section if a change has taken place, saving processing time.

The Basic Gas Mixer VI communicates with each individual flow meter used in the laboratory (*figure 3.3-3 (a) and (b)*). A read VC and write VC for each of the flow meters (N₂, O₂A, O₂B, VO₂ and CO₂) are used to allow the VI to set the desired rate and read the actual rate. If the actual does not match the set values an error message is generated and displayed on the user interface.



(a)



(b)

Figure 3.3-2: Anesthetic Flow rate Calculator VI block diagram (a) and front panel (b). (Based on work done by Dr. Ross Shonat).

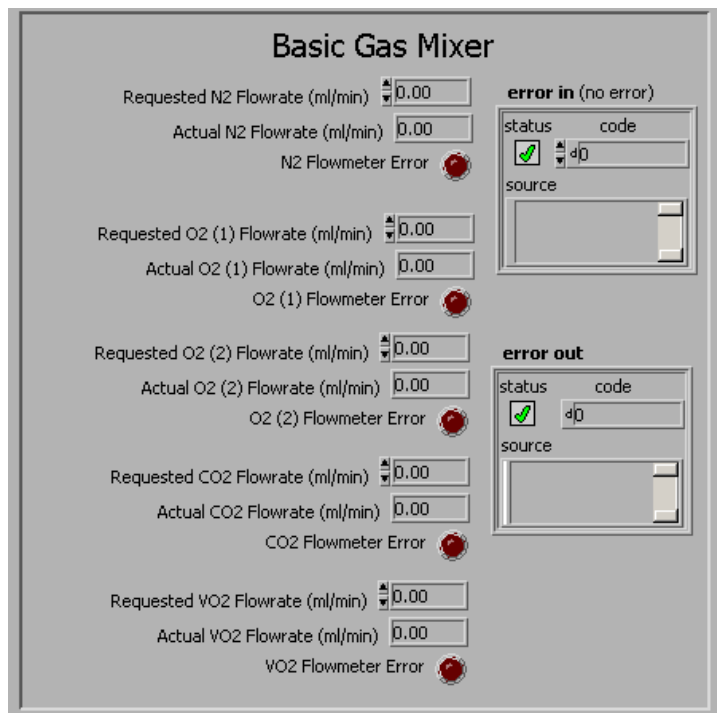
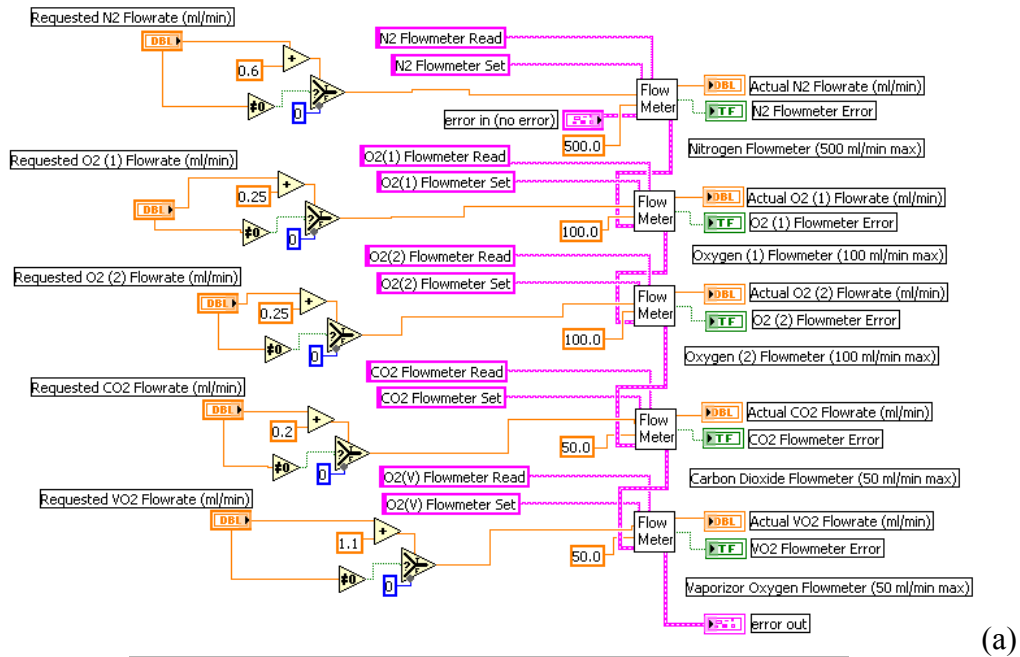


Figure 3.3-3: Basic Gas Flowmeter VI block diagram (a) and front panel (b). (Based on work done by Dr. Ross Shonat).

3.3.2. Ventilator Control

The Ventilator Control VI (*Figure 3.3-4*), designed primarily by a previous researcher Amanda Kight, had slight changes made to the input/output structure to allow for the integration of the VI with the new interface. This VI provides the user with control of such ventilator parameters as respiratory rate, tidal volume and I/E ratio as well as starting and stopping the ventilator.

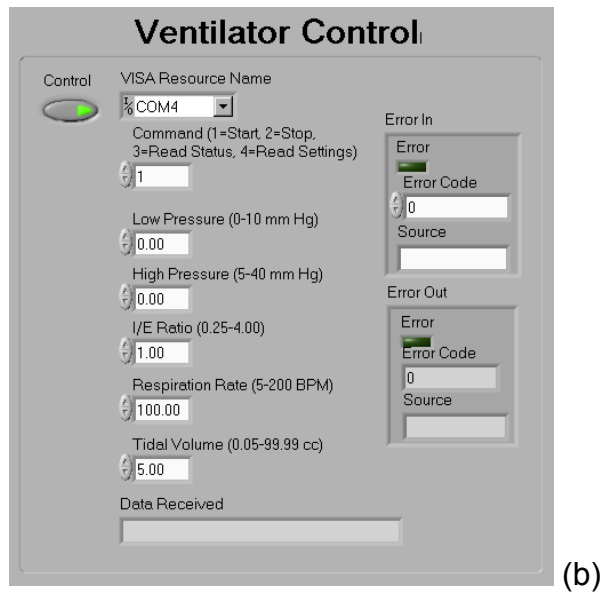
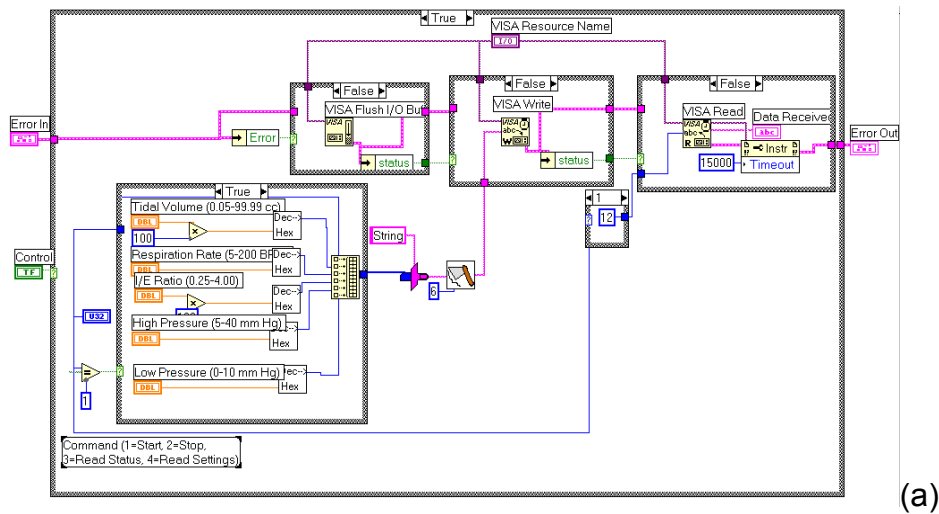
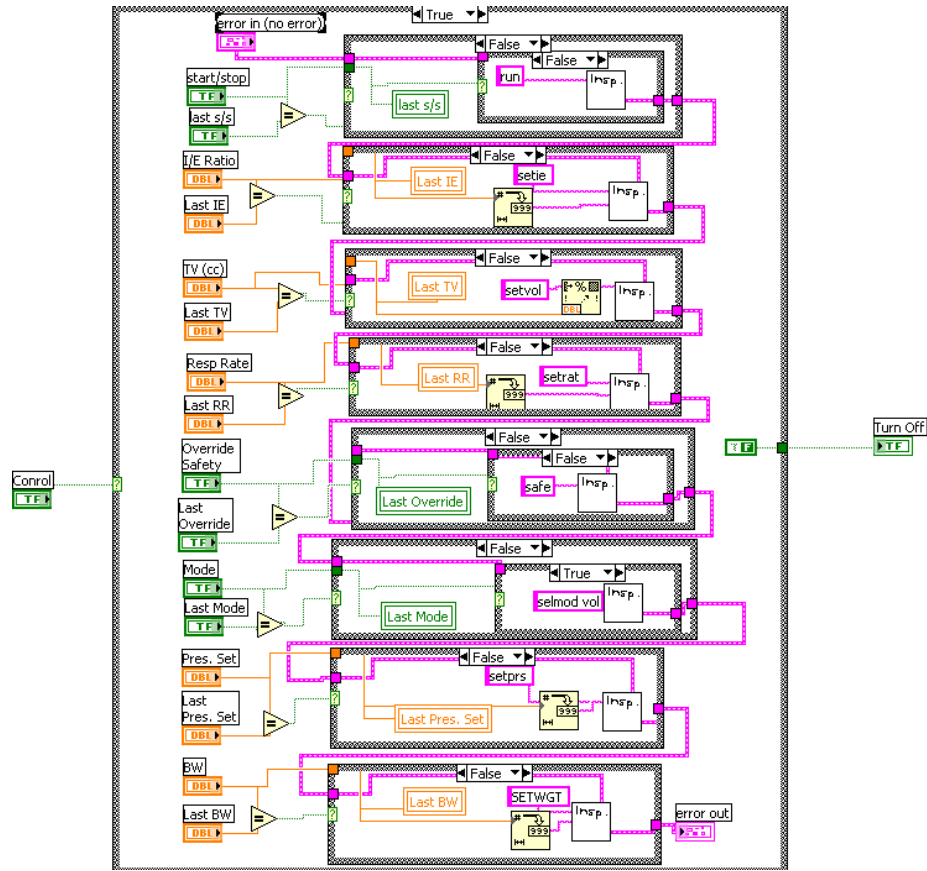
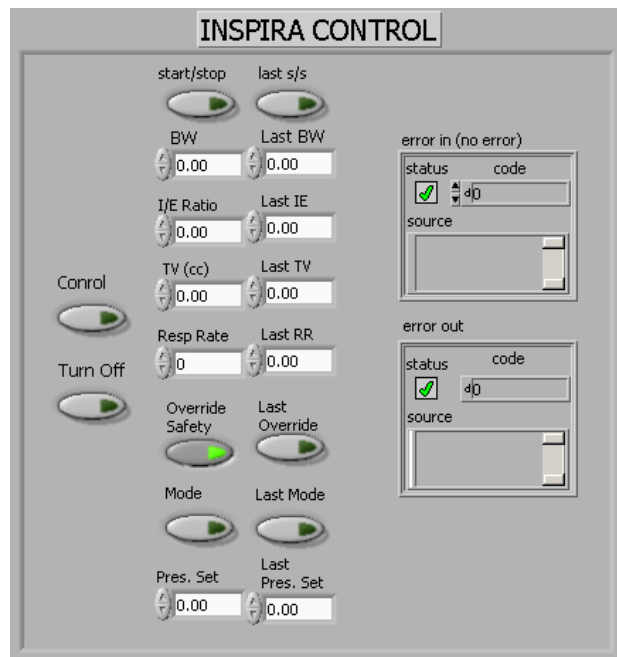


Figure 3.3-4: The Ventilator Control VI block diagram (a) and front panel display (b). (Based on work done by Amanda Kight).



(a)



(b)

Figure 3.3-5: Inspira Control VI Block diagram (a) and front panel (b).

The Inspira Control VI is able to control the Harvard Apparatus Inspira ventilator (*figure 3.3-5*). A list of ASCII commands are provided by the manufacturer and used as the basis of the control VI. The VI is designed to identify a change in the user settings and in response send the corresponding ASCII code to the ventilator via an RS/232 connection.

3.3.3. Body Temperature Control

In an attempt to develop a more elegant solution to the control of body temperature, within a +/- 0.5 °C range from the set point, a duty cycle based simple control system is used. The existing laboratory setup for the control of the animal's core body temperature consists of a circulating warm water bath/blanket with a computer-controlled solenoid valve controlling the flow, either allowing water to flow through the blanket or bypass the blanket entirely. The VI shown in *figure 3.3-6* assesses the difference between the current body temperature and the set point temperature and, depending on what range the difference in temperature falls in, assigns a duty cycle value (0 to 100 %). The system is designed to bring the animal's temperature rapidly to the set point with minimal overshoot. A summary of the ranges and their corresponding duty cycles is shown in *table 3.3-1*.

Temperature Difference (Set Point – Measured)(°C)	Duty Cycle
< 0	0%
0 – 0.25	25%
0.26 – 1.0	50%
1.0 – 3.0	66%
> 3.0	100%

Table 3.3-1: Summary of temperature difference ranges and the corresponding duty cycles

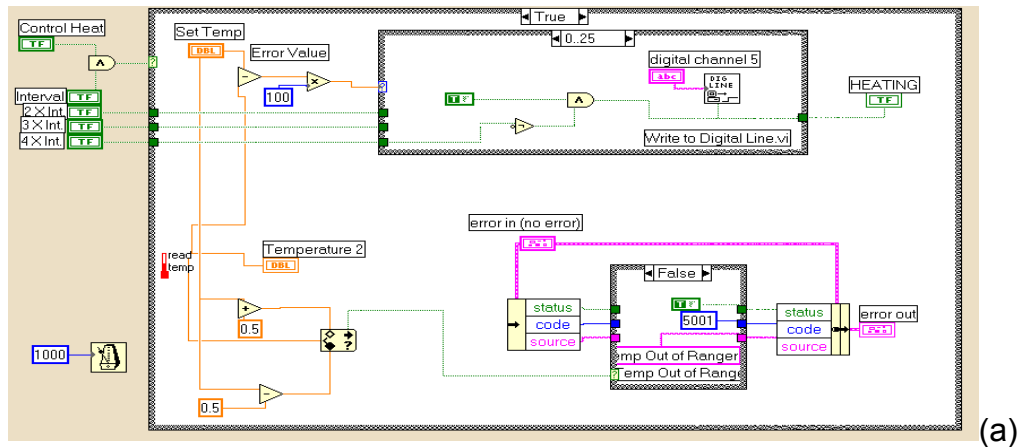


Figure 3.3-6: The water bath control VI block diagram (a) and front panel display (b).

The Duty Cycle VI provides the entire system with a series of Boolean controls that control the activity and acts as a time interval control (*figure 3.3-7*). The VI takes advantage of the iteration count in combination with a set delay function to create a repeatable time interval count. A user input is incorporated into the VI to allow for adjustment of the time intervals for greater flexibility and increased functionality.

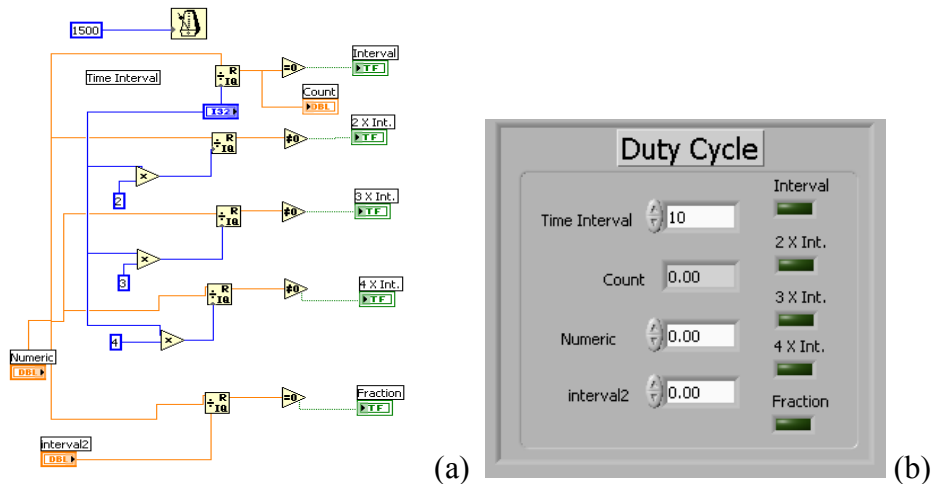


Figure 3.3-7: Duty cycle VI block diagram (a) and front panel (b)

3.4. Fuzzy Logic Control Systems

As discussed in the background section, both traditional and fuzzy logic controls have advantages and disadvantages that must be considered carefully. The advantage of the traditional control approach is that it is a time tested and proven method of producing an accurate and stable control system that is robust to outside stimuli. The major disadvantage of traditional control systems is their dependence on the accuracy and stability of the mathematical model they are based upon. For the control of anesthesia, the test subject's physiological response to the anesthetic or ventilation settings is modeled to predict the affects of changes to these parameters. To achieve a more accurate and robust control system, a multitude of parameters must be taken into account. The need for multiple inputs to improve accuracy makes the system susceptible to being adversely affected if one of the input parameters is lost or is not being monitored. This reduces user flexibility.

Fuzzy logic, on the other hand, models the decision making of an expert. For the control of anesthesia the modeling of the anesthetist rather than the test subject's physiology has many advantages. Some of the noted advantages to modeling the decisions of the anesthetist rather than the test subject's physiology are:

- “Human physiology is complex, and more difficult to model than the decision making process of the anesthetist,
- The variation between and within patients is much larger than the variation in decisions between and within anesthetists,
- A patient model cannot directly tell us what information is relevant to the anesthetist, whereas an anesthetist model can.” (De Graaf *et al* 1997)

Another advantage of fuzzy logic control is the ability to subdivide the control systems to produce a system in which the individual parameters are independent of each other. This subsystem approach allows for the development of a complex control system that is made up of fairly simple parts and has the ability to continue to function if there is an error in one of the parameter control systems. The most notable disadvantage to the use of fuzzy logic controls is that the system is only as accurate as the knowledge base it is developed from. **Table 3.4-1** provides an overview of the pros and cons for both control approaches.

To achieve a more flexible, accurate and easily implemented control system, the fuzzy logic approach was used for the BP and CO₂ control sub-systems in this application. The use of fuzzy logic control, rather than traditional control, was based on the pros and cons of the two approaches outlined in **table 3.4-1** and the success of the work done previously using this strategy (Apshari *et al* 1994, Becker *et al* 1997, Dojat

1997, Graaf *et al* 1997, Held *et al* 2000, Linkens 1999, Lowe *et al* 1999, Meier *et al* 1992, Shing *et al* 1999).

	TRADITIONAL CONTROL	FUZZY LOGIC CONTROL
PROS	<ul style="list-style-type: none"> • Time tested and proven • Accurate/Stable • Can compensate for outside stimuli 	<ul style="list-style-type: none"> • Models Anesthetist decision making • Gives direct output • Easily implemented • Shown to be affective for anesthesia control in past research (animals/humans) • Can be subdivided into independent parameter control
CONS	<ul style="list-style-type: none"> • Accuracy and stability is dependent on model accuracy • Reduced user flexibility to monitor parameters independently • Model of physiology is highly complex • Implementation can be difficult 	<ul style="list-style-type: none"> • Fairly new approach • Only as accurate as the knowledge base used

Table 3.4-1: Pros and Cons of the traditional and fuzzy logic approach to anesthesia control.

3.4.1. Blood Pressure

As discussed previously, there are three major sections to a fuzzy logic BP control system, the fuzzification, inference and defuzzification sections. The fuzzification process is achieved primarily by developing a set of membership functions. The fuzzification membership functions developed for this project are based primarily on a fuzzy logic system developed in earlier work for the control of human anesthetic depth (Meier 1992). The equation that defines the membership functions used in this research was as follows:

$$N = \exp(-K(Z - L))$$

N = Membership value

K = Width of the bell

Z = Input value

L = Shifting with reference to zero

Due to the differences in the anesthetic being used here, halothane instead of isoflurane, and the physiological differences between humans and rodents, the membership functions and rule base were altered during preliminary testing to ensure accurate output values, resulting in the rule base shown in *table 3.4-2* (Meier *et al* 1992). These alterations consisted of an increase in the offset from zero for the NB, NS, PS and PB rules for preliminary testing and the addition of a correction in the output rule base to allow for user specified reaction intensity (i.e. a lower correction value translates to a less intense reaction). These changes made to the variables are based on observations made in the laboratory.

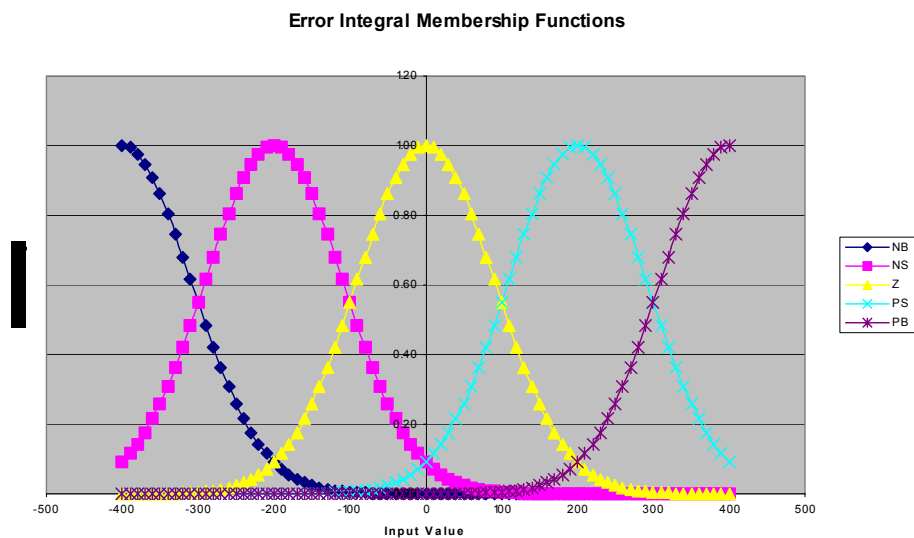


Figure 3.4-1: Preliminary membership functions for blood pressure control system.

Two input values are used for the BP control system, error (E), defined as the difference between the actual mean arterial blood pressure (MAP) value and set MAP value, and the integral of the error (IE), defined as the integral of the error value over 10 time intervals. The IE value is present in the system to compensate for any transients in the E value, ultimately producing a more stable robust system. The two input values are fit to two separate sets of membership functions based on the above equation (*figure 3.4 - I*) and the location of the input value on each of the membership curves is noted to assign a membership value for each input rule.

INPUT			OUTPUT	
Rule	E (Measured - Set)	IE (Integral Error)	Rule	Output
NB	-40	-400	Z	Set - (2 * correction Value)
NS	-20	-200	BS	Set - correction Value
Z	0	0	S	Set
PS	20	200	AS	Set + Correction Value
PB	40	400	VS	Set + (2 * Correction Value)

Table 3.4-2: Pressure controller rule base definition summary.

Once values are assigned to the two sets of input rules, for E and IE inputs, the inference process is used to obtain a single set of output rule values. This is achieved using a standard set of fuzzy logic inference operations, shown below, where Z, BS, S, AS and VS are the output rules (*see table 3.4-2*).

$$Z = \text{MAX} (\text{NBE}, \text{NBIE})$$

$$\text{BS} = \text{MAX} [\text{NSE}, \text{MIN} (\text{ZE}, \text{NSIE})]$$

$$\text{S} = \text{MIN} (\text{ZE}, \text{ZIE})$$

$$\text{AS} = \text{MAX} [\text{PSE}, \text{MIN} (\text{ZE}, \text{PSIE})]$$

$$\text{VS} = \text{MAX} (\text{PBE}, \text{PBIE})$$

Where E and IE denote which input value the rule pertains to.

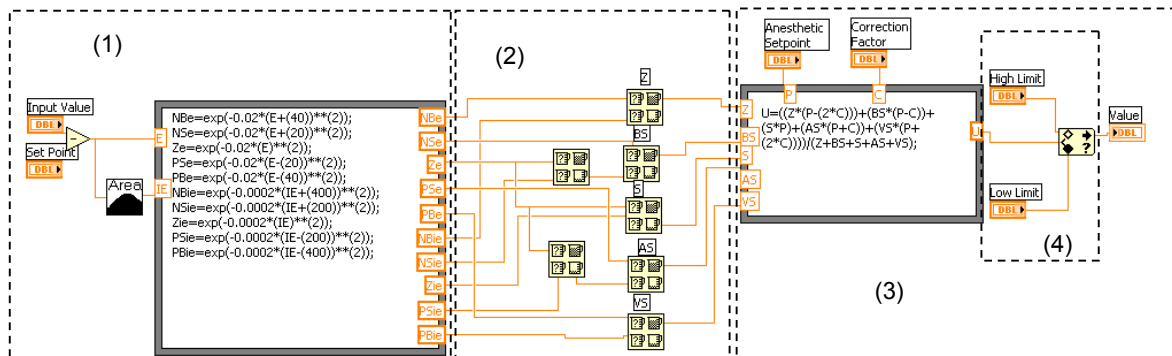
After the inference process is completed and values are assigned to each of the output rules, a crisp value for the anesthetic level using the defuzzification process is produced. A standard defuzzification operation is shown below,

$$\text{Crisp Output Value} = \frac{[(Z*(A-2C)) + (BS*(A-C)) + (Z*A) + (AS*(A+C)) + (VS*(A+2C))]}{Z + BS + S + AS + VS}$$

where A = anesthetic set point, and C = user defined correction value which must be determined by an experienced anesthetist.

The Blood Pressure Control VI shown in **figure 3.4-2** is based on the above calculations. The fuzzification process is achieved using a formula node that represents the membership functions and outputs a membership value for each of the input rules (**figure 3.4-2 box (1)**). The inference process is achieved using a series of Min/Max VI sequenced to duplicate the fuzzy logic inference operation stated previously. (**figure 3.4-2 box (2)**). The defuzzification process is completed using another formula node which takes in the output rule values obtained from the inference process and outputs a single crisp value (**figure 3.4-2 box (3)**). Safety limits are present in the VI to ensure that the system does not adjust the anesthetic level outside the limits that are defined by the user (**figure 3.4-2 box (4)**). The correction values, pressure set point, anesthetic set point upper and lower limit values are left as input values to provide flexibility to the user. The

actual MAP value is calculated using the Mean Arterial Pressure VI, which is designed to use the maximum (systolic) pressure and minimum (diastolic) pressure values obtained from the waveform processing section (*figure 3.4-3*).



(a)

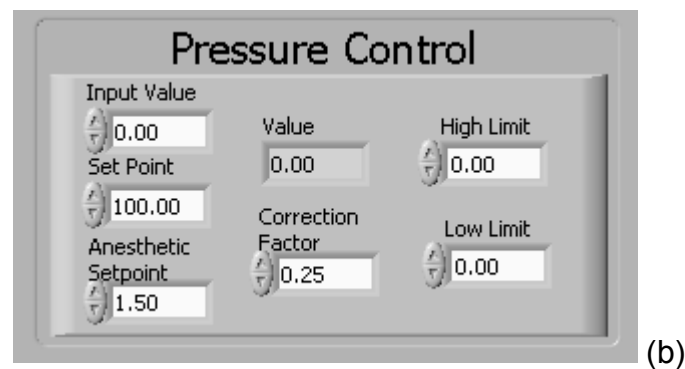
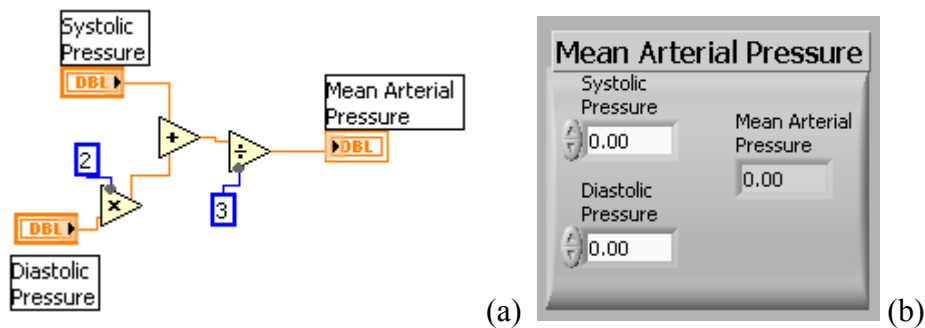
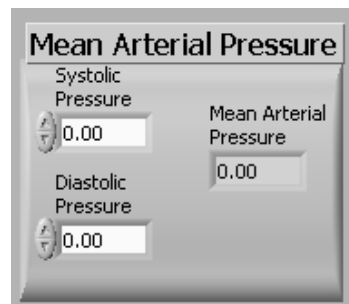


Figure 3.4-2: Blood Pressure Control VI block diagram (a) showing the fuzzification, inference, defuzzification operations and the safety limits (boxes 1, 2, 3 and 4 respectively) and front panel display (b).



(a)



(b)

Figure 3.4-3: Mean Arterial Pressure VI block diagram (a) and front panel (b)

3.4.2. End Tidal CO₂ Control

As with the pressure control system, the CO₂ control system is comprised primarily of the three major processing steps of fuzzification, inference, and defuzzification. But, unlike the pressure control system, the CO₂ control system presented a unique challenge because of a lack of previous work done on controlling CO₂ levels in anesthetized rodents. Because of this, the membership function sets required for the fuzzification process were based primarily on observations performed in the laboratory. These observations and available physiological data for both humans and animals indicated that the relationship between the change in respiratory rate/tidal volume and change in ET_{CO₂} was linear (*figure 3.4.4*). Therefore, the mathematical relationship that produces the desired linear membership functions (*figure 3.4-5*) is shown below:

$$N = \text{MAX} (0, (1 - \text{ABS}(Z - L)))$$

N = Membership value

Z = Input value

L = Shifting with reference to zero

Five membership functions were used per input based on optimization studies done during previous research (Meier *et al* 1992).

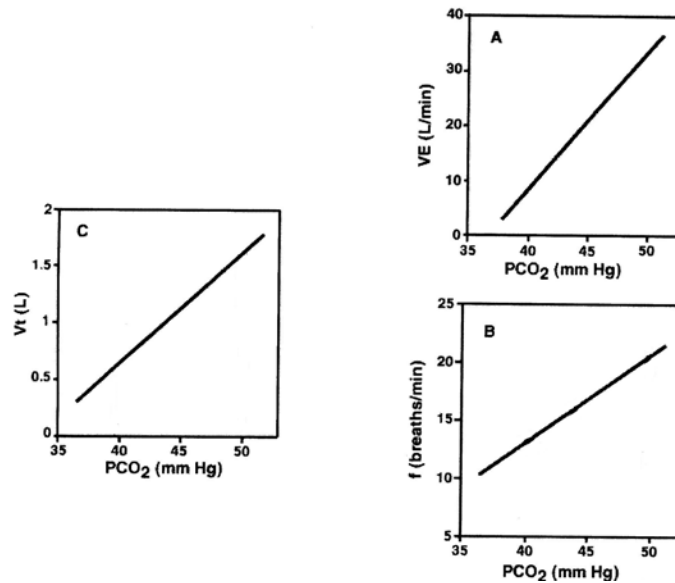


Figure 3.4-4: Plots of (A) increased ventilation with increased pCO₂ levels, due to (B) increased RR and (C) increased TV (Letsky 1992) .

The two input parameters for this system are E and IE, where E is defined as the difference between the actual %CO₂ measured by the micro-capnometer and the set %CO₂ value, and IE is defined as the integral of the E value over 10 time intervals. There were two major output parameters identified for the control of CO₂, Respiration rate (RR), the rate at which the animal's lungs are inflated and deflated, and tidal volume (TV), the volume of gas that is forced into the lungs with each breathe.

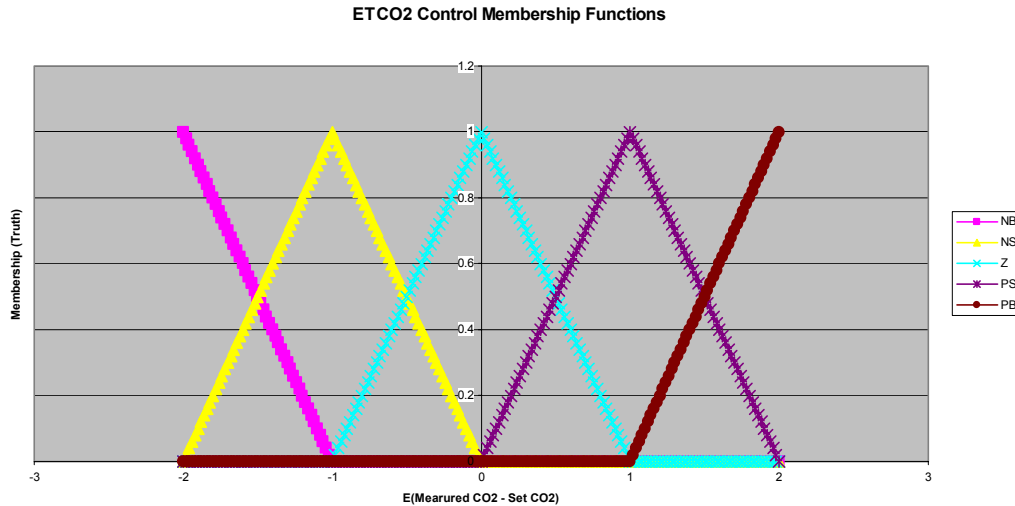


Figure 3.4-5: Fuzzification membership functions for the *E* input rule base.

The linear relationship between O_2 concentrations and the RR and TV are used as the basis for the control system output rule base (*table 3.4-3*), resulting in a more drastic increase in TV/RR for more drastic changes in $ETCO_2$. In order to simplify the action of the control system, a scaling factor approach was adopted for the output rule set. The scaling factor allows for the development of a single output rule set and single crisp output value used to scale the set point values of RR and TV. Once the output rule set is established, it is possible to develop a set of inference operations (shown below) to convert the values assigned to the input rule sets into values for the output rule set (*see table 3.4-3*).

$$Z = \text{MAX} (NBE, NBIE)$$

$$BS = \text{MAX} [NSE, \text{MIN} (ZE, NSIE)]$$

$$S = \text{MIN} (ZE, ZIE)$$

$$AS = \text{MAX} [PSE, \text{MIN} (ZE, PSIE)]$$

$$VS = \text{MAX} (PBE, PBIE)$$

Where *E* and *IE* denote which input value the rule pertains to.

INPUT			OUTPUT	
Rule	E (Measured - Set)	IE (Integral Error)	Rule	Output
NB	-2	-20	Z	Set – (0.5* correction Value)
NS	-1	-10	BS	Set – (0.25*correction Value)
Z	0	0	S	Set
PS	1	10	AS	Set + Correction Value
PB	2	20	VS	Set + (2 * Correction Value)

Table 3.4-3: ETCO₂ controller rule base definition summary.

After the inference process is completed and values are assigned to the each of the output rules it is possible to obtain a crisp value for the scaling factor using the defuzzification process. Using a standard fuzzy logic defuzzification operation and the following was obtained (C = Correction Value).

$$\text{Output} = \frac{((Z*(1-(0.5*C)))+(BS*(1-(0.25*C)))+(S*1)+(AS*(1+(C)))+(VS*(1+(2*C))))}{Z + BS + S + AS + VS}$$

An additional processing step was added to the system after noting an effect of the animal's pO_2 value on the ventilation (TV and RR) values (**figure 3.4-4**). The additional processing step allows the user to enter the animal's pO_2 obtained from a manual blood gas measurement. The value of the pO_2 entered by the user is used to scale the correction factor, resulting in a variable adjustment of RR and TV depending on the pO_2 value entered. A summary of the pO_2 ranges and the scaling associated with them is shown in **table 3.4-4**. A default value of 100mmHg is automatically entered into the pO_2 field if no measured pO_2 is entered by the user.

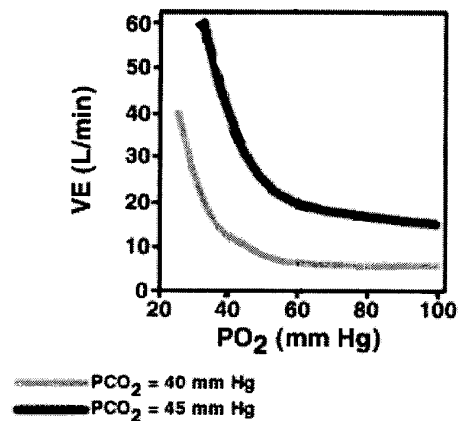


Figure 3.4-6: Graph showing the change in ventilation due to changes in oxygen concentration (Letsky 1992)

PO ₂ Range (mmHg)	Scaling
49 and lower	2* Correction Value
50 - 74	1.5*Correction Value
75 - 99	1.25* Correction Value
100 and higher	1* Correction Value

Table 3.4-4: Correction value scaling factors for various pO₂ ranges.

The ETCO₂ Control VI shown in *figure 3.4-6* is based on the above calculations. The fuzzification process is achieved using a formula structure that represents the membership functions and outputs a membership value for each of the input rules (*figure 3.4-5 box (1)*). The inference process is achieved using a series of Min/Max VIs sequenced to duplicate the fuzzy logic inference operations stated previously (*figure 3.4-6 box (2)*). The defuzzification process is achieved using another formula structure which takes in the output rule values obtained from the inference process and outputs a single crisp value (*figure 3.4-6 box (3)*). Scaling of the correction value was achieved using a case structure with the pO₂ range as the criteria for which case to use (*figure 3.4-*

6 box (4)). The correction value, CO₂ set point, pO₂, RR set point and TV set point values are left as input values to provide flexibility to the user.

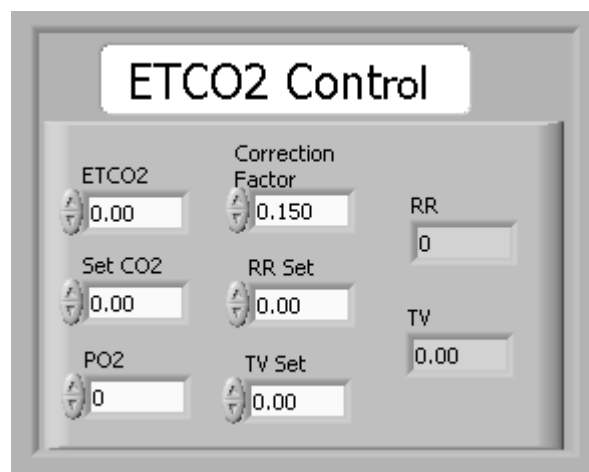
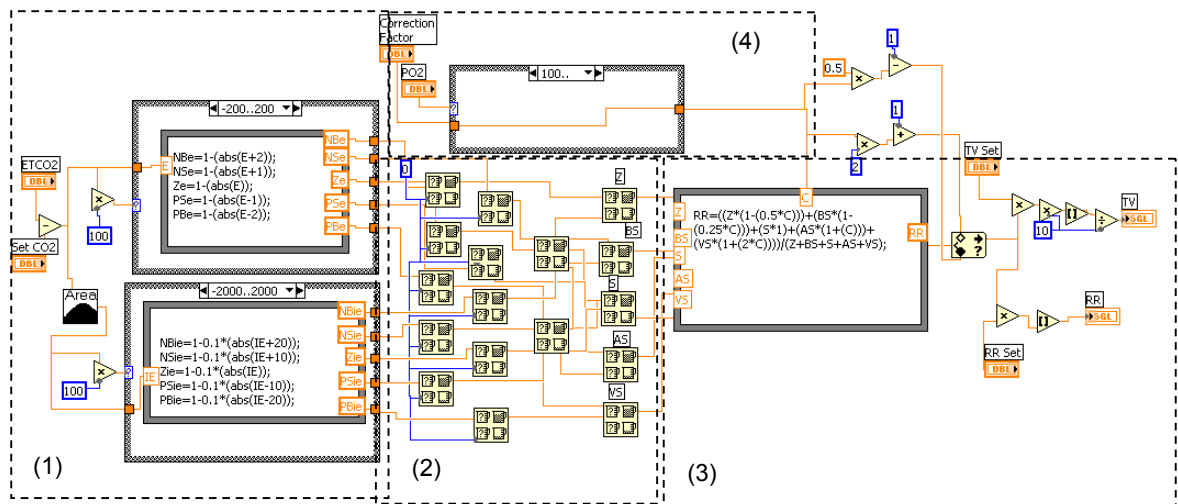


Figure 3.4-7: ETCO₂ Control VI block diagram (a) showing the fuzzification, inference and defuzzification operations (boxes 1, 2 and 3 respectively) and (b) front panel display.

3.5. Data Transfer System

The VI used to automatically write the patient's monitored parameters to a text file, is shown in *figure 3.5-1*. The Write to File VI is also capable of placing markers in

the data and a text description describing the marked event. The event marker capability makes the analysis of the data and the recreation of the events during the procedure more convenient and accurate. An example of data collected using this VI, and its event marking capability, is shown in *figure 3.5-2*.

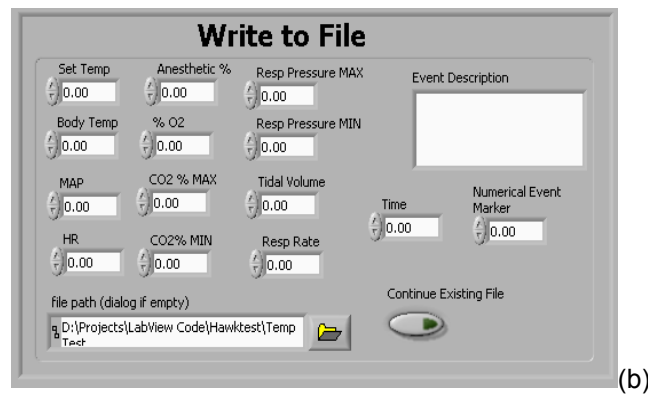
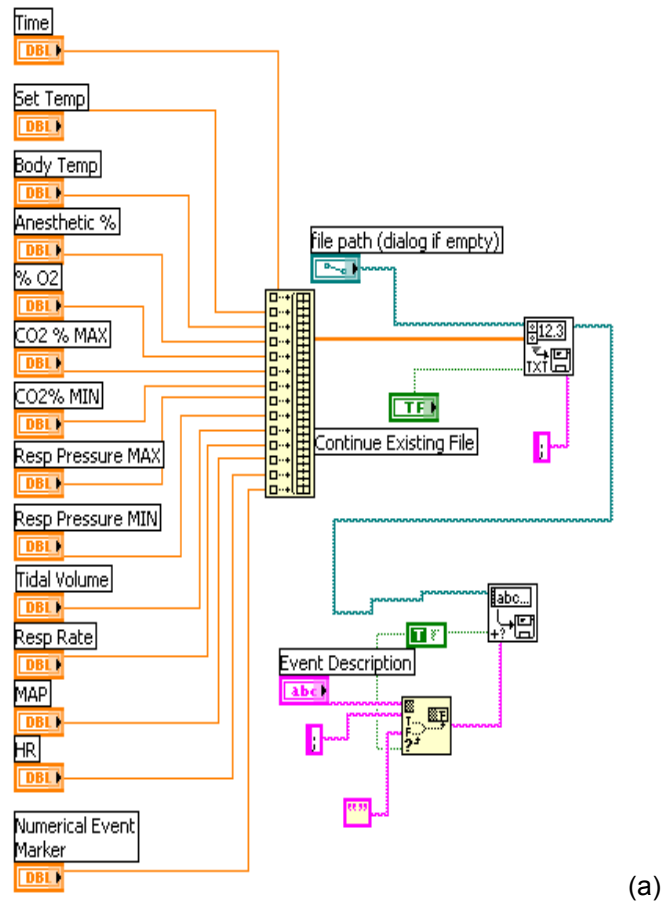


Figure 3.5-1: the Write to File VI block diagram (a) and front panel display (b).

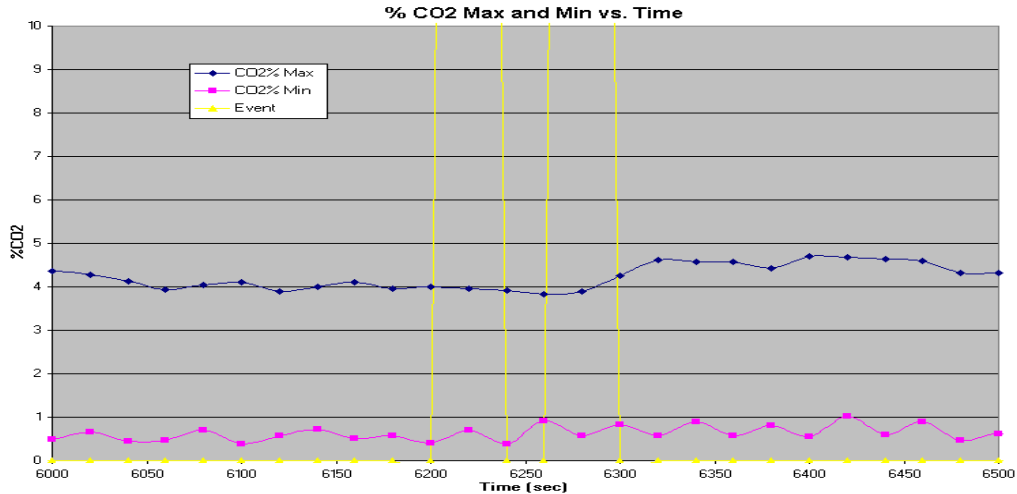


Figure 3.5-2: An example of the data collected using the write to file VI and analyzed using Excel, note the vertical lines indicating a marked event (in this case images being taken).

3.6. User Interface

The User Interface VI is used to provide the user with an easy to use single screen for anesthesia monitoring and control and is created by combining all of the VIs discussed in the previous sections (*figure 3.5-1*). The front panel of this VI is designed to incorporate all of the user-defined inputs and display all of the acquired data and waveforms. In order to ensure that the gathering of essential data and manipulation of key parameters is expedited, the interface is separated into subsets defined by function. These sub-sets include Ventilator Control, Anesthetic Control, Temperature Control, File Transfer, Airway Pressure, ETCO₂ and BP. In addition to these sub-sets, two large waveform displays are incorporated to display airway pressure %CO₂ and BP (*figure 3.5-2*).

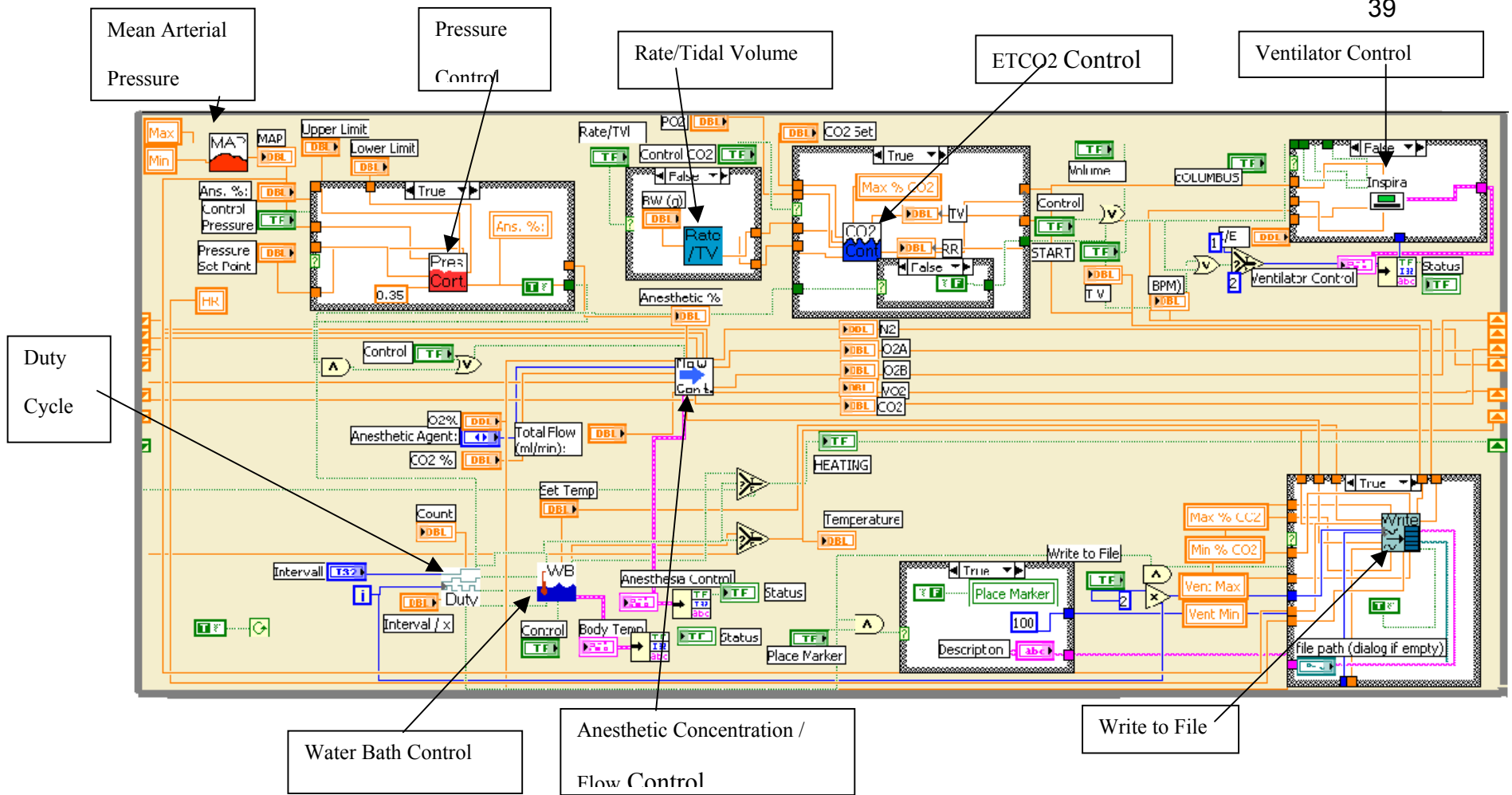


Figure 3.6-1: User interface VI block is made up of the previously discussed VIs

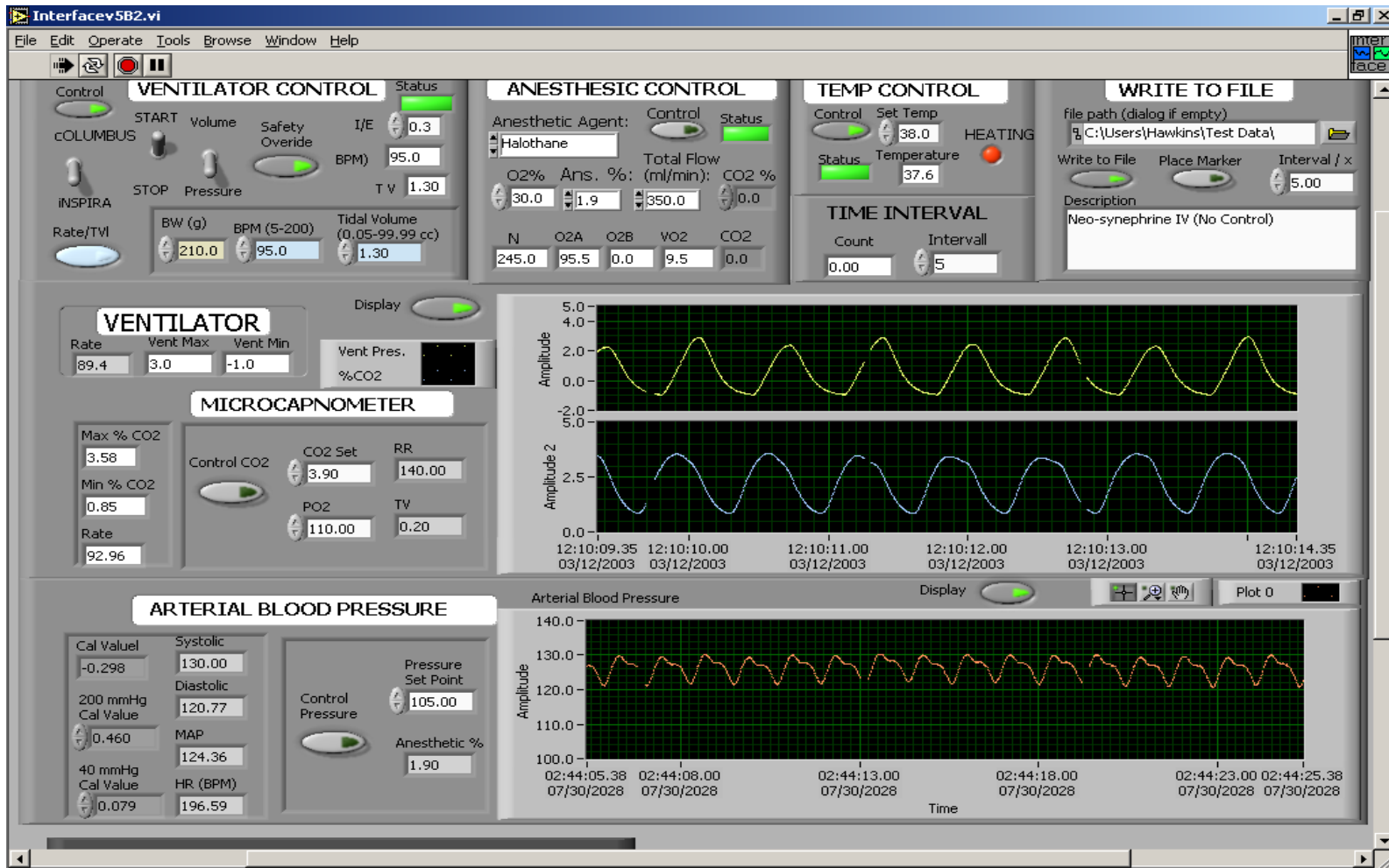


Figure 3.6-2: Interfacev2 VI block diagram (a) and front panel interface (b)

3.6.1. Interface Hierarchy

The following is a block diagram representation of the hierarchy of the VIs used to create the user interface:

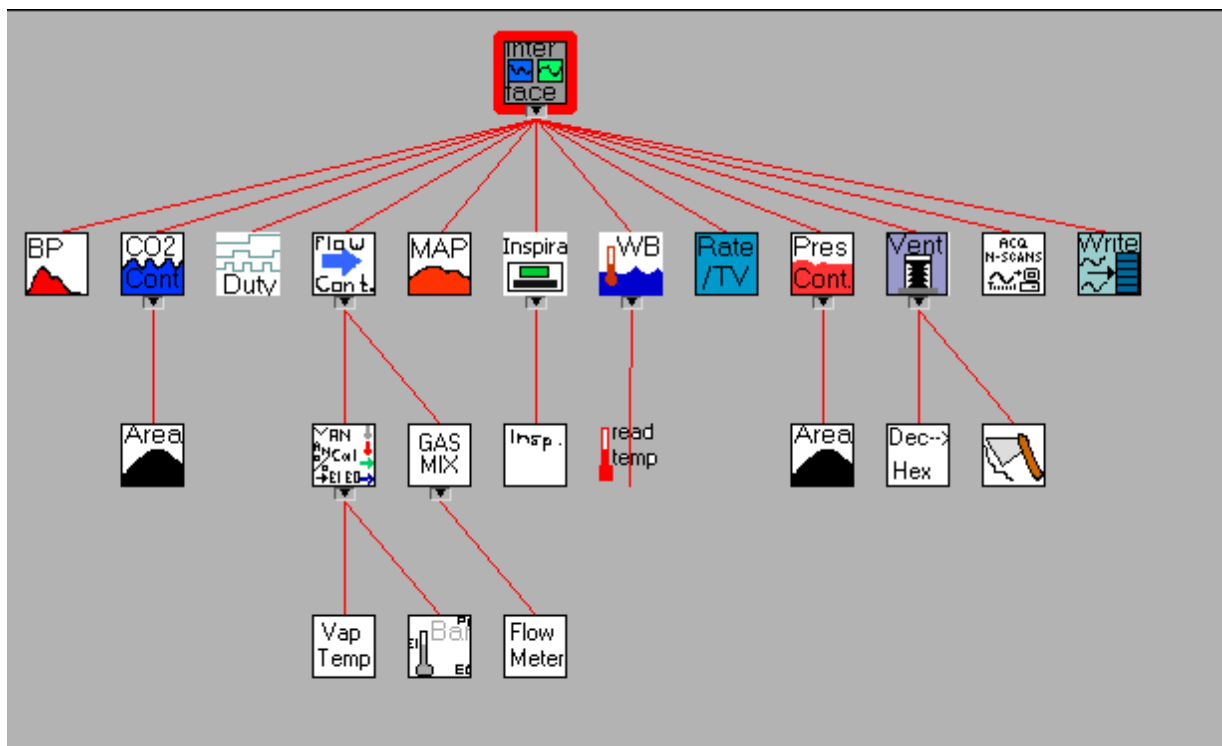


Figure 3.6-3: Block diagram showing the hierarchy of the sub-VIs used to make the interface VI.

4. METHODS

The system that was developed to achieve the goals set forth at the start of this project had to be tested for safety, efficacy and stability. This was achieved using both *in-vitro* and *in-vivo* experiments. The *in-vivo* testing was completed using a total of 10 rats, which underwent both short and long-term perturbation experiments to assess the capabilities of the system. The following sections describe the methods used to complete these experiments.

4.1. *In-Vitro Testing*

In order to test the performance, safety and efficacy of the body temperature control system before it was tested on any animals, a rat phantom was designed and built. It was created using a plastic conical vial filled with distilled water into which the rectal thermometer was placed. The phantom was placed on the heated stage and covered with the heating blanket.

In-Vitro testing of the blood pressure and ETCO₂ control systems was not possible due to a lack of an acceptable rat phantom for these parameters. Though there are mathematical models (rat) that exist that can model the physiological reaction to both anesthetic changes and changes in RR and TV, the interfacing of such models with the existing system was not feasible since the model would have to produce a waveform (analog) output that could be sampled by the system, which is currently not available.

4.2. *In-Vivo Experiments*

The true capabilities of the control systems were tested using live animals that were under continuous monitoring by an anesthetist. The testing consisted of two major

portions; the short-term perturbation tests and the long-term perturbation tests. The testing was separated in this manner to better evaluate the system's stability and ability to regulate in two different time response situations, one which models such events as rapid un-sustained pressure changes due to surgical activity and the other which models long lasting pressure changes due to loss of blood or fluid infusion. During both sets of experiments, the ETCO₂ control system was evaluated, when available. All *in-vivo* experiments were conducted in accordance with the protocols approved by the institutes Institutional Animal Care and Use Committee (IACUC) at the Worcester Polytechnic Institute.

Each rat was anesthetized at the start of experiments using an induction chamber (**figure 4.2-1 (a)**), which was filled with a mixture of N₂, O₂, and halothane saturated O₂. The interface was used to control the concentrations of the gases and monitor the actual flow rates. Once the rat lost consciousness, an anesthesia mask was affixed over its snout allowing for sustained anesthesia while the tracheotomy procedure was completed (**figure 4.2-1 (b)**). While the mask was in place, the halothane concentration was reduced to ~2.5% to reduce the chances of over anesthetization while maintaining depth. The tracheotomy procedure consisted of exposing the trachea via surgical dissection and inserting a Teflon cannula into the trachea. After the tracheal cannula was placed (**figure 4.2-1 (c)**) it was connected to the gas mixture and the animal was allowed to breathe freely until labored breathing was detected by the surgeon or the anesthetist, at which time the ventilator was started with an appropriate respiratory rate and tidal volume chosen based primarily on the animal's body weight.

The placement of the tracheal cannula allowed for the monitoring of %CO₂ by the micro-capnometer. Prior to the beginning of each experiment the micro-capnometer was calibrated using pure N₂ and 5% CO₂ calibration gas. At this point the temperature probe was placed into the rectum of the rat and body temperature control was started (set point of 38 °C). In addition, the Write to File function was activated at this point of the procedure to gather available data at a typical rate of 1 data set / (10 sec), though the sampling rate did vary from experiment to experiment due to changes in the processor and memory load on the computer.

The left femoral vein and artery were exposed via surgical dissection. Once exposed, the left femoral artery was catheterized with Intramedic brand PE50 polyethylene tubing. The catheter was pre-filled with heparinized saline (10 units/ml) to reduce the risk of coagulation during the procedure. The arterial catheter was connected to the pressure transducer, which was calibrated with a sphygmomanometer prior to the start of each experiment (40 mmHg and 200 mmHg calibration points), allowing for BP monitoring. The femoral artery catheter was also used as the withdrawal point for blood gas samples (~0.25 ml blood/sample). The left femoral vein was also catheterized with PE50 polyethylene tubing and used for the administration of fluids and vasoactive drugs.

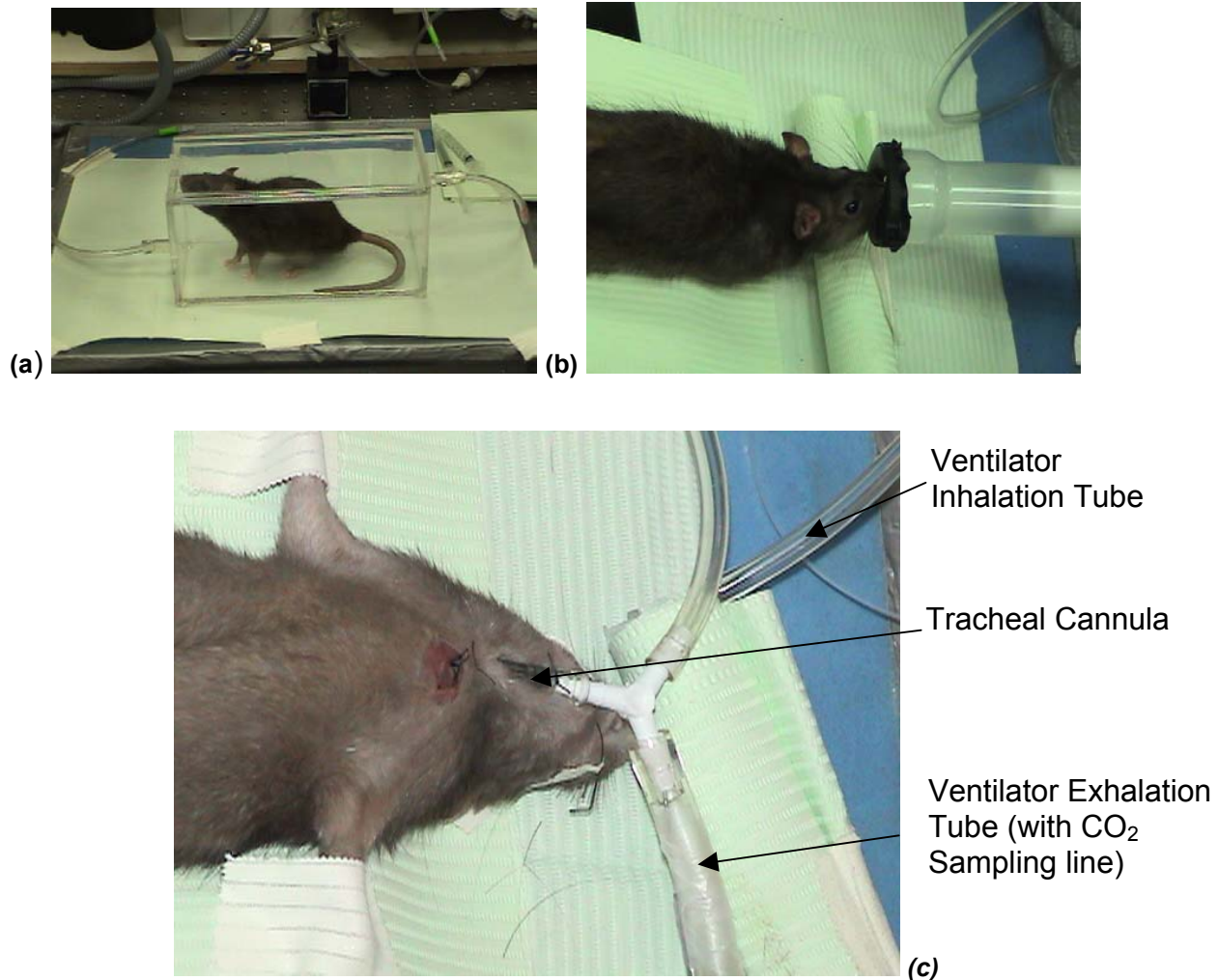


Figure 4.2-1: Digital images of a rat (a) in an induction chamber (b) with the anesthesia mask over its snout and (c) with the tracheal cannula inserted and connected to the ventilator inhalation and exhalation tubing.

4.2.1. Short-term Perturbation

The short-term perturbation tests were performed initially to test the ability of the control system to return the BP to the set level following a short drastic change in BP. In this set of experiments, the BP of the rat was monitored in situations where no control

was present and where automated control was activated. CO₂ was not controlled during this set of experiments due to complications with the ventilator being used at the time.

During this set of experiments, 4 rats (R1 – R4) were tested once they had reached a stable state after being instrumented as previously described. Once a stable state was achieved, a 1 µg injection of epinephrine (0.1 ml of 10 µg/ml epinephrine diluted in sterile saline solution) was administered IA. The order of the controlled or no-control conditions was randomized. After injection, the BP was allowed to reach a stable level before moving on to the next test (time between injections varied greatly between animals).

4.2.2. Long-term Perturbation

Long-term perturbation tests were performed to determine the systems ability to control BP and ETCO₂ during a situation of prolonged pressure fluctuation. These experiments were designed to induce conditions of either hypertension or hypotension to fully access the system. In these experiments, the animal's BP was manipulated using vasoactive drugs. As with the short term perturbation testing, these tests were randomized and performed under both controlled and no-controlled situations. During the long term perturbation experiments, the CO₂ controller was activated in conjunction with the BP controller and deactivated during the no control situation.

During this set of experiments, 6 rats LTP1 – LTP6, were tested once they reached a stable state after being instrumented as previously described. Once a stable physiological state was achieved, the animal was forced into a hypertensive state using a 5 µg/(kg*min) dose of neo-synephrine, a vasoconstriction drug, maintained for a 10-

minute period. The infusion was administered IV in the left femoral artery and a Cole Parmer syringe pump was used to ensure a constant infusion rate. For these experiments the neo-syneprine was diluted to a concentration of 15 $\mu\text{g}/\text{ml}$ in Lactated Ringers Solution (LRS). Controlled and no-control situations were tested.

A hypotensive state was achieved using sodium nitroprusside, a drug that causes vasodilatation, at a dose of 1 $\mu\text{g}/(\text{kg}\cdot\text{min})$ and maintained for a 10-minute period. The infusion was administered IV in the left femoral artery and a Cole Parmer syringe pump was used to ensure a constant infusion rate. For these experiments, the neo-syneprine was diluted to a concentration of 3 $\mu\text{g}/\text{ml}$ in Lactated Ringers Solution (LRS). Again, controlled and no-control situations were tested.

5. RESULTS

5.1. *Body Temperature Results*

The temperature of the rat phantom was monitored and the results of one of these experiments is shown in *figure 5.1-1*. After testing the control system on the rat phantom to ensure safety and stability, the system was tested on an actual rat. The results of one such experiment are shown in *figure 5.1-2*. The control system was able to maintain the temperature of the water within the ± 0.5 °C range throughout several trial runs, and was able to achieve this while ramping to the set point temperature in an acceptable period of time. The control system, once at set temperature (37 °C), stayed within the 0 and 25 % duty cycle regions for the majority of the test runs, meaning that the wear on the solenoid was reduced. The oscillations seen in the temperature over time were estimated to be a result of the heating and cooling of the metal stage and were not further investigated, since the temperature remained within the acceptable range.

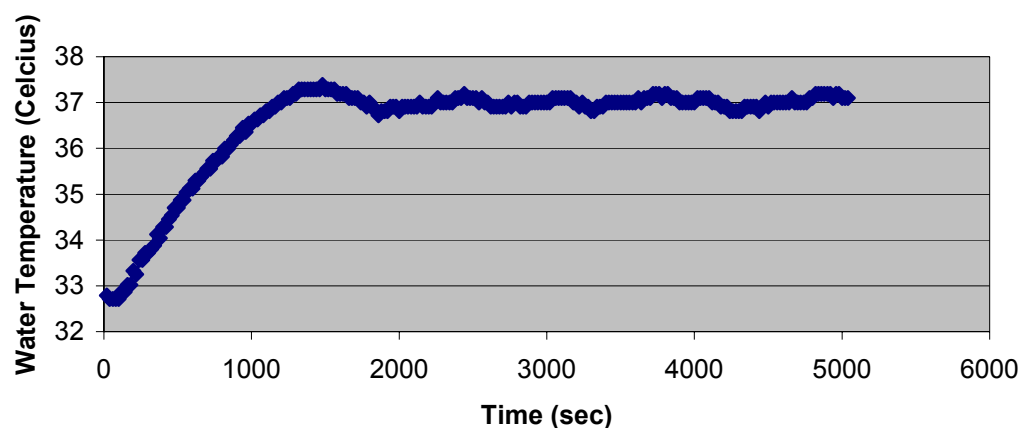


Figure 5.1-1: Test data for control of water temperature in a rat substitute (With a set point of 37 degrees Celsius).

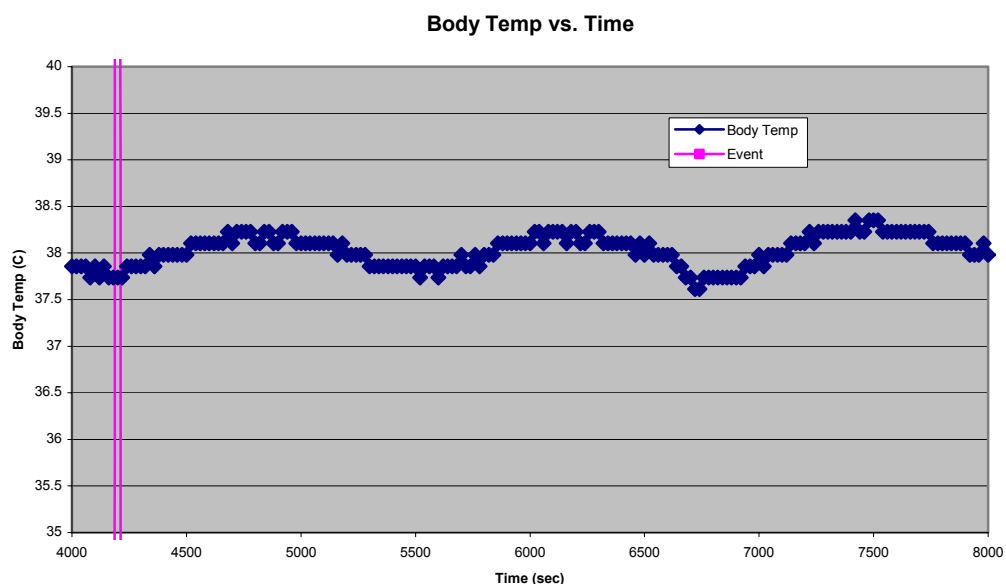


Figure 5.1-2: A sample of the data collected during a preliminary animal procedure (set point Temperature of 38 degrees Celsius).

5.2. Short term Perturbation Results

During the short-term perturbation testing the user interface was set to save data every twenty seconds. The acquired data were saved to a text file and later converted to Excel^R format for further analysis. An example of a resulting data set is shown in *table 5.2-1*. The data pertaining to the epinephrine injections were isolated and the time course was adjusted to reflect the time relative to injection. The adjustment of the time course to relative time allowed for the direct comparison of the physiological reaction before, during and after injection under control and no-control conditions.

The important variables for the evaluation of the control system were identified as the deviation of the measured MAP from the set point (baseline) MAP and the control variable % anesthetic. Due to the natural variation in animals, the MAP deviation value was expressed as a percent deviation from the MAP set point to allow for the direct

comparison of the different animals' data sets. The % MAP deviation was calculated as follows:

$$\% \text{ MAP deviation} = \frac{(\text{Measured MAP} - \text{Set point MAP}) * 100}{\text{Set point MAP}}$$

Once the % MAP deviation was calculated, a plot of the % anesthetic and % MAP deviation vs. time for both the control and no-control conditions was produced for each animal. A representative plot from animal R-1 is shown in *figure 5.2-1& 5.2-2* and the plots for all data yielding animals are included in *Appendix A*. The % anesthetic for the no-control condition was excluded from these plots because it did not change. Of the four animals tested, three animals yielded data for both the control and no-control conditions, while one only yielded data for the no-control condition and was removed from further analysis.

For a statistical analysis of these results, the root mean square (RMS) value of the % MAP deviation for both the control and no control conditions was calculated (for a ~250 seconds interval) A paired t-test analysis was used to determine if there was a significant decrease in the % MAP deviation (as expressed by the RMS values) while under automated control. A summary of the calculated values of RMS and the results of the paired t-test are shown in *table 5.2-2*

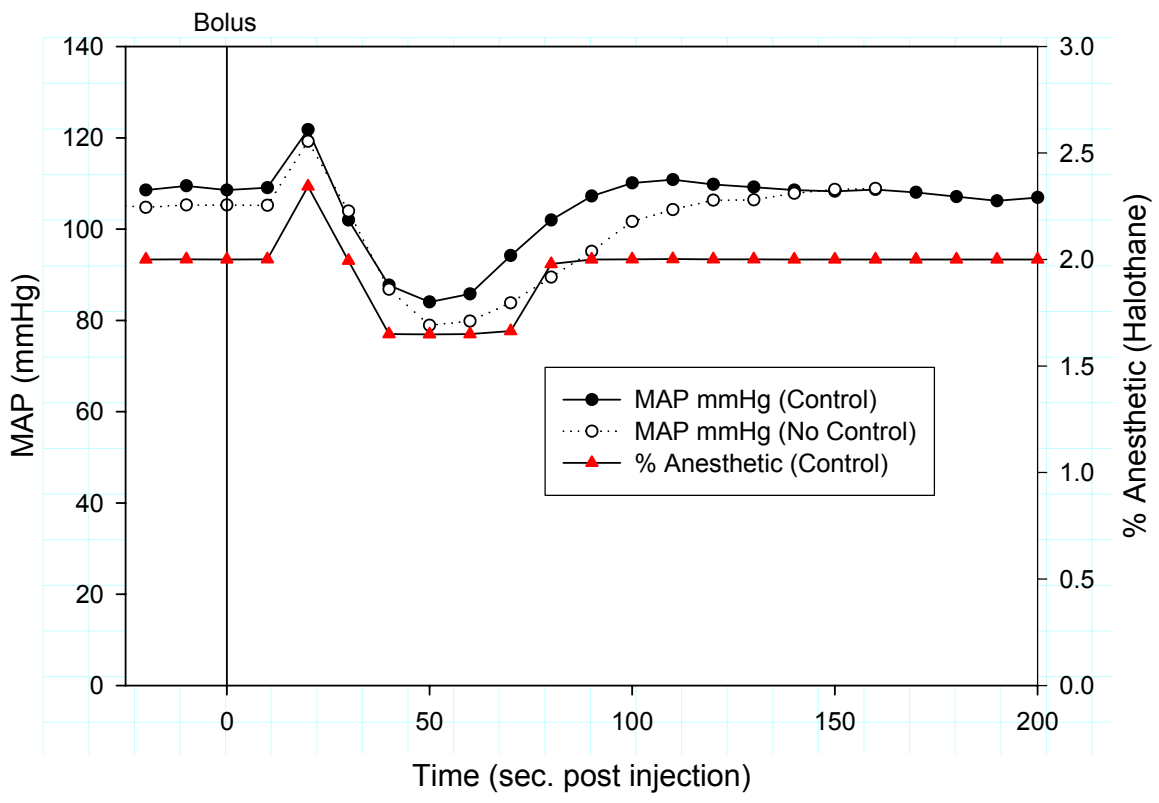


Figure 5.2-1: Animal R-1 epinephrine test data showing MAP under control (closed circles) and no-control (open circles) conditions and % anesthetic (closed triangles) vs. time.

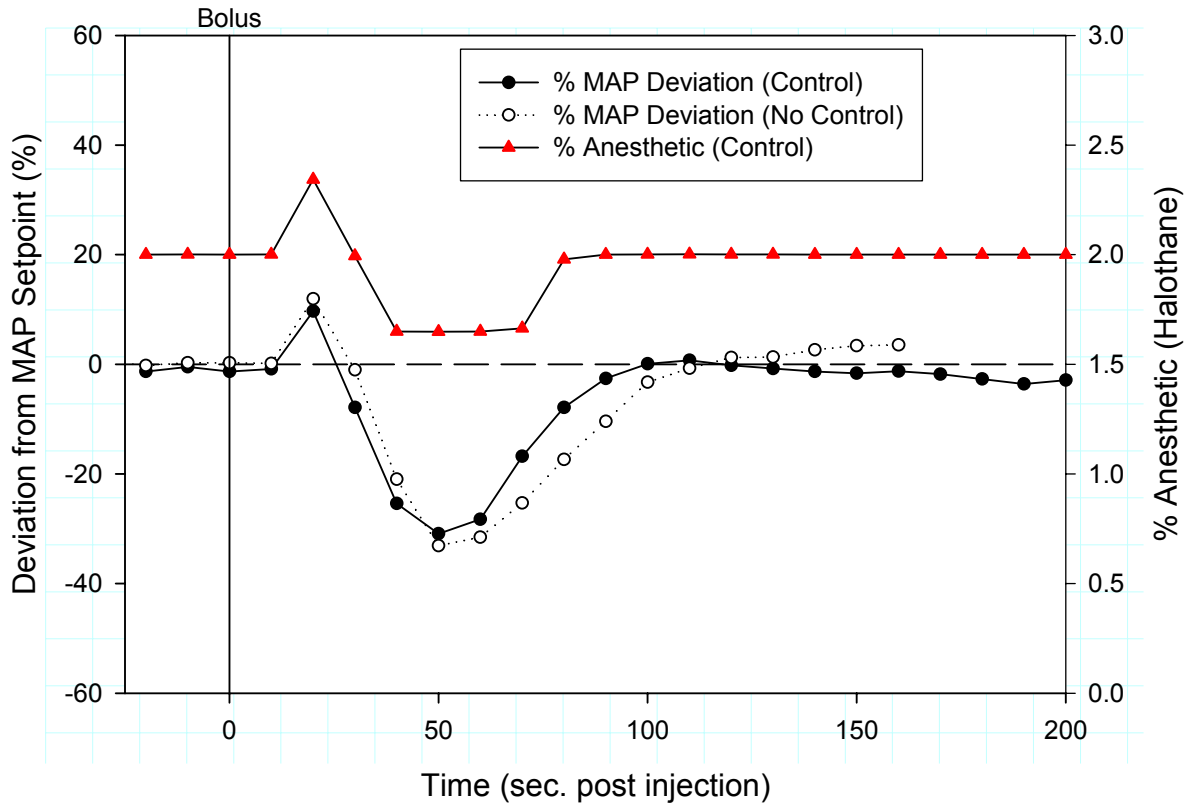


Figure 5.2-2 Animal R-1 epinephrine test data showing % MAP deviation under control (closed circles) and no-control (open circles) conditions and % anesthetic (closed triangles) vs. time.

Animal: R-1 Strain: Sprague Dawley Test: Epinephrine (No Control)													Date: 03/19/03			
Time (post Inj.)	Temp Set (°C)	Actual Temp. (°C)	An. % (Halothane)	O2%	CO2 % MAX	CO2 % MIN	Vent Press. MAX	Vent. Press. MIN	Tidal Volume (cc)	Resp. Rate (BPM)	MAP (mmHg)	Event Marker	Event	Set Pressure (mmHg)	Dev. From MAP	% Dev. From MAP
-180	38	38.10	2.00	32	4.87	1.77	3.51	-1.2	2.7	93	105.06	0	No event	105	0.06	0.06
-170	38	38.10	2.00	32	5.04	1.67	6.64	-1.2	2.7	93	105.06	0	No event	105	0.06	0.06
-160	38	38.10	2.00	32	5.30	1.55	2.05	-1.2	2.7	93	104.96	0	No event	105	-0.04	-0.04
-150	38	38.10	2.00	32	5.34	1.73	5.31	-1.2	2.7	93	105.17	0	No event	105	0.17	0.16
-140	38	38.10	2.00	32	5.36	1.71	5.82	-1.2	2.7	93	105.68	0	No event	105	0.68	0.64
-130	38	38.10	2.00	32	5.56	1.91	5.37	-1.1	2.7	93	104.76	0	No event	105	-0.24	-0.23
-120	38	38.10	2.00	32	5.83	1.78	4.69	-1.1	2.7	93	104.45	0	No event	105	-0.55	-0.53
-110	38	38.10	2.00	32	5.67	2.61	5.65	-1.2	2.7	93	104.96	0	No event	105	-0.04	-0.04
-100	38	38.10	2.00	32	5.83	1.91	5.71	-1.1	2.7	93	104.35	0	No event	105	-0.66	-0.63
-90	38	38.10	2.00	32	5.89	1.75	6.35	-1.2	2.7	93	104.86	0	No event	105	-0.14	-0.14
-80	38	37.98	2.00	32	5.95	1.67	6.22	-1.2	2.7	93	105.06	0	No event	105	0.06	0.06
-70	38	37.98	2.00	32	5.91	1.69	1.12	-1.2	2.7	93	105.78	0	No event	105	0.78	0.74
-60	38	37.98	2.00	32	5.48	1.60	4.06	-1.2	2.7	93	105.68	0	No event	105	0.68	0.64
-50	38	38.10	2.00	32	6.12	1.78	5.32	-1.2	2.7	93	105.58	0	No event	105	0.58	0.55
-40	38	37.98	2.00	32	6.02	2.20	3.65	-1.1	2.7	93	105.68	0	No event	105	0.68	0.64
-30	38	37.98	2.00	32	5.98	1.83	4.25	-1.1	2.7	93	105.47	0	No event	105	0.47	0.45
-20	38	37.98	2.00	32	6.00	2.59	4.91	-1.2	2.7	93	104.76	0	No event	105	-0.24	-0.23
-10	38	37.86	2.00	32	6.11	1.95	5.47	-1.2	2.7	93	105.27	0	No event	105	0.27	0.25
0	38	37.86	2.00	32	5.95	1.95	5.39	-1.2	2.7	93	105.27	100	1 ug epi (no control)	105	0.27	0.25
10	38	37.86	2.00	32	6.08	1.75	4.62	-1.1	2.7	93	105.17	0	No event	105	0.17	0.16
20	38	37.86	2.00	32	5.31	1.63	4.06	-1.2	2.7	93	119.23	0	No event	105	14.23	11.93
30	38	37.86	2.00	32	5.31	1.72	2.54	-1.2	2.7	93	103.93	0	No event	105	-1.07	-1.03
40	38	37.86	2.00	32	4.69	2.19	5.63	-1.1	2.7	93	86.80	0	No event	105	-18.21	-20.97
50	38	37.86	2.00	32	4.98	1.53	4.58	-1.1	2.7	93	78.89	0	No event	105	-26.11	-33.09
60	38	37.86	2.00	32	5.67	1.73	6.88	-1.0	2.7	93	79.82	0	No event	105	-25.18	-31.55
70	38	37.98	2.00	32	3.77	1.63	5.91	-0.9	2.7	93	83.82	0	No event	105	-21.18	-25.27
80	38	37.98	2.00	32	4.31	1.67	5.28	-1.2	2.7	93	89.46	0	No event	105	-15.54	-17.37
90	38	37.86	2.00	32	4.16	1.89	5.83	-1.1	2.7	93	95.11	0	No event	105	-9.89	-10.40
100	38	37.98	2.00	32	4.75	1.72	6.50	-1.0	2.7	93	101.68	0	No event	105	-3.32	-3.27
110	38	37.98	2.00	32	5.28	1.82	6.63	-1.1	2.7	93	104.24	0	No event	105	-0.76	-0.73
120	38	37.86	2.00	32	5.53	1.90	6.15	-1.1	2.7	93	106.29	0	No event	105	1.29	1.22
130	38	37.86	2.00	32	5.79	2.30	7.10	-1.2	2.7	93	106.40	0	No event	105	1.40	1.31
140	38	37.86	2.00	32	5.56	2.17	5.60	-1.2	2.7	93	107.83	0	No event	105	2.83	2.63
150	38	37.86	2.00	32	5.91	1.79	7.20	-1.0	2.7	93	108.66	0	No event	105	3.65	3.36
160	38	37.86	2.00	32	5.82	2.35	5.70	-1.2	2.7	93	108.86	0	No event	105	3.86	3.55

Table 5.2-1 Representative data set for animal R-1 showing formatted data for an epinephrine injection test under no- control conditions.

Animal #	R-1	R-1	R-1
RMS % MAP Deviation No Control	12.53	11.959	9.428
RMS % MAP Deviation Control	9.242	10.806	8.570
D	3.291	1.153	0.859
D	1.767	s	1.327
T	2.306	p	< 0.20

Table 5.2-2: Summary of calculated RMS values and Paired t-test results

5.3. Long-term Perturbation results

For all long-term perturbation testing, the interface was set to save data to a text file approximately every four seconds. Once saved to the text file, as with the short-term perturbations, the data was transferred to an Excel^R spreadsheet for further analysis. A representative data set is shown in *table 5.3-1*. Since there were two types of long-term perturbations, Neo-Synephrine (hypertension) and sodium nitroprusside (hypotension) the data was separated by type of infusion and control or no-control conditions. As with the short-term perturbation results, the % MAP deviation was identified as the key evaluation parameter for these tests while the % anesthetic was the major control variable. As with the previous experiments, the time scale for these experiments was adjusted to represent

relative time post infusion start to allow the data from the control and no-control tests to be directly compared.

Of the six animals tested, only four yielded data for the neo-syneprine testing (LTP-2, LTP-3, LTP-4, LTP-6). A representative plot of % MAP deviation and % anesthetic vs. time for the Neo-Syneprine injection testing is shown in *figure 5.3-1& 5.3-2* and the plots for all data yielding animals are included in *Appendix B*.

Animal: LTP-3		Strain: Brown Norway			Test: Sodium Nitroprusside (Control)							Sex: Female			Date: 03/12/03		
Time (post Inj.)	Temp Set (°C)	Actual Temp. (°C)	An. % (Halot hane)	O2%	CO2 % MAX	CO2 % MIN	Vent Press. MAX	Vent. Press. MIN	Tidal Volume (cc)	Resp. Rate (BPM)	MAP (mmHg)	HR (BPM)	Event Marker	Event	Set Pressure (mmHg)	Dev. From MAP	% Dev. From MAP
-344	38	37.86	1.80	30	5.26	0.11	2.78	-1.03	1.5	77	95.83	315	100	Pressure control started 95	95	0.83	0.87
-334	38	37.86	2.50	30	4.86	0.10	2.78	-1.03	1.5	77	94.60	315	0	No event	95	-0.41	-0.43
-324	38	37.98	2.50	30	5.24	0.12	2.81	-1.03	1.5	77	94.60	316	0	No event	95	-0.41	-0.43
-320	38	37.98	2.50	30	5.26	0.11	2.78	-1.03	1.5	77	94.80	315	0	No event	95	-0.20	-0.21
-316	38	37.98	2.50	30	5.25	0.12	2.73	-1.03	1.5	77	95.93	315	0	No event	95	0.93	0.98
-312	38	37.98	2.15	30	5.21	0.10	2.81	-1.03	1.5	77	94.49	313	0	No event	95	-0.51	-0.53
-308	38	37.98	1.80	30	5.05	0.11	2.76	-1.03	1.5	77	94.60	313	0	No event	95	-0.41	-0.43
-304	38	37.86	1.80	30	5.08	0.10	2.81	-1.03	1.5	77	90.49	313	0	No event	95	-4.51	-4.75
-300	38	37.98	1.80	30	5.33	0.12	2.73	-1.03	1.5	77	93.16	314	0	No event	95	-1.84	-1.94
-296	38	37.98	1.80	30	5.34	0.16	2.81	-1.05	1.5	77	92.65	312	0	No event	95	-2.36	-2.48
-292	38	37.98	1.80	30	5.46	0.17	2.76	-1.03	1.5	77	92.03	312	0	No event	95	-2.97	-3.13
-288	38	37.98	1.80	30	5.58	0.21	2.76	-1.03	1.5	77	92.24	313	0	No event	95	-2.77	-2.91
-284	38	37.98	1.80	30	5.68	0.21	2.76	-1.03	1.5	77	92.75	313	0	No event	95	-2.25	-2.37
-280	38	37.98	1.80	30	5.65	0.22	2.73	-1.03	1.5	77	93.47	313	0	No event	95	-1.53	-1.61
-276	38	37.86	1.80	30	5.65	0.22	2.73	-1.03	1.5	77	92.75	313	0	No event	95	-2.25	-2.37
-272	38	37.98	1.80	30	5.50	0.19	2.78	-1.03	1.5	78	93.36	314	0	No event	95	-1.64	-1.72
-268	38	37.98	1.80	30	5.70	0.23	3.03	-1.03	1.5	77	93.36	315	0	No event	95	-1.64	-1.72
-264	38	37.98	1.80	30	5.67	0.21	3.00	-1.05	1.5	77	94.29	313	0	No event	95	-0.71	-0.75
-260	38	37.98	1.80	30	5.53	0.21	2.98	-1.03	1.5	78	93.98	314	0	No event	95	-1.02	-1.07
-256	38	37.98	1.80	30	5.49	0.22	2.98	-1.03	1.5	77	94.80	314	0	No event	95	-0.20	-0.21
-252	38	37.98	1.80	30	5.59	0.21	2.93	-1.03	1.4	75	94.60	313	0	No event	95	-0.41	-0.43
-248	38	37.98	1.80	30	5.53	0.19	2.76	-1.03	1.4	76	96.65	313	0	No event	95	1.65	1.73
-244	38	37.98	1.80	30	5.53	0.18	2.78	-1.03	1.4	76	96.96	315	0	No event	95	1.96	2.06
-240	38	37.98	1.80	30	5.71	0.19	2.73	-1.05	1.4	76	97.57	315	0	No event	95	2.57	2.71
-236	38	37.98	1.80	30	5.74	0.19	2.78	-1.05	1.4	77	99.21	317	0	No event	95	4.21	4.43
-232	38	37.98	1.80	30	5.68	0.21	2.76	-1.05	1.4	76	98.39	317	0	No event	95	3.39	3.57
-228	38	37.98	1.80	30	5.64	0.18	2.71	-1.03	1.4	76	99.52	317	0	No event	95	4.52	4.76
-224	38	37.98	1.81	30	5.60	0.19	2.66	-1.03	1.4	76	100.24	318	0	No event	95	5.24	5.52
-220	38	37.98	1.81	30	5.74	0.18	2.78	-1.05	1.4	76	100.03	320	0	No event	95	5.03	5.30
-216	38	37.86	1.81	30	5.73	0.19	2.78	-1.03	1.4	77	100.34	318	0	No event	95	5.34	5.62
-212	38	37.98	1.80	30	5.65	0.18	2.71	-1.05	1.4	76	98.80	318	0	No event	95	3.80	4.00
-208	38	37.98	1.81	30	5.62	0.14	2.76	-1.03	1.4	76	98.39	318	0	No event	95	3.39	3.57
-204	38	37.98	1.81	30	5.40	0.11	2.56	-1.03	1.4	76	98.08	318	0	No event	95	3.08	3.25
-200	38	37.86	1.80	30	5.50	0.08	2.71	-1.05	1.4	76	97.57	318	0	No event	95	2.57	2.71
-196	38	37.98	1.80	30	5.43	0.10	2.78	-1.05	1.4	75	95.21	317	1	No event	95	0.21	0.22
-164	38	37.86	1.77	30	5.27	0.09	2.73	-1.03	1.4	75	87.82	313	0	No event	95	-7.18	-7.56
-160	38	37.98	1.80	30	5.46	0.09	2.71	-1.03	1.4	74	91.00	312	0	No event	95	-4.00	-4.21
-156	38	37.98	1.79	30	5.32	0.09	2.73	-1.05	1.4	75	89.57	313	0	No event	95	-5.43	-5.72

Table 5.3-1: Representative data set for animal LTP-3 showing formatted data for an Sodium Nitroprusside infusion test under control conditions.

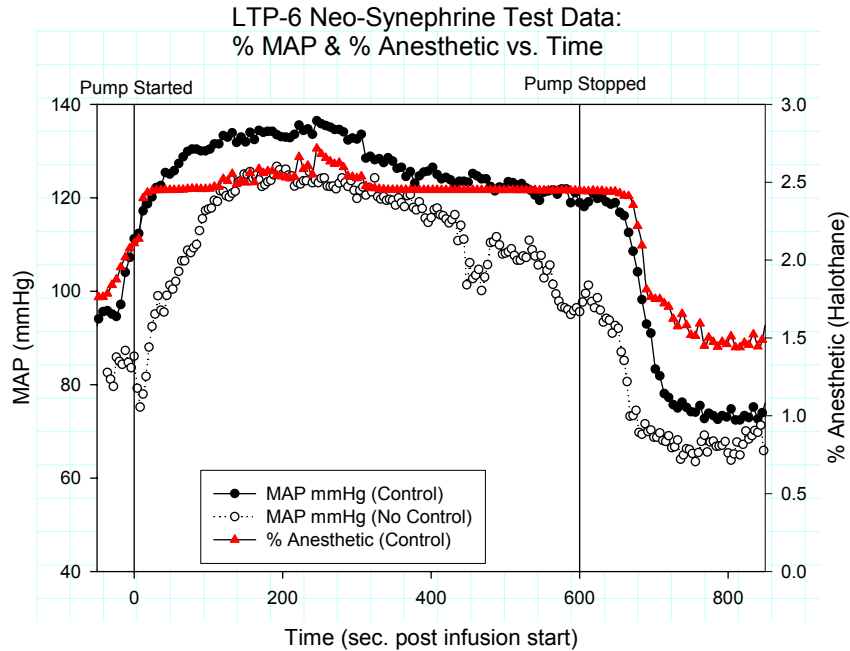


Figure 5.3-1: Animal LTP-6 Neo-Syneprine infusion test data showing MAP under control (closed circles) and no-control (open circles) conditions and % anesthetic (closed triangles) vs. time.

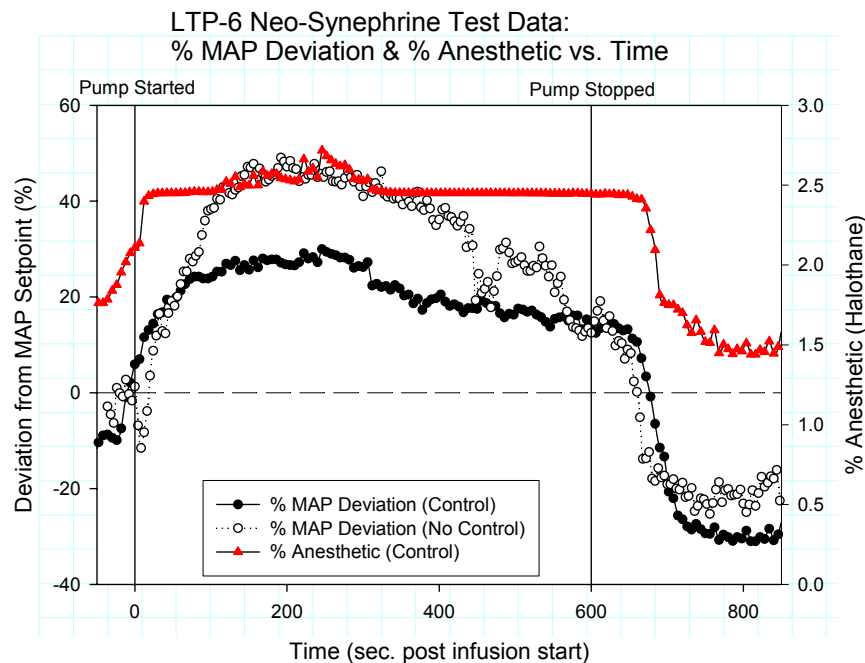


Figure 5.3-2: Animal LTP-6 Neo-Syneprine infusion test data showing % MAP deviation under control (closed circles) and no-control (open circles) conditions and % anesthetic (closed triangles) vs. time.

Of the six animals tested only four animals yielded data for the sodium nitroprusside infusion tests (LTP-2, LTP-3, LTP-5, LTP-6). A representative plot of % MAP deviation and % anesthetic vs. time for the sodium nitroprusside infusion testing is shown in *figure 5.3-3 & 5.3-4* and the plots for all data yielding animals are included in *Appendix C*.

As with the short-term perturbation a quantitative evaluation of the data from the long-term perturbations was achieved by performing a paired t-test analysis on the calculated RMS values from each test. The results of the RMS and t-test calculations for Neo-Synephrine and sodium nitroprusside infusion tests are shown in *table 5.3-2* and *table 5.3-3* respectively.

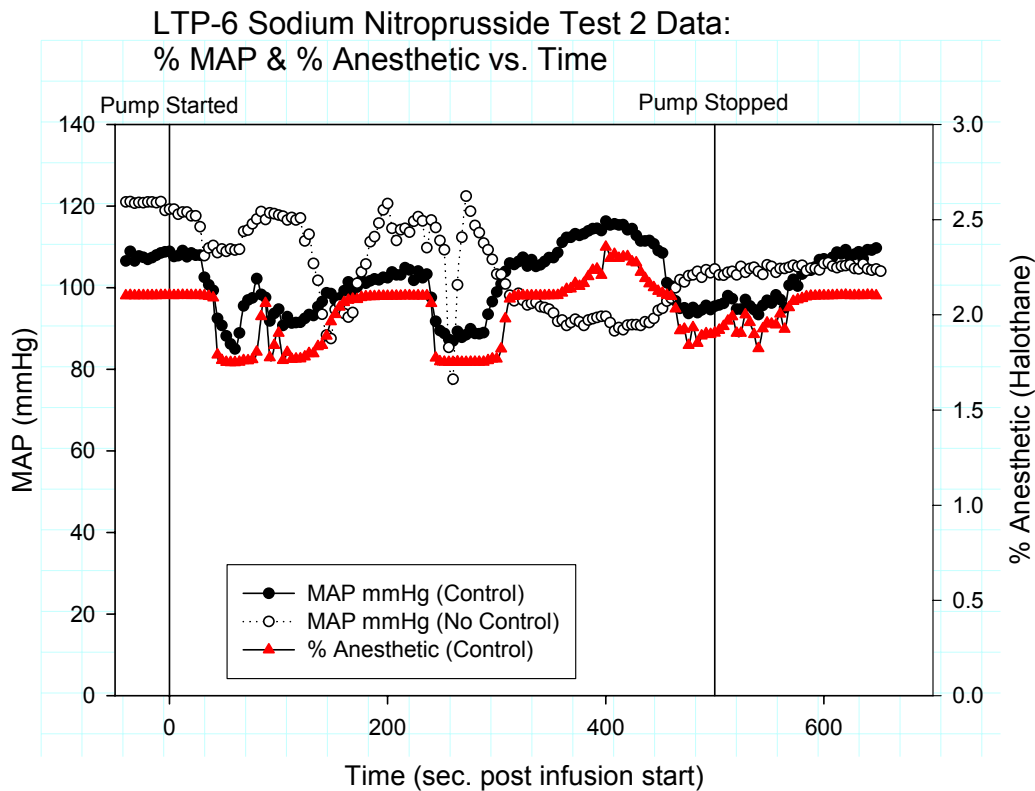


Figure 5.3-3: Animal LTP-6 sodium nitroprusside infusion test data showing MAP under control (closed circles) and no-control (open circles) conditions and % anesthetic (closed triangles) vs. time.

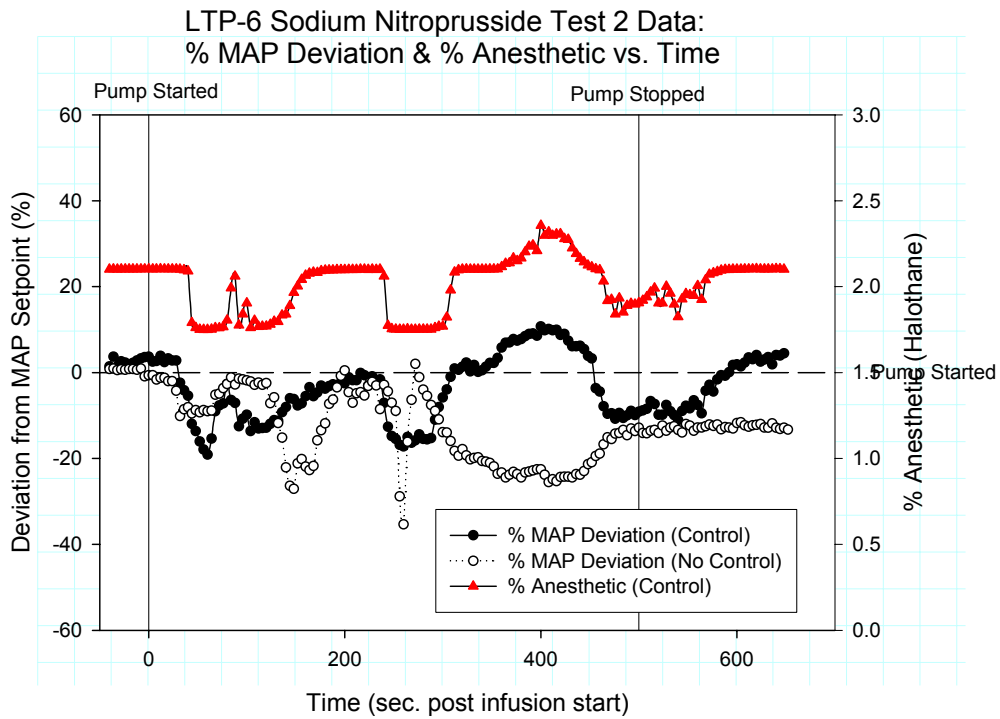


Figure 5.3-4: Animal LTP-6 sodium nitroprusside infusion test data showing % MAP deviation under control (closed circles) and no-control (open circles) conditions and % anesthetic (closed triangles) vs. time.

Neo-Syneprine infusion Data Analysis Results					
Animal #	LTP2	LTP3	LTP4A	LTP4B	LTP6
RMS % MAP Deviation No-Control	17.34	25.93	17.93	17.93	30.70
RMS % MAP Deviation Control	12.12	30.95	27.38	15.06	22.38
d	5.21	-5.02	-9.45	2.87	8.31
D	0.39	s	7.39		
t	0.117	P		< 0.50	

Table 5.3-2: Summary of calculated RMS values and Paired t-test results for the Neo-Syneprine infusion experiments.

Sodium Nitroprusside infusion Data Analysis Results						
Animal #	LTP2	LTP3	LTP5A	LTP5B	LTP6A	LTP6B
RMS % MAP Deviation No-Control	15.71	8.37	35.74	10.49	18.83	14.59
RMS % MAP Deviation Control	11.04	6.60	18.42	9.47	14.04	8.02
d	4.68	1.77	17.32	1.02	4.78	6.57
D	6.02	S	5.90			
t	2.499	p		< 0.10		

Table 5.3-3: Summary of calculated RMS values and Paired t-test results for sodium nitroprusside infusion experiments.

The overall stability and consistency of the system was analyzed by comparing the MAP values for each animal at the same time relative to infusion start for each of the long-term experiments. Mean and standard deviation values for each time point (relative to infusion start) during both the control and no-control conditions were calculated for the Neo-Syneprine and sodium nitroprusside infusion experiments. The resulting plots of mean and standard deviation values against time (post infusion start) are shown in *figures 5.3-4* and *5.3-5*, respectively.

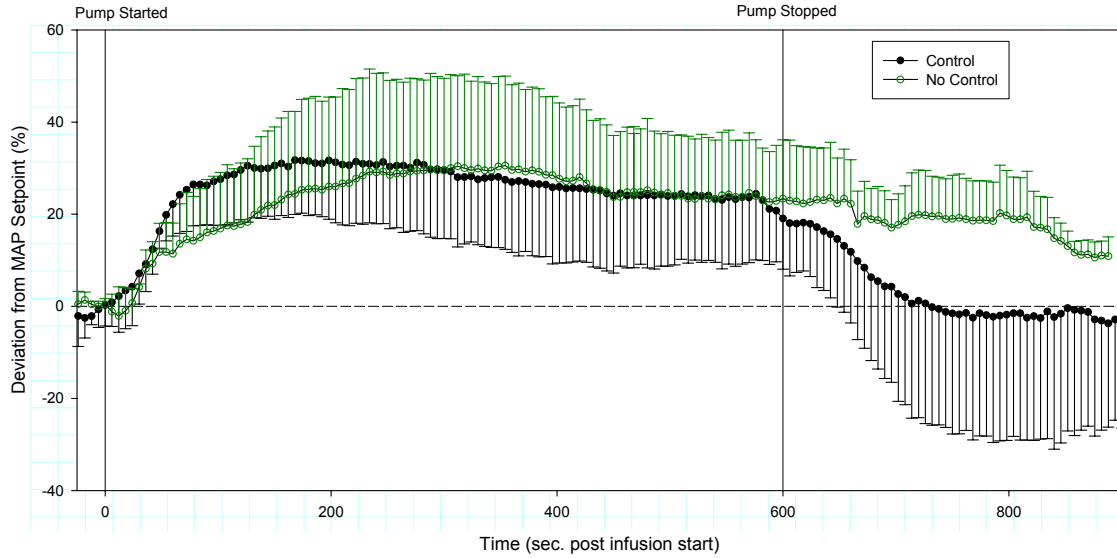


Figure 5.3-5: Neo-syneprhine testing mean and standard deviation vs. time for control (closed circles, negative error bars) and no-control (open circles, positive error bars).



Figure 5.3-6: Sodium nitroprusside testing mean and standard deviation vs. time for control (closed circles, negative error bars) and no-control (open circles, positive error bars).

5.4. CO₂ controller Results

Attempts were made to use the CO₂ control system during the short-term perturbation tests but were unsuccessful due to limitations of the Columbus Instruments ventilator being used at the time. Prior to the start of the long-term perturbation testing, a beta version of the Harvard Apparatus Inspira was used. The Inspira was able to handle the demands of the control system and allowed for the use of the CO₂ controller during the long term testing. Though no specific perturbations were performed, it was possible to collect data for each animal and observe the reactions of the control system to changes in ETCO₂. The key parameter for evaluation of the CO₂ control system was identified as the MAX % CO₂ and the major control variables were identified as tidal volume and respiratory rate. Due to calibration issues with the micro-capnometer, all % CO₂ values are one half that of the actual value. Representative plots of ETCO₂, tidal volume and respiration rate vs. time are shown in *figures 5.4-1 and 5.4-2* and plots for all of the LTP animals can be found in *Appendix D*.

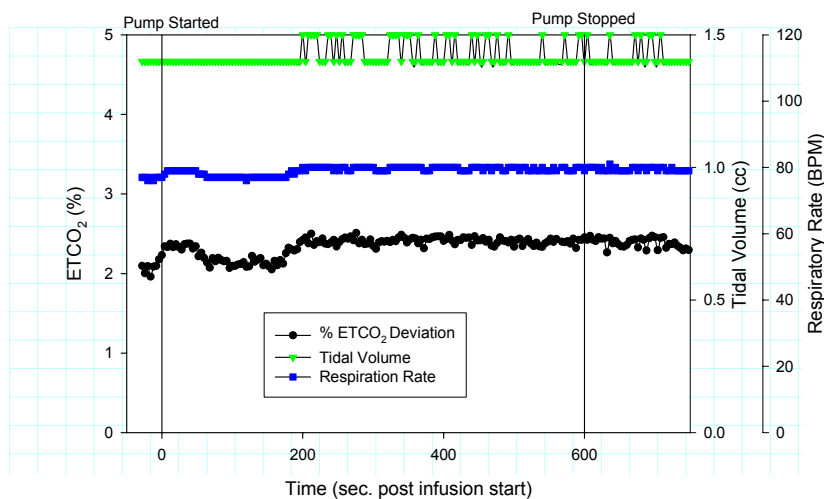


Figure 5.4-1: Representative plot of % CO₂ (closed circle) tidal volume (closed triangle) and respiratory rate (Closed square) vs. time for animal LTP-3.

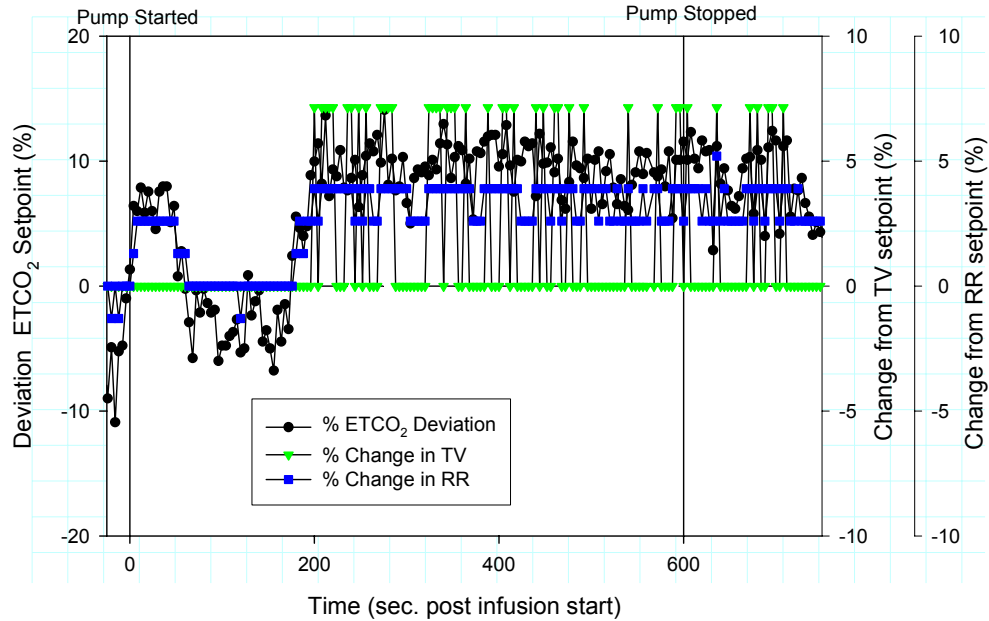


Figure 5.4-2: Representative plot of % CO₂ deviation (closed circle) change in TV set point (closed triangle) and change in RR set point (Closed square) vs. time for animal LTP-3.

5.5. Steady state observations

During the long-term perturbation testing, animal LTP-5 was allowed to stabilize and then placed on pressure and CO₂ control with no perturbations for a period of ~45 min. This was done to assess the normal variation of an animal's physiology when no active procedures are taking place and the system's ability to maintain the set points in this situation. Though no quantitative data can be obtained since the n is equal to 1, qualitative information can be gleaned by examining the resulting plots (*figures 5.5-1 - 5.5-4*).

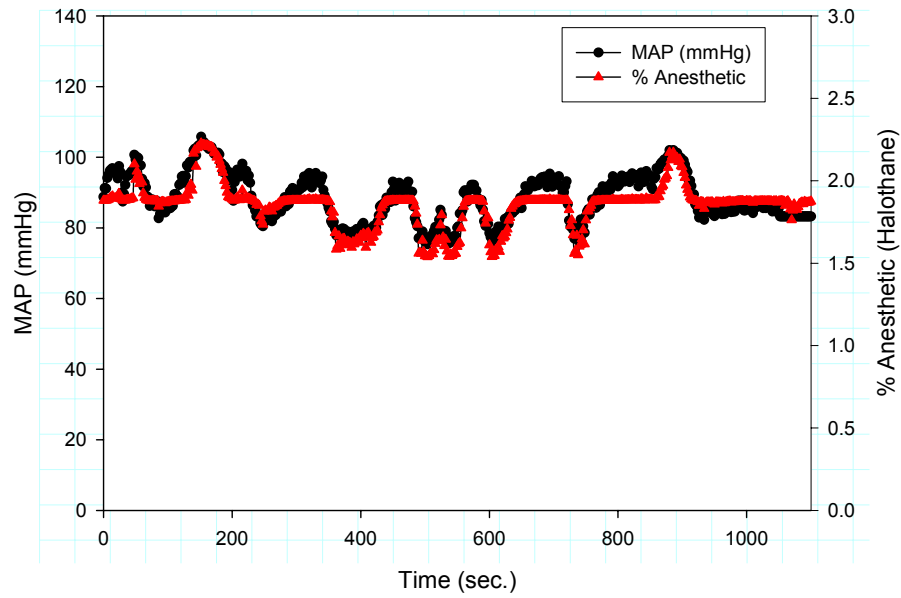


Figure 5.5-1: Animal LTP-5 steady state test data showing MAP under control (closed circles) and % anesthetic (closed triangles) vs. time.

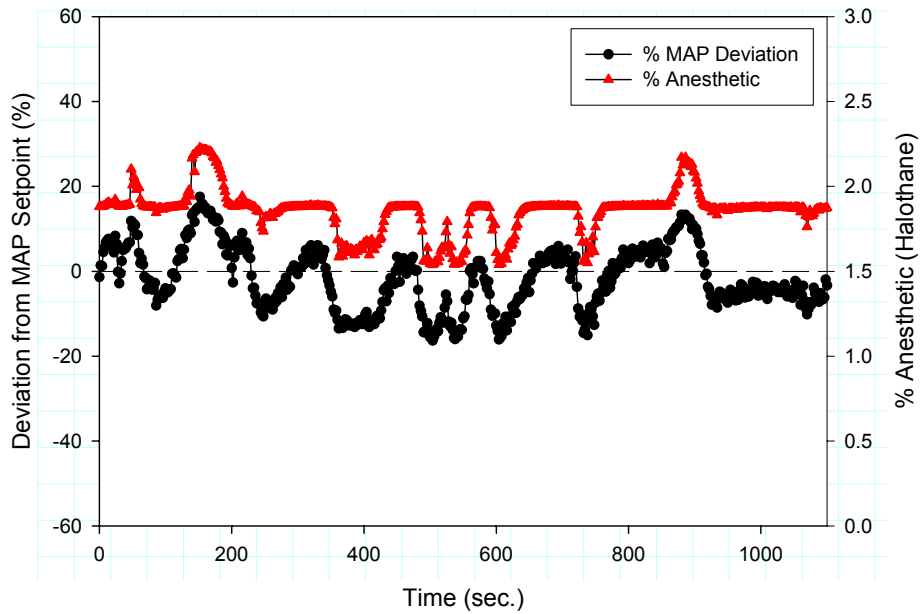


Figure 5.5-2: Animal LTP-5 steady state test data showing % MAP deviation under control (closed circles) and % anesthetic (closed triangles) vs. time.

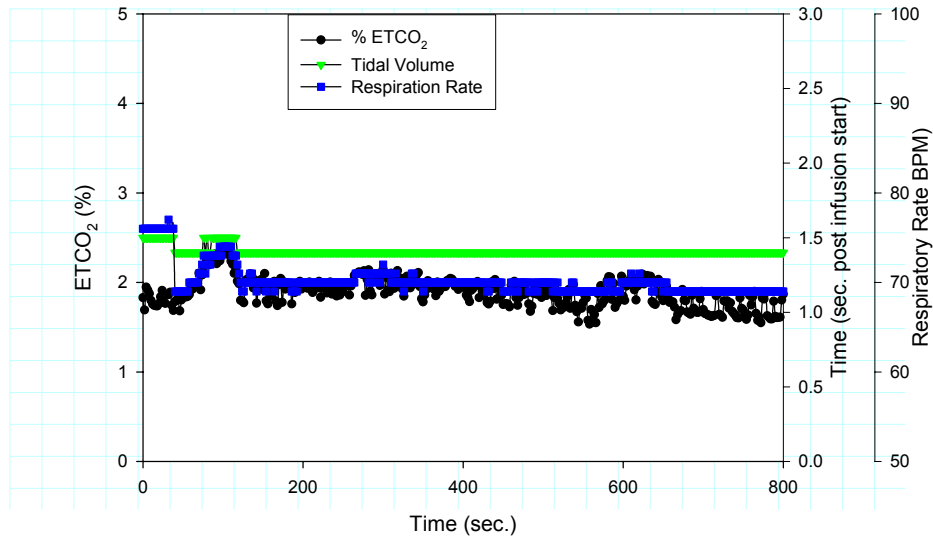


Figure 5.5-3: Animal LTP-5 steady state data showing % CO_2 (closed circle) tidal volume (closed triangle) and respiratory rate (Closed square) vs. time.

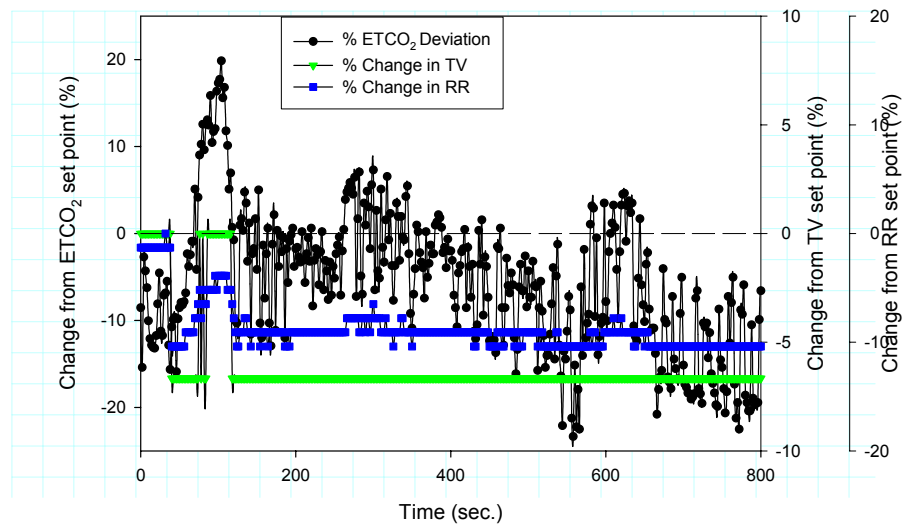


Figure 5.5-4: Animal LTP-5 steady state data showing % CO_2 deviation (closed circle) % change in tidal volume (closed triangle) and % change in respiratory rate (Closed square) vs. time.

6. DISCUSSION

6.1. *Significance of results*

The major aim of this project was the maintenance of an anesthetized rodent's physiological state using an automated control system. The data collected for the various perturbation tests indicate that the system in all cases is reacting to the perturbations in a predicted, safe and stable manner, but that a number of limitations exist. The pressure and anesthetic percent data from the short-term (epinephrine) perturbation tests showed that the control system was able to identify a change from the set pressure and adjust the anesthetic percentage in an attempt to correct the deviation (*Appendix A*). However, results of the paired t-test analysis revealed that no statistical differences were found ($p < 0.20$) between the control and no-control conditions, suggesting that while the system was able to respond to changes in BP, anesthetic changes have a much longer time response and can not effectively blunt a dramatic short-term change in BP.

The Neo-Synephrine perturbation pressure and anesthetic percent data (*Appendix B*) indicated that, as with the epinephrine testing, the system was able to appropriately adjust the anesthetic percentage in response to a change in the MAP, but that the change in anesthetic concentration was not able to counteract the pressure increase caused by the vasoconstrictive drug. The lack of a drop in MAP even in the presence of the upper safety limit anesthetic concentration indicates that there is an unknown mechanism that is limiting the anesthetic agent's ability to depress MAP or limiting the delivery of the anesthetic agent in general. Results from the paired t-test analysis showed that there was no statistical difference between the RMS deviation values for control and no-control ($p < 0.50$).

The sodium nitroprusside perturbation pressure and anesthetic percent data collected from the four animals showed that the system was able to adjust the anesthetic concentration and reduce the % MAP deviation in the control situation compared to the no-control (*Appendix C*). Paired t-test analysis was performed on the calculated RMS values for % MAP deviation, giving a t value of 2.499, proving that the control condition was a significant improvement ($p < 0.10$) over the no-control condition to a confidence level between 90% and 95 % ($t_0 = 2.015$ and $t_0 = 2.579$, respectively).

The %CO₂, TV and RR data obtained throughout the long-term perturbation tests (*Appendix D*) shows that the system was able to maintain the ETCO₂ under near steady state conditions (the perturbations used had little effect on ETCO₂). Though this is not a perturbation experiment it is an important indicator of the systems stability and efficacy under normal conditions.

6.2. Future Work

The presence of a significant improvement in the hypotension perturbation testing with no prior optimization of the control system indicates that further work should be completed that analyzes and optimizes the activity of the pressure controller. A number of variables exist in the system that could directly affect the ability of the system to effectively and safely maintain the desired set point. Additional hypotension testing should be completed in conjunction with this optimization to increase the number of data points available for statistical analysis.

As stated previously, the inability of the system to reduce MAP during the Neo-Synephrine (hypertension) experiments even in the presence of increased anesthetic

concentration suggests that an unknown mechanism exists which limits the anesthetic's ability to reduce the elevated MAP. Additional hypertension testing should be completed using a different drug or a method that minimizes the fluctuation of systemic parameters other than the blood pressure to fully evaluate the situation and identify the limitation.

Additional short and long term perturbation experiments should be completed using alternative inhalant anesthetics. The use of an alternative anesthetic may provide a more rapid response or a different MAP depressing mechanism that could allow for increased effectiveness for short-term fluctuations and situation modeled in the Neo-Synephrine infusion test. The interface developed for this project already contains functionality that allows for the selection of alternative anesthetics.

Because all of the perturbations performed during this project considered only the control or no-control conditions, additional testing should be completed which considers a positive control. In order to achieve this, an anesthetist should attempt to control the set points of the animal during perturbations and these results should be compared to the results obtained during automated control. This testing can identify any limitations in halothane's ability to control BP and allow for the validation of the system's decision making.

Though all of the testing that was completed in this project was done on rats, mice are another important animal model in the lab. In order to complete this testing for the pressure control system a reliable means for acquiring the BP of a mouse must be developed. Arterial cannulation in the mouse is extraordinarily difficult and not employed in this project.

Perturbation testing of the ETCO₂ control system should be completed to assess that system's ability to maintain the set point %CO₂ in non-steady state conditions. Possible perturbations include the addition of CO₂ gas to the inhaled gas mixture or injection of bicarbonate.

6.3. Conclusions

The four specific goals for this project were to 1) Develop a computer-controlled monitoring system (based on LabVIEW^R) capable of “real time” data acquisition and display of body temperature, end tidal CO₂ (ETCO₂), ventilator pressure and blood pressure, 2) Develop a communications capability allowing for the control of laboratory instrumentation, such as the ventilator, heating bath and gas flow meters, 3) Develop a computer-based control system (using LabVIEW^R) for maintaining body temperature, ETCO₂, and blood pressure., 4) Design a user interface that incorporates the above subsystems and an event marker and file transfer system.

The project was successful in producing a single user interface capable of “real-time” acquisition, display, transfer and evaluation of physiological data from an anesthetized animal and, based on this evaluation, manipulation of the available control variables in an attempt to maintain a predetermined set point. The *in-vivo* testing completed in this project proved that the system was able to significantly improve the deviation from the set pressure while under control in the hypotension condition.

Though both the short-term and hypertension testing showed no significant improvement, the system successfully manipulated the anesthetic percentage in a safe and

stable manner in response to changes in MAP. The results for the hypertension testing suggest that unknown mechanisms exist that limit the anesthetic agent's ability to depress MAP or limit the delivery of the anesthetic agent in general.

Though no quantitative analysis was done, the qualitative data for the CO₂ control system obtained during the long-term perturbation testing showed that the system can safely and effectively adjust the TV and RR values to maintain a ETCO₂ level close to the set point.

Though currently limited, this system is an important first step towards a fully automated monitoring and control system and can be used as the basis for further research investigating alternate anesthetic agents and optimization of the control algorithms.

7. REFERENCES

- Afshart, A. and C. Georgescu (1994). "A Fuzzy Model-Based Optimal Control Strategy." EMTL-Schlumberger Industries, France: 120-125
- Allen, Robert, David Smith (2001). "Neuro-fuzzy closed-loop control of depth of anesthesia." Artificial Intelligence in Anesthesia 21: 185-191
- American College of Veterinary Anesthesiology (1995). "Suggestions for monitoring anesthetized veterinary patients." JAVMA 206 (7)
- Becker, Kurt, Bernhard Thull, Horst Kasmacher-Leidinger, Johannes Stemmer, Gunther Rau, Gunther Kalff, Hans-Jergen Zimmerman (1997). "Design and validation of an intelligent patient monitoring and alarm system based on a fuzzy logic process model." Artificial Intelligence in Medicine 11: 33-53
- Boutilette, Michael Paul, Kevin James McNamara, Colleen Marie O'Rourke (2000). "Development of a Computer Controlled Anesthesia Machine for Mice" Major Qualifying Project, Worcester Polytechnic Institute Biomedical Engineering Department.
- Brule, James A. (1985). "Fuzzy Systems: A Tutorial." <http://www.austinlinks/Fuzz/tutorial/.html> 1985
- Chu, Kuch-Shiu, and Andrew Hunter (1999) "GA Design of Crisp-Fuzzy logic Controllers." School of Computing and Information Systems, University of Sunderland
- Dojat, M., F. Pachet, Z. Guessoum, D. Touchard, A. Harf, L. Brochard (1997). "NeoGanesh: a working system for the automated control of assisted ventilation in ICUs." Artificial Intelligence in Medicine 11: 97117
- Dorsch, Jerry A., Susan E. Dorsch, 1984. Understanding Anesthesia Equipment Construction Care and Complications. Baltimore, MD. Williams & Wilkins
- Dulkara, T., K. Irikura, Z. Huang, N. Panahian, and M. A. Moskowitz (1995). "Cardiovascular Responses Under Controlled and Monitored Physiological Conditions in the Anesthetized Mouse." Journal of Cerebral Blood Flow and Metabolism 15 (4): 631638
- Frei, C. W., M. Derighetti and A. M. Zbinden (1997). "Modelling for control of mean arterial blood pressure (MAP) during Anesthesia." Presented at 2nd MATHMOD, Vienna
- Gaines, B. R. "Fuzzy Reasoning and the Logic of Uncertainty."

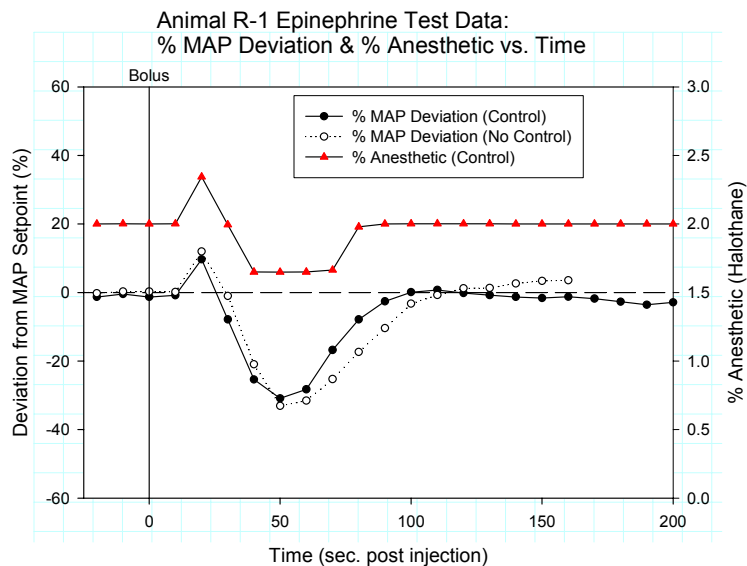
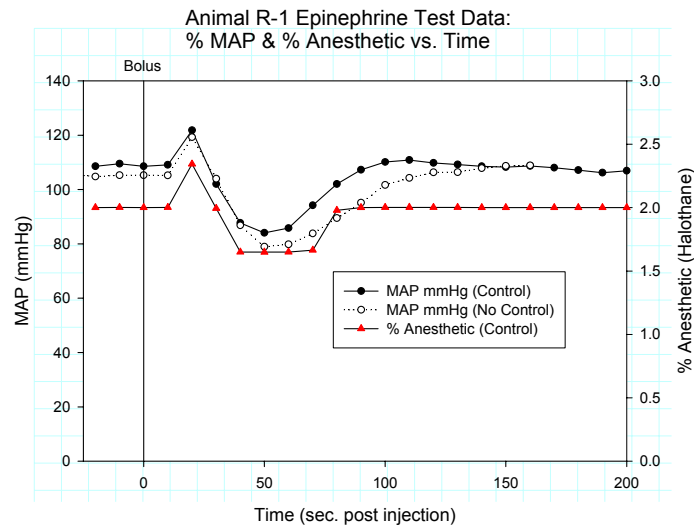
- Graal, P.M.A. de, G.C. van den Eljkel, H.J.L.M. Vullings, B.A.J.M. de Mol (1997). "A decision-driven design of a decision support system in anesthesia." Artificial Intelligence in Medicine 11: 141-153
- Guettler, Norbert, Dejan Vukajlovic, Alexander Berkowtson, Britta Schulte, Ali Erdogen, Joerg Carisson, Joerg Neuzner, Hanz Pitschner (2001). "Affect of Vagus Blockage with Atropine on Heart-Rate Turbulence." *PACE* 24(4): 539-786
- Horstkotte, Erik (2000). "Fuzzy expert systems." <http://www.austinlinks/fuzzy-expert-systems/.html> 2000
- Horstkotte, Erik (2000). "Fuzzy Logic Overview." <http://www.austinlinks/fuzzy/overview/.html> 2000
- Jain, L.C. (2000). "Industrial Applications of Fuzzy Systems." Knowledge-Based Intelligent Engineering Systems (KES) Center, University of South Australia
- Johnson, G. Allan, Ph.D., Daniel H. Turnbull, Ph.D. Elaine G. Fitzsimons, M.S. (1999). "In-Vivo Microscopy: Technologies and Applications." Duke Center for In Vivo Microscopy, NIH/NICRR
- Jones, Richard W., Michael J. Harrison, Andrew Lowe (2001). "Computerized anesthesia monitoring using fuzzy trend templates." Artificial Intelligence in Medicine 21: 247-251
- Ko, J.C.H (2002). "Pharmacology: Inhalation Anesthetics." *Veterinary Medicine*, Oklahoma State University February 8, 2002
- Kubota, Toru, Christine M. Mahler, Charles F. McTiernan, Clarence C. Wu, Marc D. Feldman and Arthur M. Feldman (1998). "End-systolic pressure:-dimension relationship of in situ mouse left ventricle." J Mol Cell Cardiol 30: 357-363
- Langari, Reza (1996). "Hierarchal Approach to Fuzzy Logic Control." Department Mechanical Engineering, Texas A & M University.
- Linkens, D.A. (1992). "Adaptive and Intelligent Control in Anesthesia." *IEE Control Systems* December 1992: 6-11
- Linkens, D. A., 1994. *Intelligent Controls in Biomedicine*. Bristol, PA. Taylor and Francis Ltd.
- Linkens, D.A., M.F. Abbod (1998). "Intelligent Control of Anesthesia." *IEE*: 271-274
- Linkens, D.A., L. Vefgin (1997), "Recognition of patient anesthetic levels: neural network systems, principal components analysis and canonical discriminant variates." Artificial Intelligence in Medicine 11: 155-173

- Lowe, Andrew, Michael J. Harrison, Richard W. Jones (1999). "Diagnostic monitoring in anesthesia using fuzzy trend templates for matching temporal patterns." Artificial Intelligence in Medicine 16: 183-199
- McAllister, M. Luisa, John Dockery, Sergei Ovchinmikov, Klaus-Peter Adisassinig (1985). "Tutorial on Fuzzy Logic in Simulation." Proceedings of the 1985 winter simulation conference: 40-44
- Meler R., J. Nieuwland, A.M. Zbinden and S.S. hacisolihzade (1992). Fuzzy Logic Control of Blood Pressure during Anesthesia." IEEE Control Systems: 12-17
- Morari, Memfred (2001). "Challenges and Opportunities in Process Control." AIChe Journal 27 (10): 21952392
- Mortier, Eric P., Michel M. R. F. Struys (2001), "Monitoring the depth of anesthesia using bispectral analysis and closed-loop controlled administration of propofol." Best Practice & Research Clinical Anesthesiology 15 (1): 6376
- Olansen, Jon B. and Eric Rosow, 2002. Virtual Bio-Instrumentation: Biomedical, Clinical and Healthcare Applications in LabVIEW. Upper Saddle River, NJ. Prentice Hall PRT
- Qingyang Hu, Rose, David W. Petr (2000). "A Predictive Self-Tuning Fizzy-Logic Feedback Rate Controller." IEEE Transactions on Networking 8 (6): 697-709
- Rao, Ramesh R., B. Wayne Bequette and Rob J. Roy (2000). "Control of hemodynamic and anesthetic states in critical care patients." Chemical and Biomedical Engineering Departments, Renselaer Polytechnic Institute
- Roberts, Dr. John (1994). "Control of Carbon Dioxide Levels during Neuro-anesthesia: Current Practice and an Appraisal of our Reliance on Capnography." Anesthesia & Intensive Care
- Seiber, T. J., C. W. Frei, M. Derighetti, P. Peigenwinter, D. Leibundgut, and A. M. Zbinden (2000). "Model-based automatic feedback control versus human control of end-tidal isoflurane concentration using low-flow anesthesia ." British Journal of Anesthesia 85 (6): 818825
- Shieh, Jian Shing, Derek Arthur Linkens, and John E. Peacock (1999). "Hierarchal Rule-Based and Self-Organizing Fuzzy Logic Control for Depth of Anesthesia." IEEE Transactions on Systems MAN and Cybernetics – Part C 29 (1): 98—109
- Short, Charles E., 1987. Principles & Practice of Veterinary Anesthesia. Baltimore, MD: Williams and Wilkins

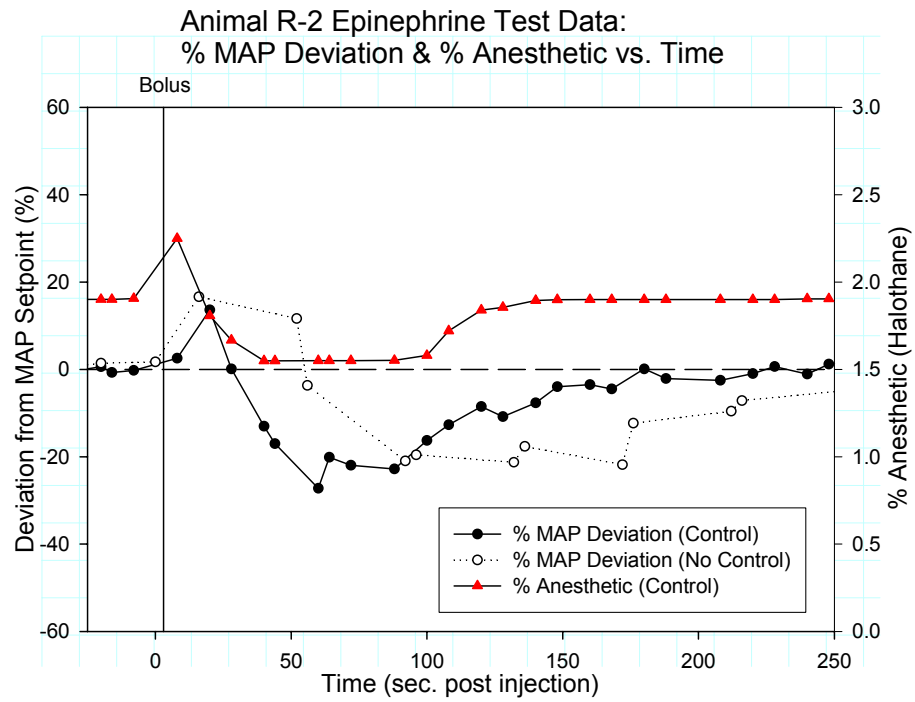
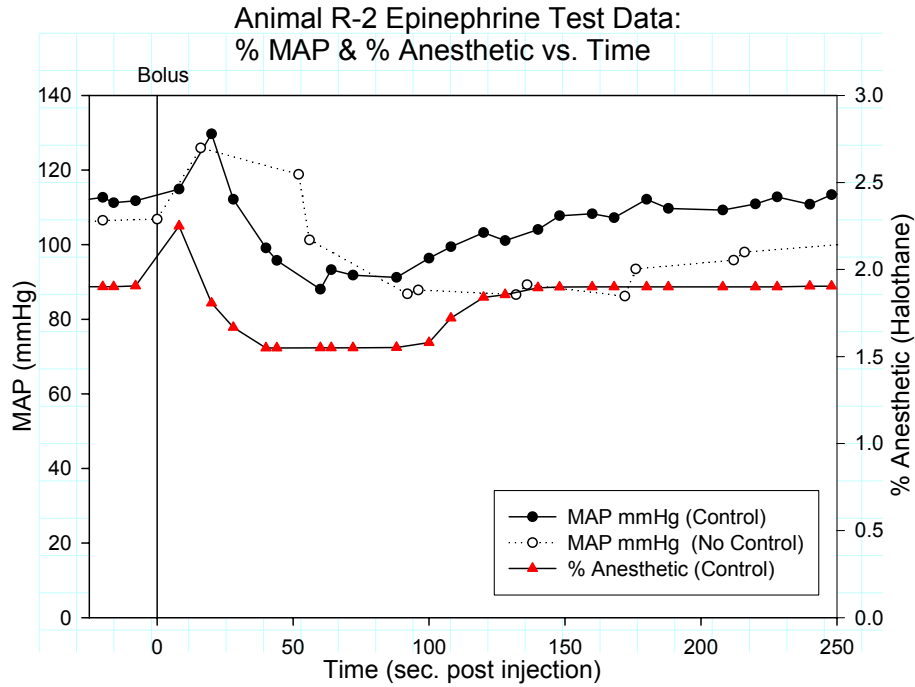
- Szolovits, Peter, 1982. Artificial Intelligence in Medicine. Washington, D.C., American Association for the Advancement of Science
- Valke, Christian and Howard Jay Chizech (1997). "Closed-Loop Drug Infusion for Control of Heart Rate Trajectory in Pharmacological Stress Tests." IEEE Transactions on Biomedical Engineering 44 (3): 185-195
- Whitely, J. P., D. J. Gavaghan and C. E. W. Hahn (2001). "Modeling inert gas exchange in tissue and mixed-venous blood return to the lungs." Journal of Theoretical Biology 209: 431-443
- Zadeh, Lotfi A., Janusz Kacprzyk, 1992, FUZZY LOGIC FOR THE MANAGEMENT OF UNCERTAINTY. New York, NY: John Wiley & sons Inc.

Appendix A: Epinephrine Injection Data Plots

The following plots are summary plots of the calculated % NAP deviation for both the control and no-control condition and % anesthetic in the control condition vs. relative time post injection.

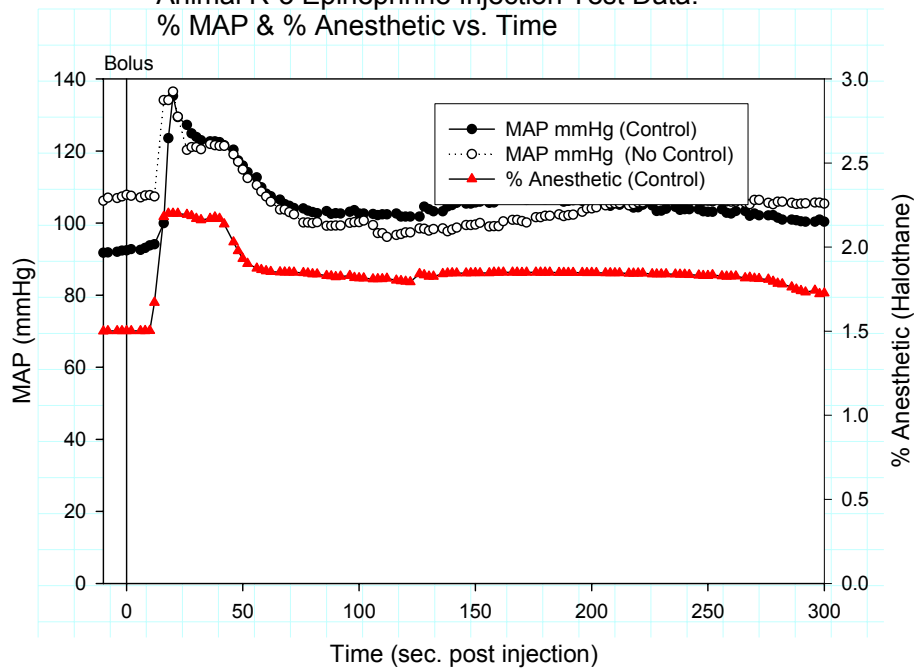


Control Condition	RMS Value (%)	Pressure Set-point (mmHg)	Anesthetic Set-point (%)
Control	9.24	110	2.0
No-Control	12.53	105	NA

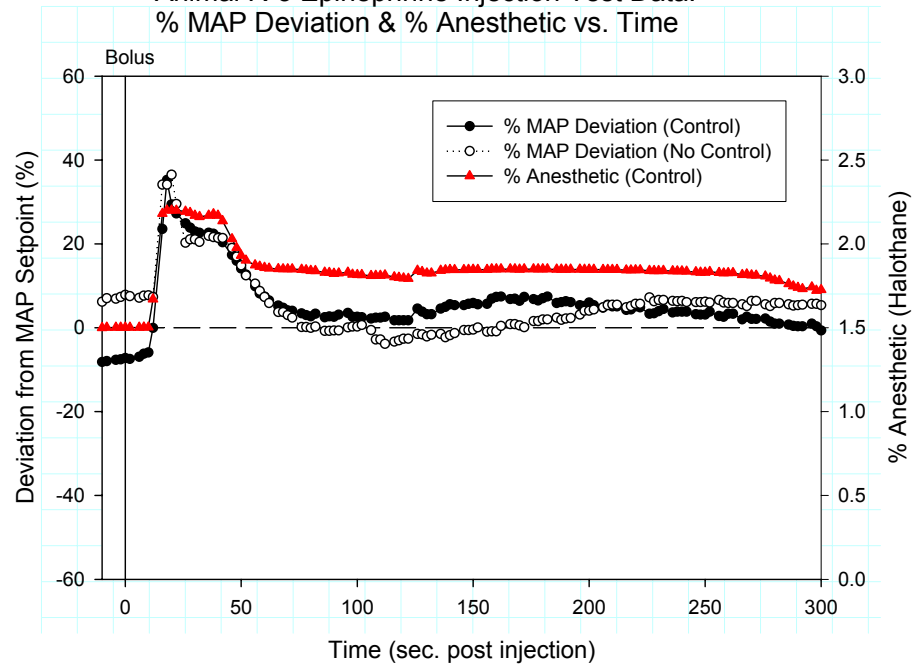


	RMS Value	Pressure Set-	Anesthetic Set-
Control Condition	(%)	point (mmHg)	point (%)
Control	10.8	112	1.9
No-Control	11.96	105	NA

Animal R-3 Epinephrine Injection Test Data:
% MAP & % Anesthetic vs. Time



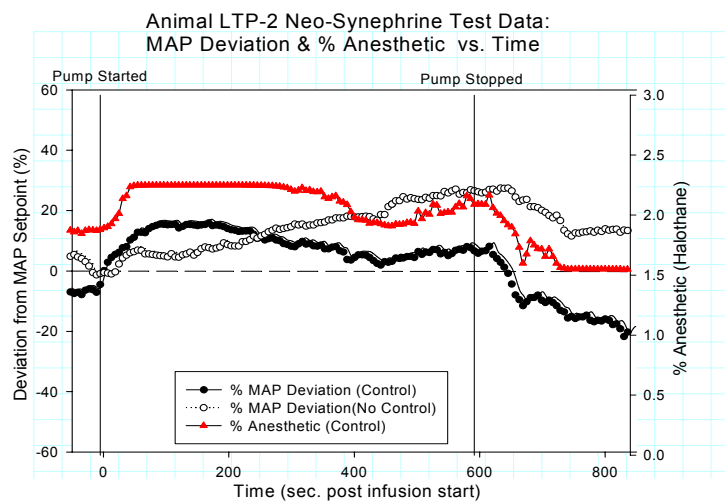
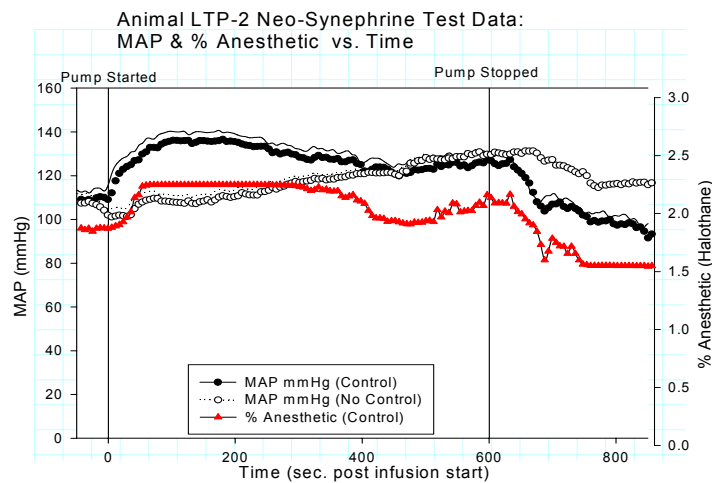
Animal R-3 Epinephrine Injection Test Data:
% MAP Deviation & % Anesthetic vs. Time



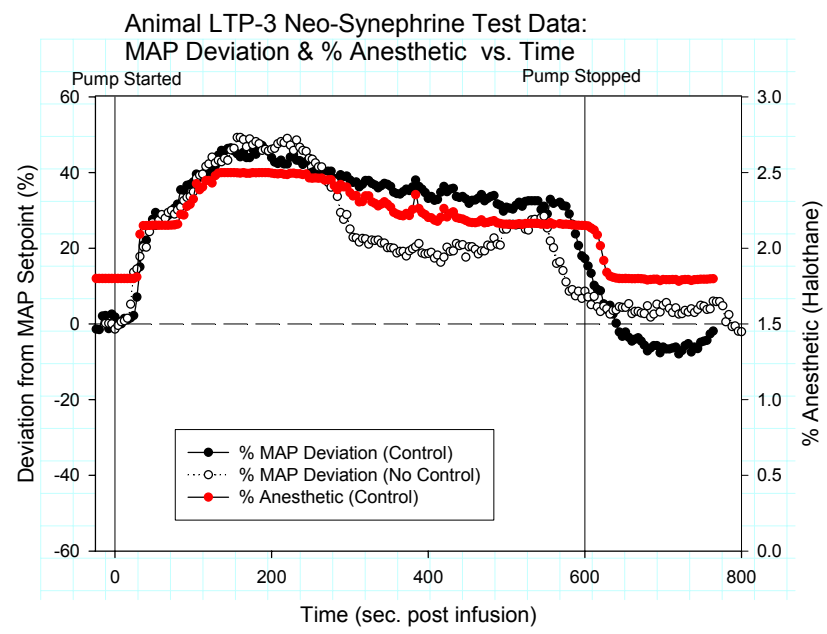
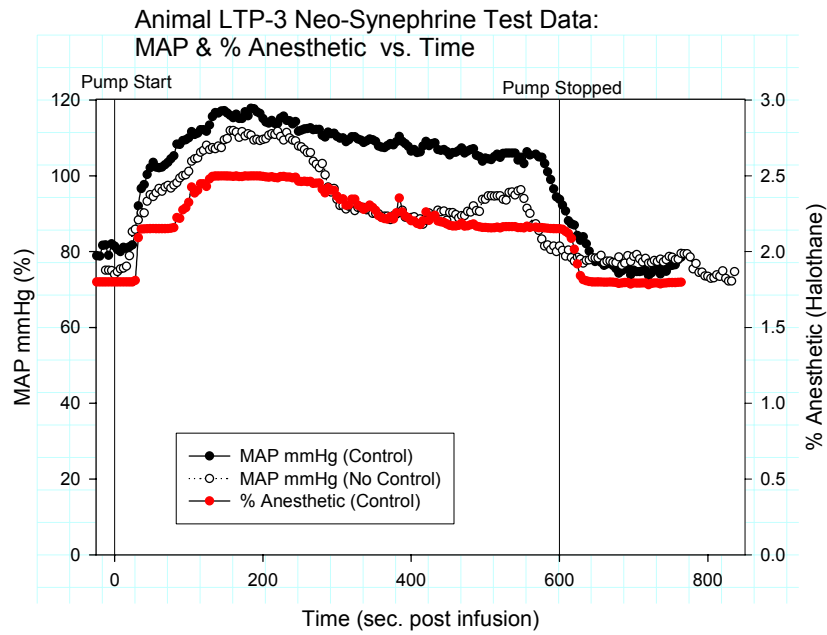
Control Condition	RMS Value (%)	Pressure Set-point (mmHg)	Anesthetic Set-point (%)
Control	8.57	100	1.5
No-Control	9.43	100	NA

Appendix B: Neo-Syneprine Infusion Data plots

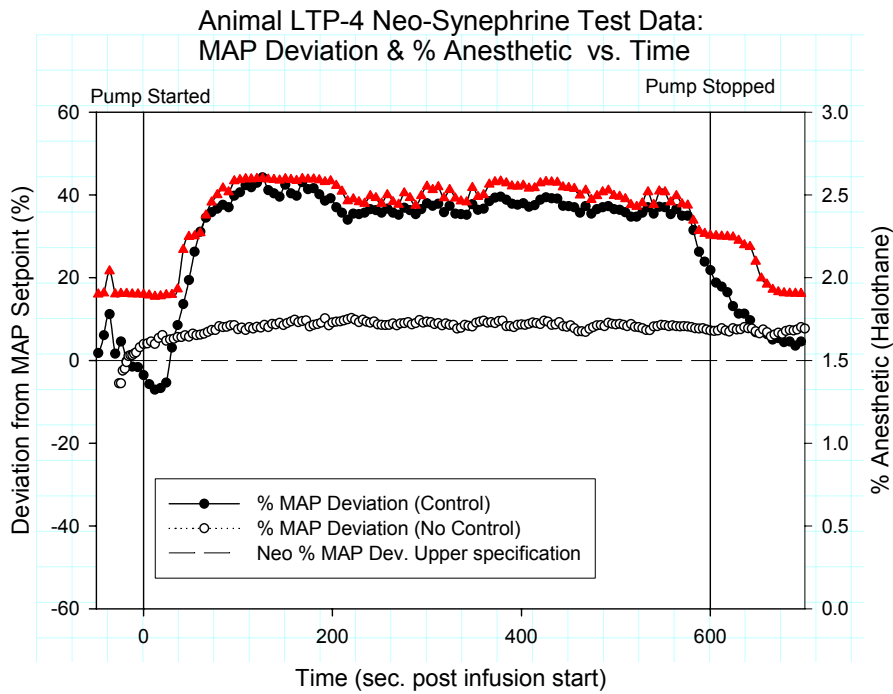
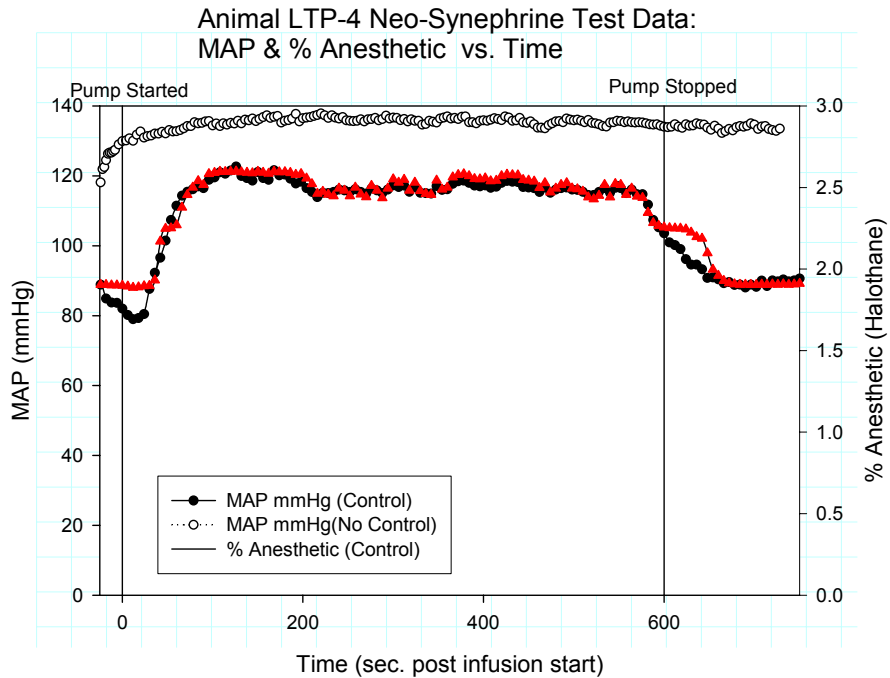
The following are plots of MAP and % MAP deviation for both the control and no-control conditions as well as % anesthetic for the control condition vs. relative time post infusion start for all of the animals which yielded data for the neo-syneprine infusion tests.



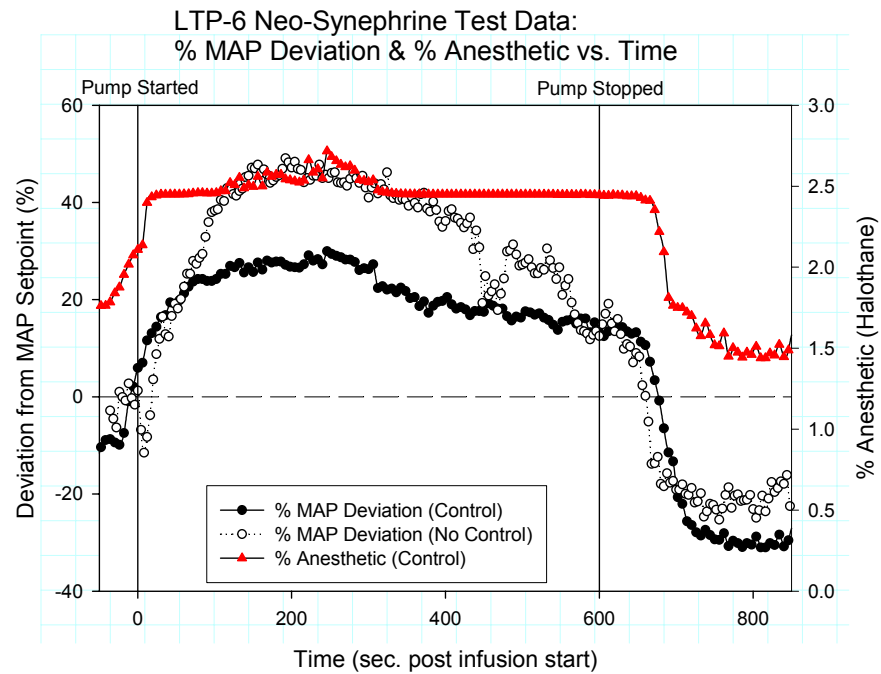
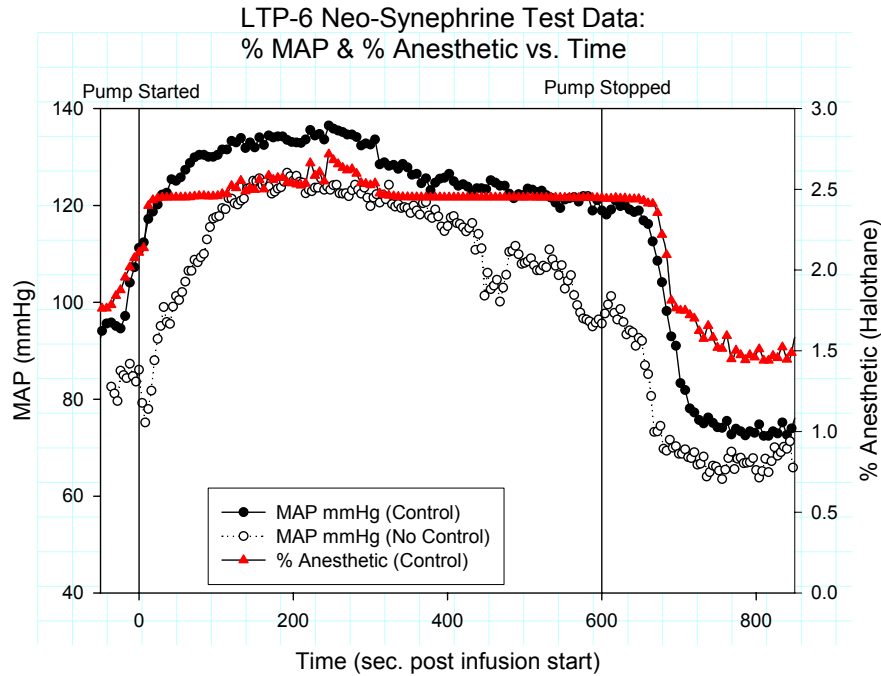
	RMS Value	Pressure Set-	Anesthetic Set-
Control Condition	(%)	point (mmHg)	point (%)
Control	12.12	120	1.9
No-Control	17.34	105	NA



Control Condition	RMS Value (%)	Pressure Set-point (mmHg)	Anesthetic Set-point (%)
Control	30.95	80	1.8
No-Control	25.93	75	NA



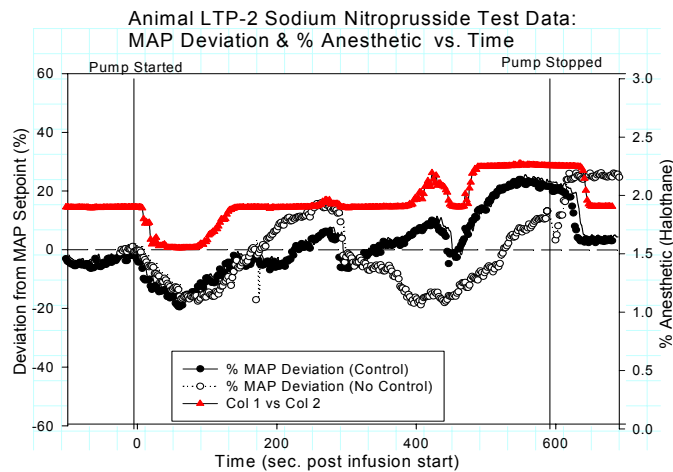
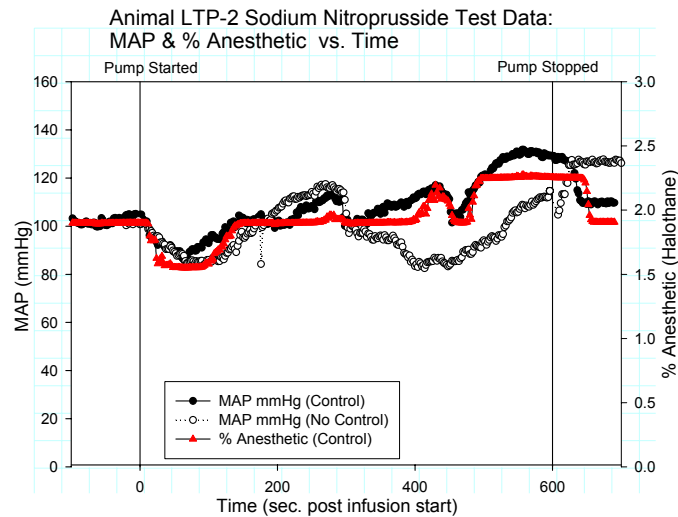
Control Condition	RMS Value (%)	Pressure Set-point (mmHg)	Anesthetic Set-point (%)
Control	27.38	85	1.9
No-Control	17.93	125	NA



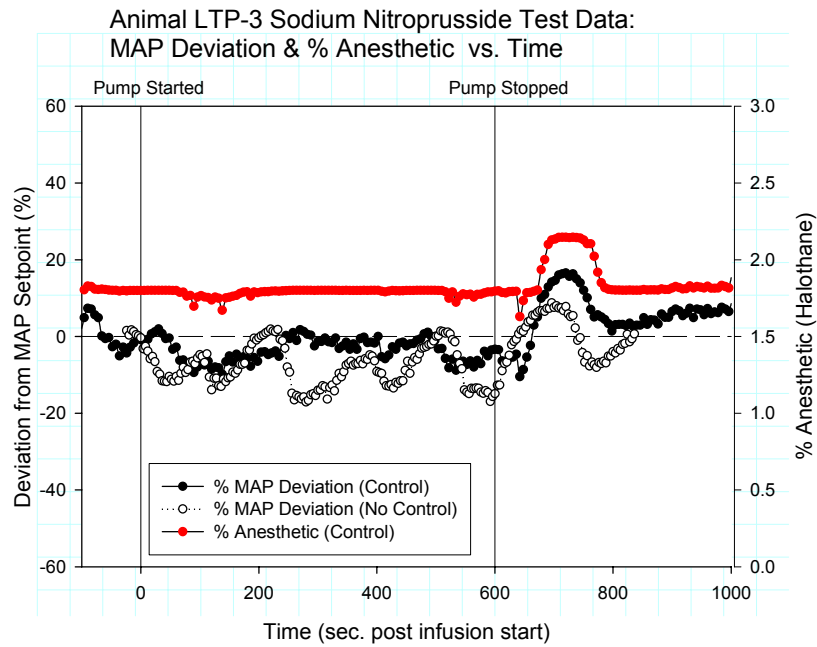
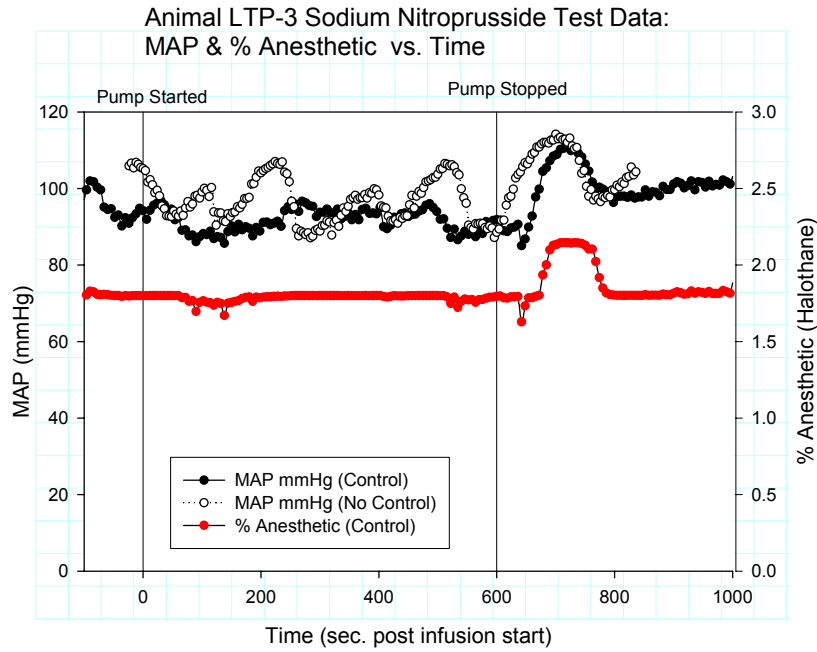
Control Condition	RMS Value (%)	Pressure Set-point (mmHg)	Anesthetic Set-point (%)
Control	22.38	105	2.1
No-Control	30.70	85	NA

Appendix C: Sodium Nitroprusside Infusion Data Plots

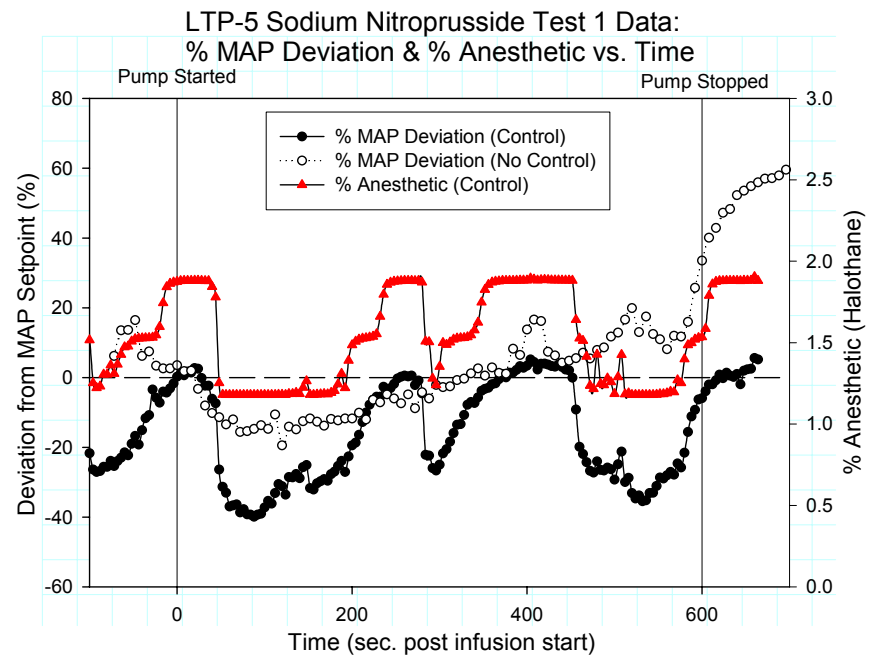
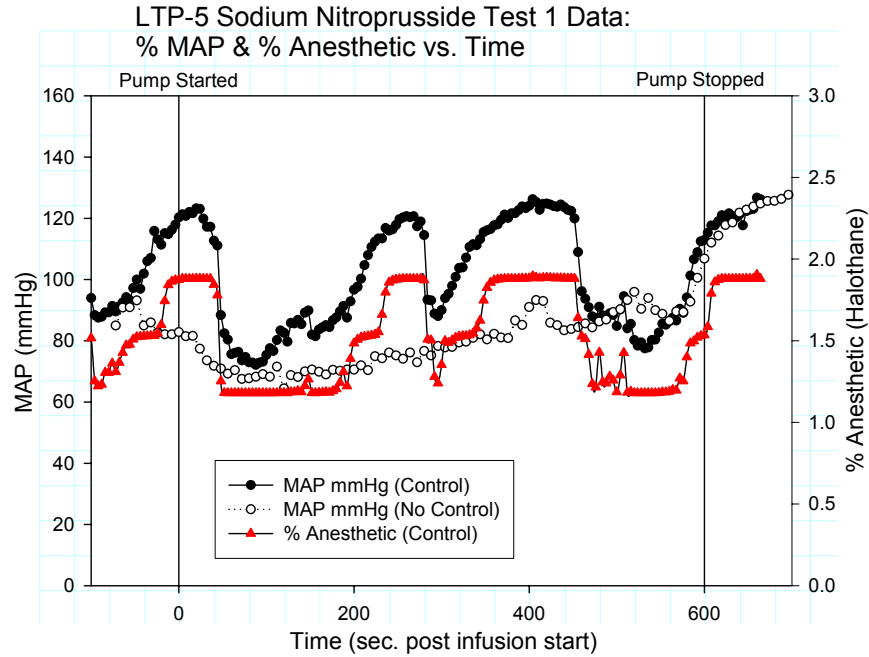
The following are plots of MAP and % MAP deviation for both the control and no-control conditions as well as % anesthetic for the control condition vs. relative time post infusion start for all of the animals which yielded data for the sodium nitroprusside infusion tests.



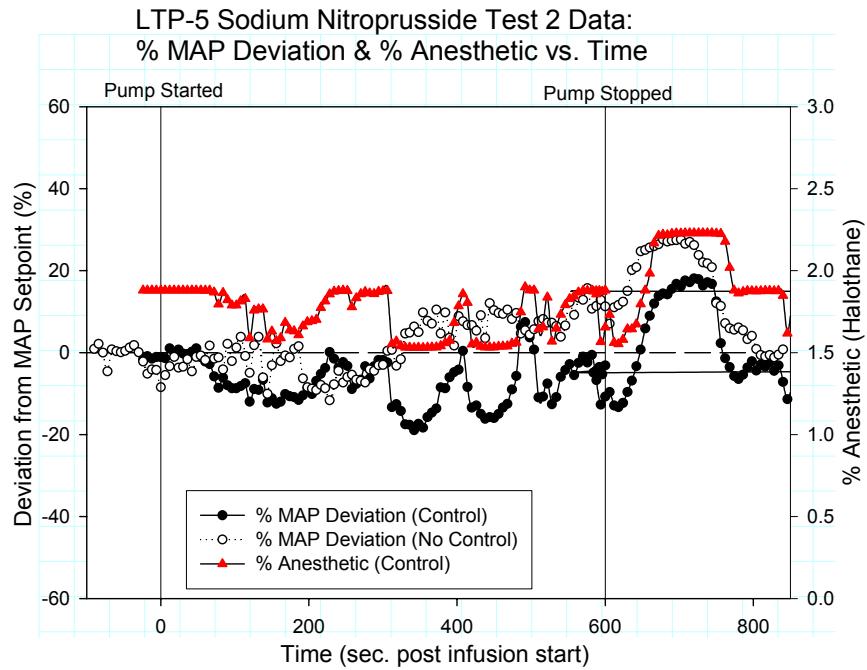
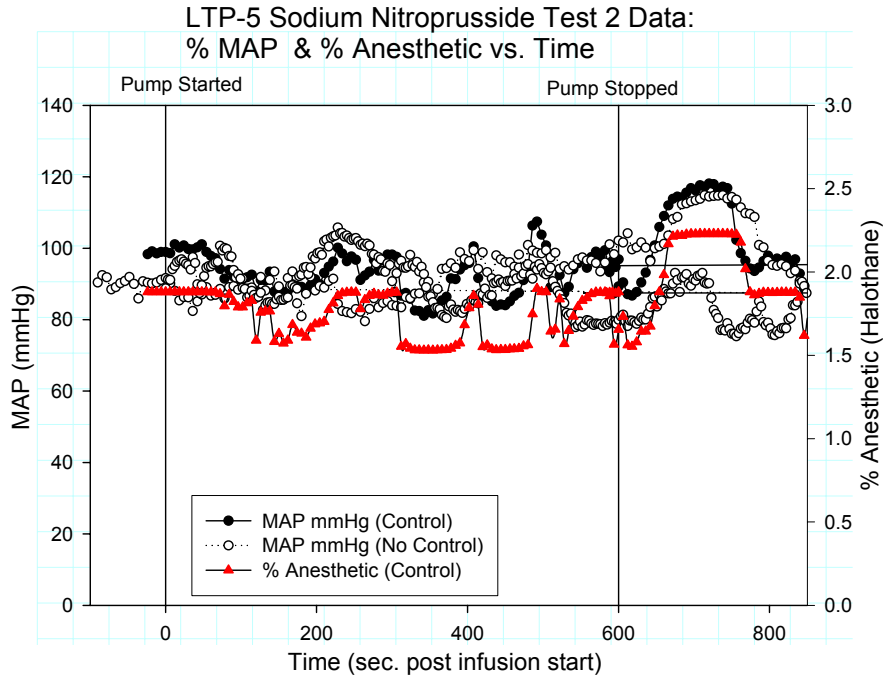
	RMS Value	Pressure Set-	Anesthetic Set-
Control Condition	(%)	point (mmHg)	point (%)
Control	11.04	105	1.9
No-Control	15.71	100	NA



	RMS Value	Pressure Set-	Anesthetic Set-
Control Condition	(%)	point (mmHg)	point (%)
Control	6.60	95	1.8
No-Control	8.37	105	NA

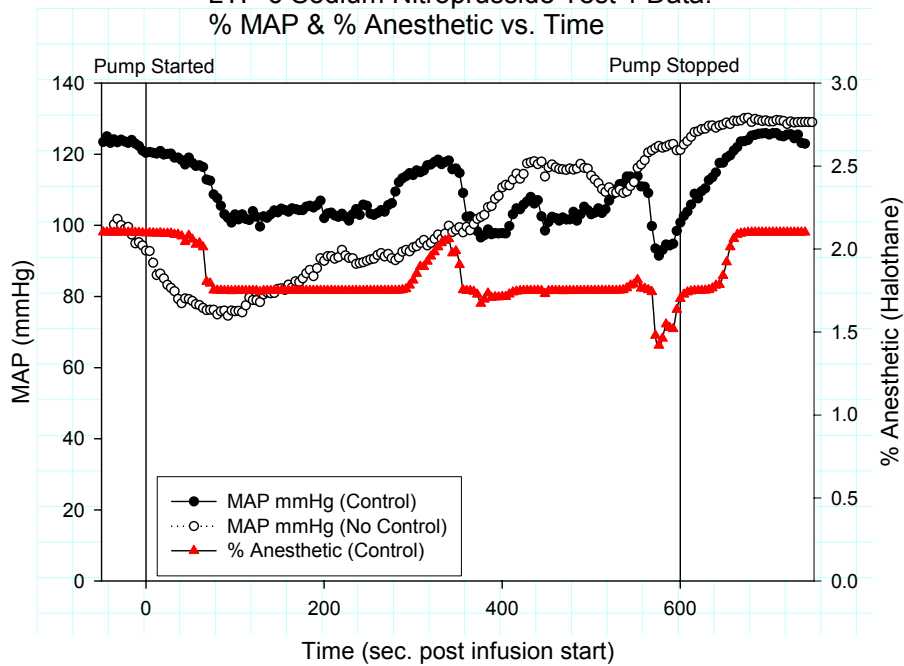


Control Condition	RMS Value (%)	Pressure Setpoint (mmHg)	Anesthetic Setpoint (%)
Control	18.42	120	1.8
No-Control	35.74	80	NA

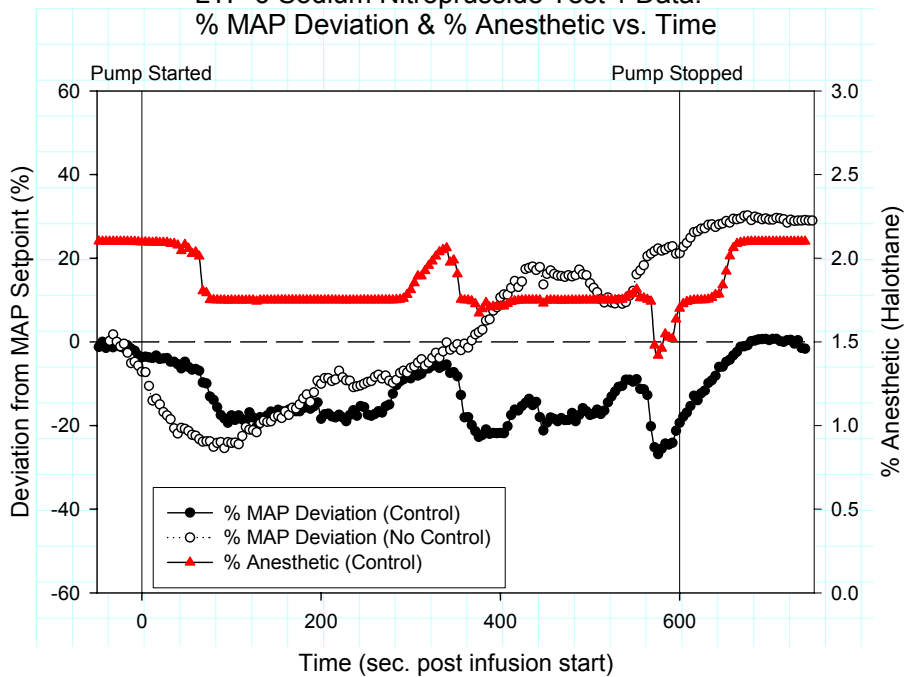


Control Condition	RMS Value (%)	Pressure Set-point (mmHg)	Anesthetic Set-point (%)
Control	18.42	120	1.8
No-Control	35.74	80	NA

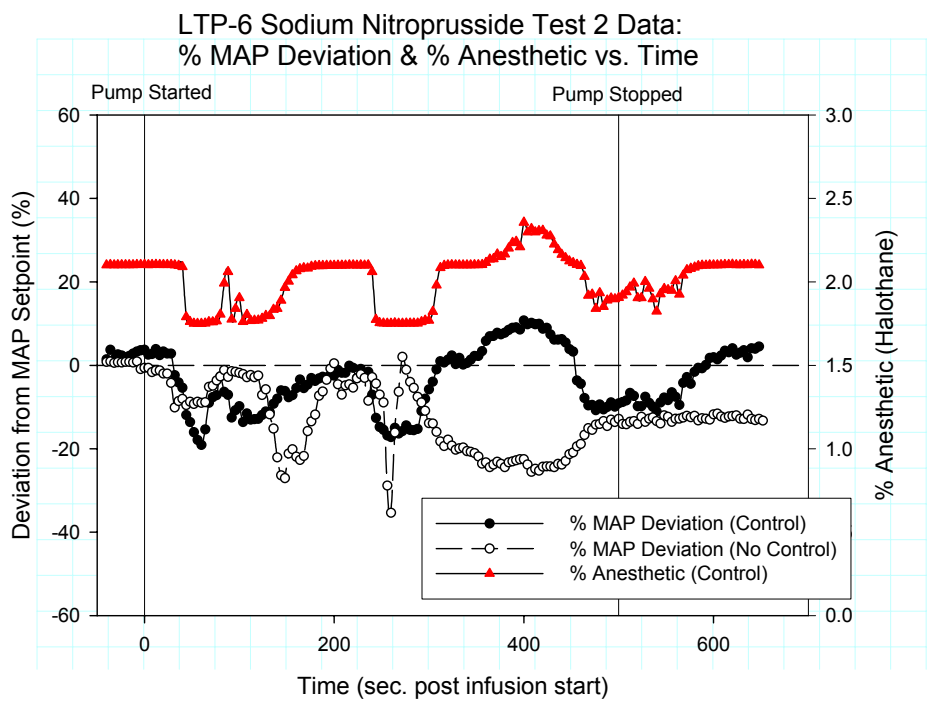
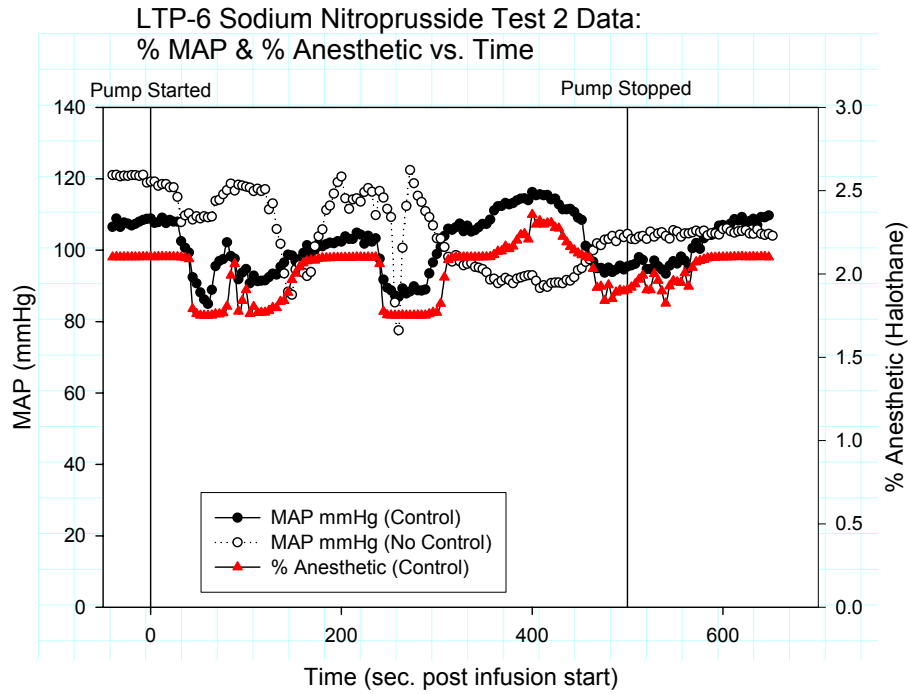
LTP-6 Sodium Nitroprusside Test 1 Data:
% MAP & % Anesthetic vs. Time



LTP-6 Sodium Nitroprusside Test 1 Data:
% MAP Deviation & % Anesthetic vs. Time



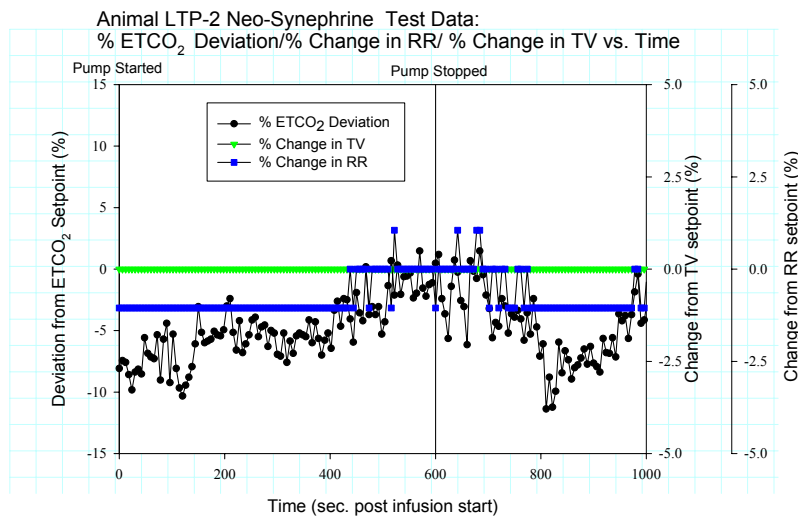
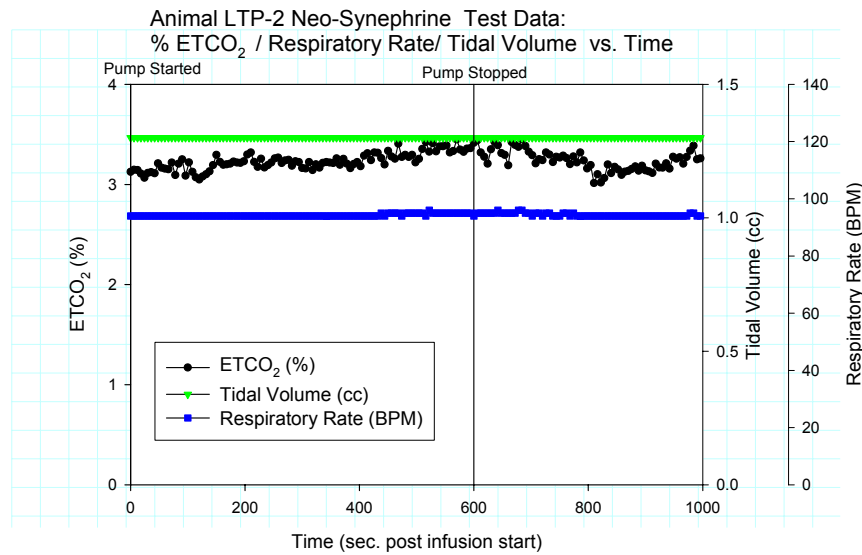
	RMS Value (%)	Pressure Set-point (mmHg)	Anesthetic Set-point (%)
Control Condition			
Control	14.04	125	2.1
No-Control	18.83	100	NA



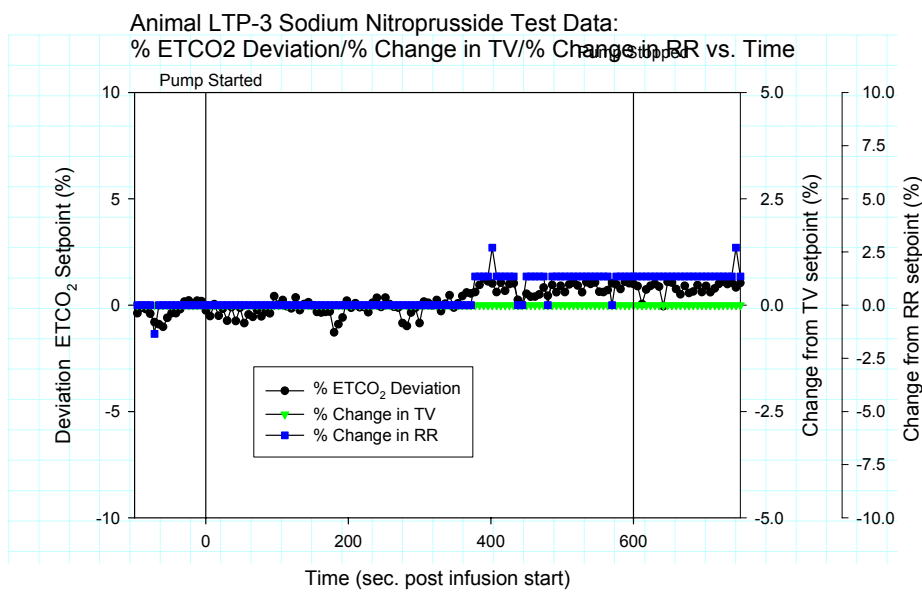
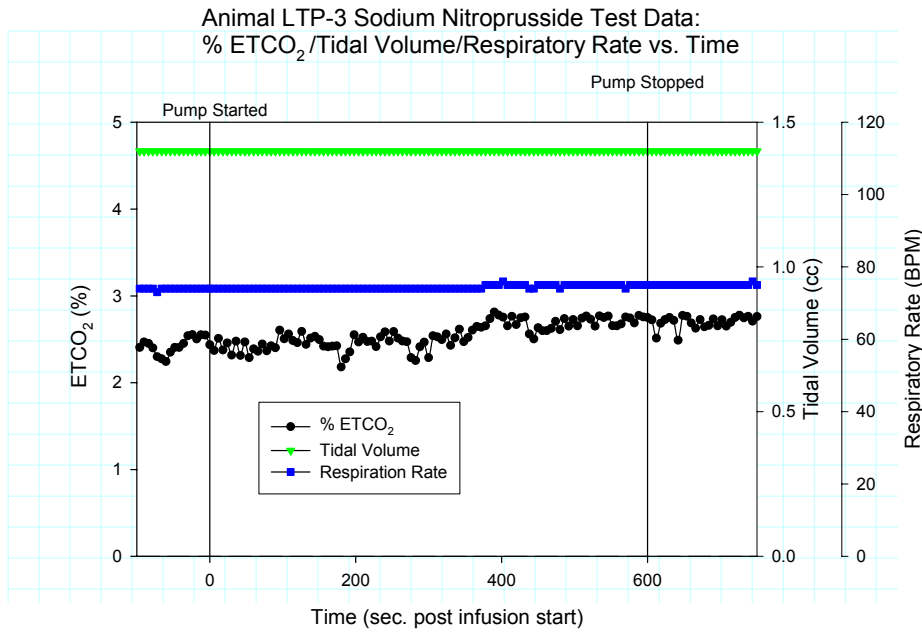
	RMS Value	Pressure Set-	Anesthetic Set-
Control Condition	(%)	point (mmHg)	point (%)
Control	8.02	105	2.1
No-Control	14.59	120	NA

Appendix D: ETCO₂ Data Plots

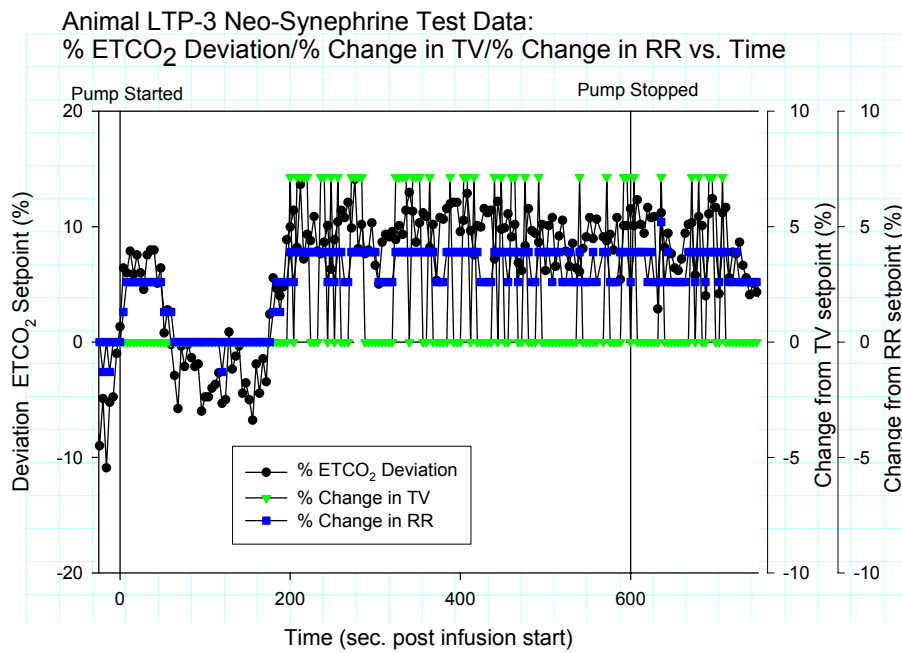
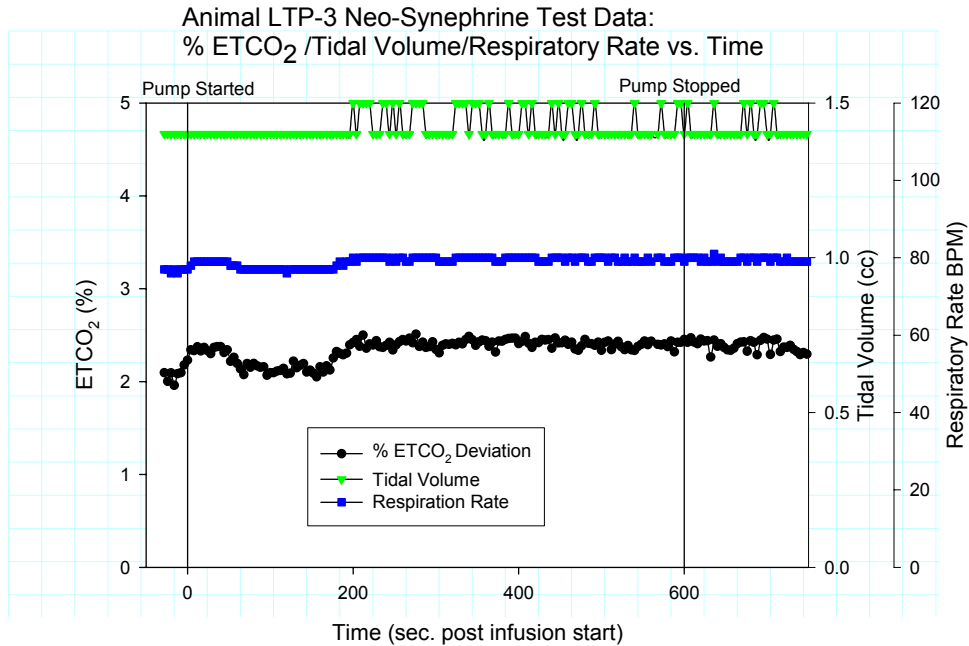
The following are plots of % CO₂, tidal volume and respiratory rate vs. time and %change in ETCO₂, %change in TV and % change in RR vs. time for the animals that yielded data for the ETCO₂ control system.



Parameter	Set-point	Units
ETCO ₂ %	3.4	%
Tidal Volume	1.3	cc
Respiratory Rate	95	BPM

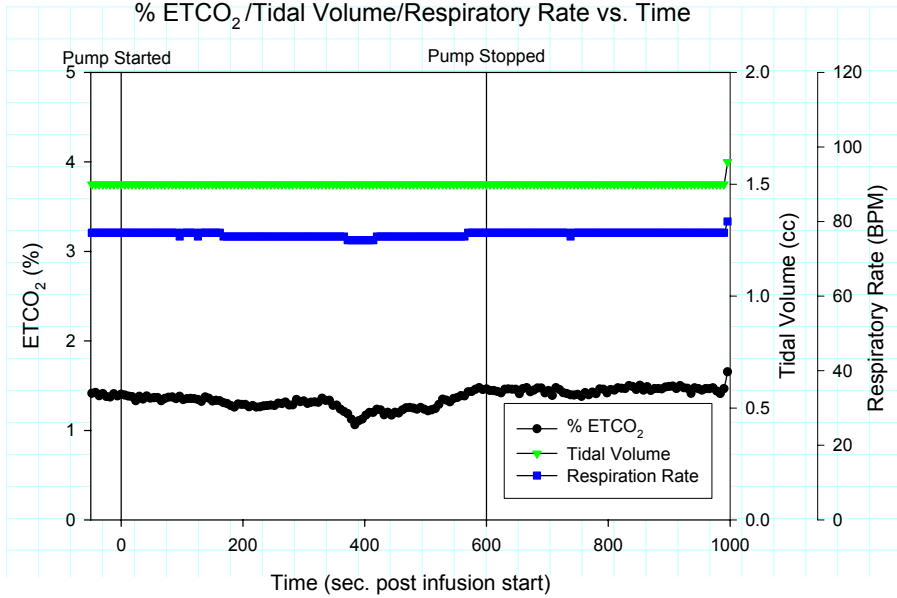


Parameter	Set-point	Units
ETCO ₂ %	2.5	%
Tidal Volume	1.4	cc
Respiratory Rate	74	BPM

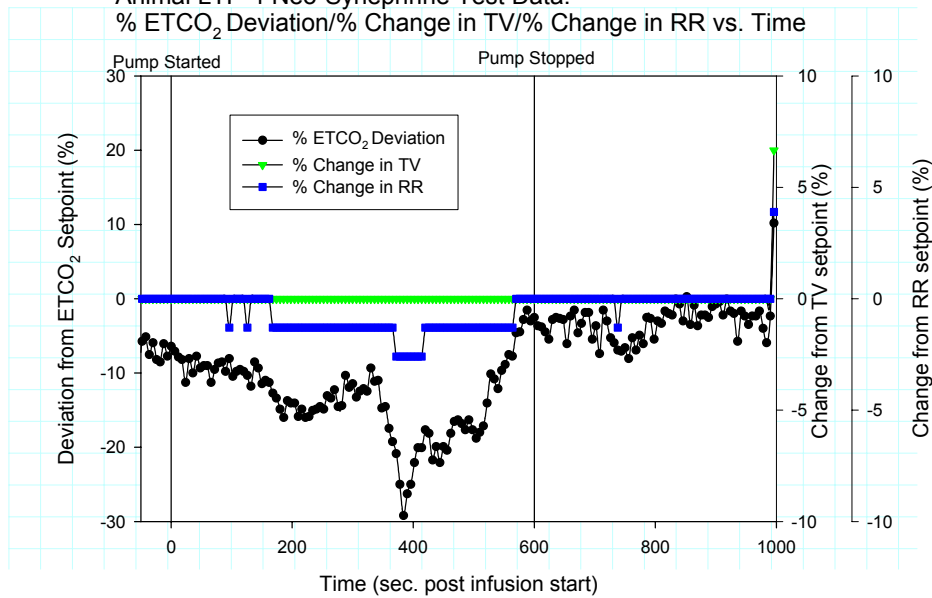


Parameter	Set-point	Units
ETCO ₂ %	2.2	%
Tidal Volume	1.4	cc
Respiratory Rate	77	BPM

Animal LTP-4 Neo-Syneprine Test Data:
% ETCO₂/Tidal Volume/Respiratory Rate vs. Time

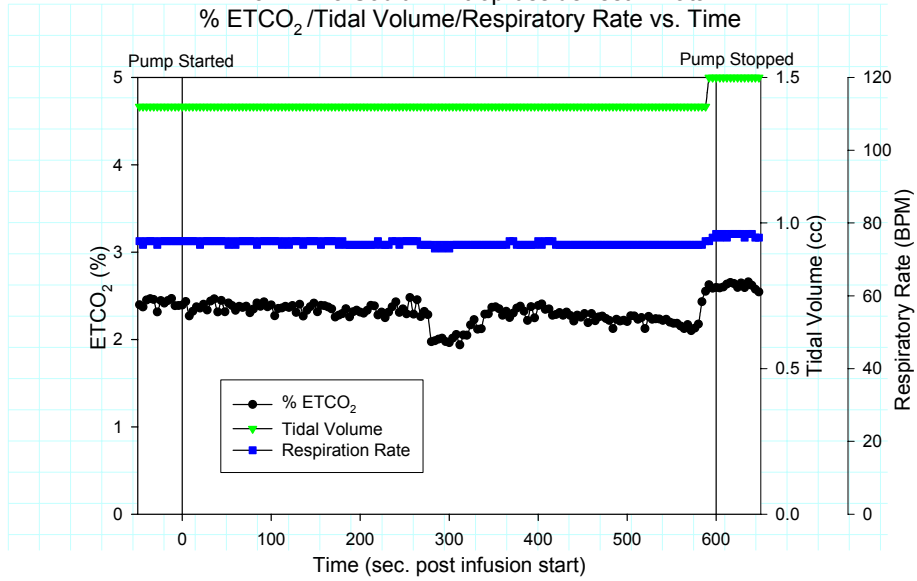


Animal LTP-4 Neo-Syneprine Test Data:
% ETCO₂ Deviation/% Change in TV/% Change in RR vs. Time

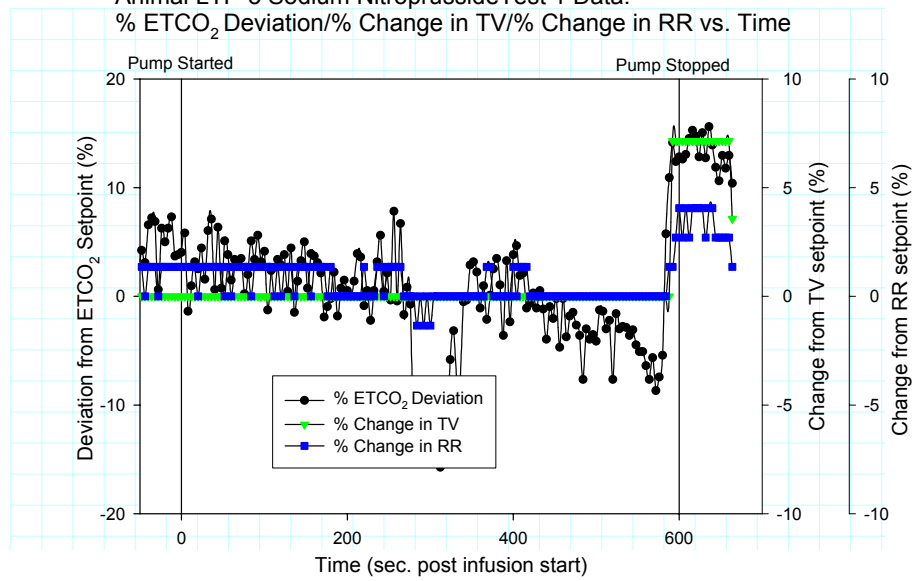


Parameter	Set-point	Units
ETCO ₂ %	1.5	%
Tidal Volume	1.5	cc
Respiratory Rate	77	BPM

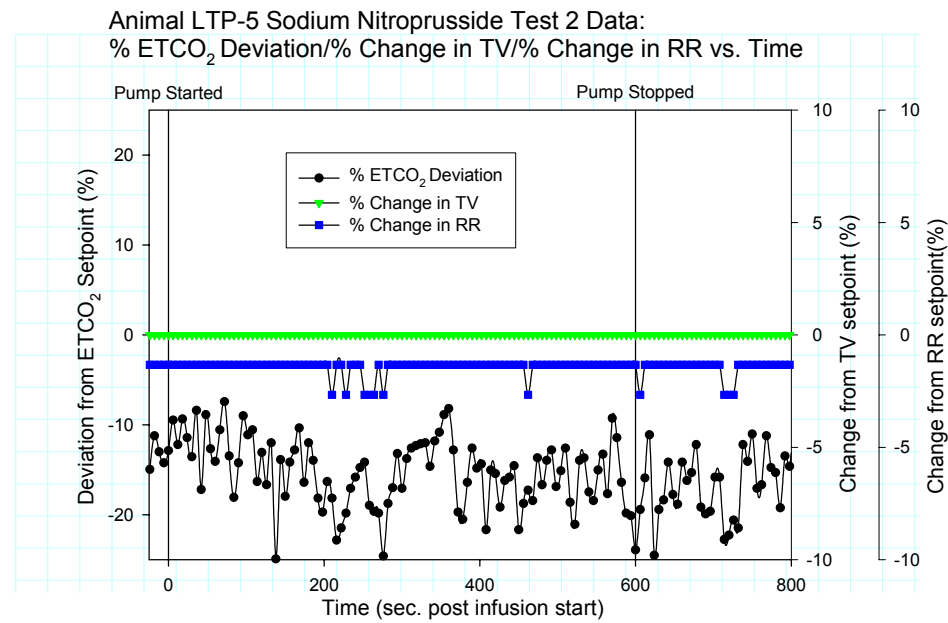
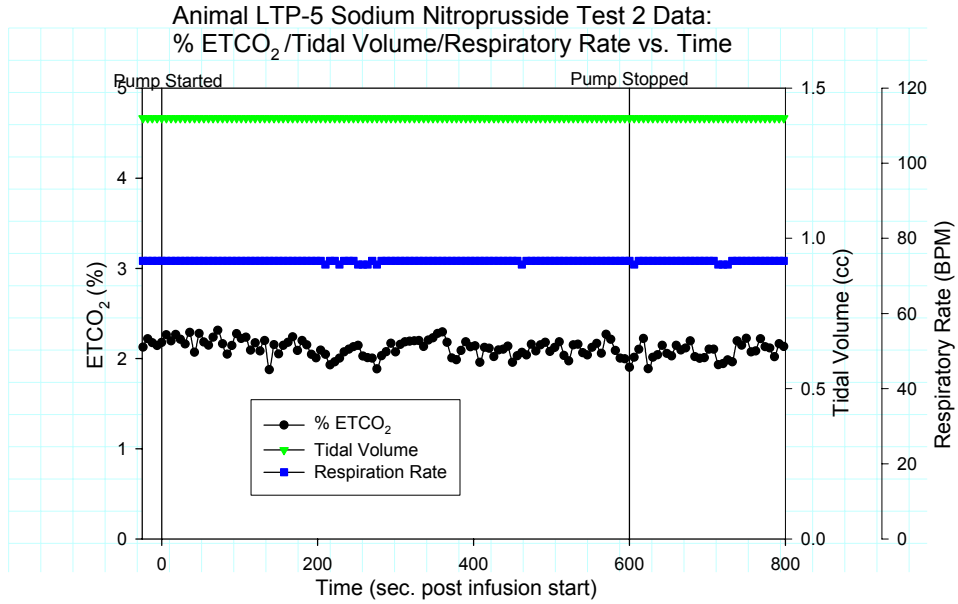
Animal LTP-5 Sodium Nitroprusside Test 1 Data:
% ETCO₂/Tidal Volume/Respiratory Rate vs. Time



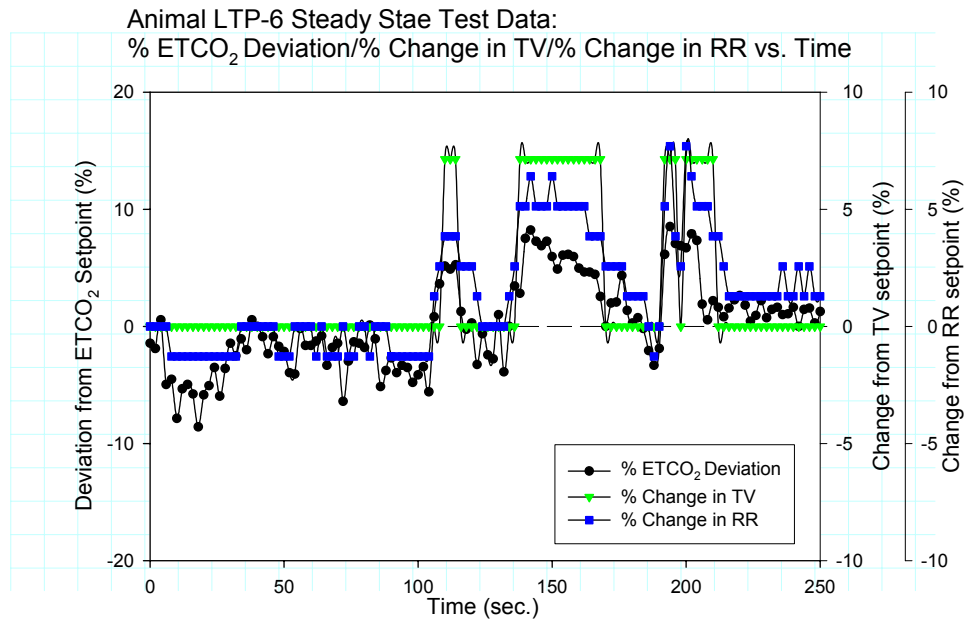
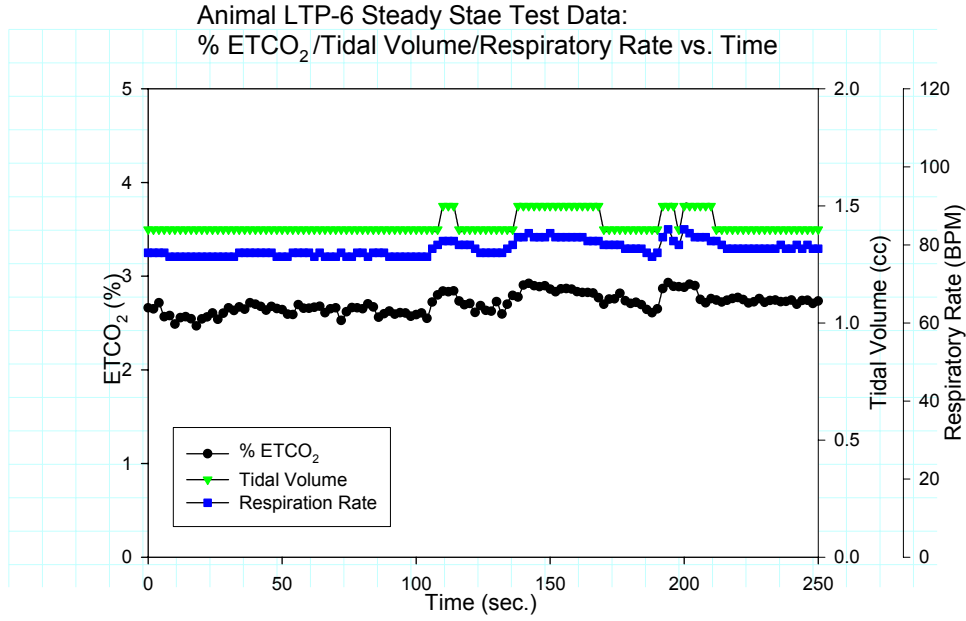
Animal LTP-5 Sodium Nitroprusside Test 1 Data:
% ETCO₂ Deviation/% Change in TV/% Change in RR vs. Time



Parameter	Set-point	Units
ETCO ₂ %	2.3	%
Tidal Volume	1.4	cc
Respiratory Rate	74	BPM



Parameter	Set-point	Units
ETCO ₂ %	2.5	%
Tidal Volume	1.4	cc
Respiratory Rate	75	BPM



Parameter	Set-point	Units
ETCO ₂ %	2.7	%
Tidal Volume	1.4	cc
Respiratory Rate	78	BPM